Department of Physics and Astronomy
University of Heidelberg

Master Thesis in Physics
submitted by

Julian Bollig

born in Bernkastel-Kues (Germany)

Year of submission

2020

5D Holographic Implementation of Softened Symmetry Breaking in the Composite Higgs Framework

This Master Thesis has been carried out by
Julian Bollig
at the
MPI for nuclear physics (MPIK)
under the supervision of
Dr. Florian Goertz
MPIK

Second Referee: Prof. Dr. Manfred Lindner (MPIK)

ABSTRACT

In this thesis the spectrum of top partners in the minimal composite Higgs model with fundamental fermionic representation is explored. It is shown that by using a recently developed softened symmetry breaking mechanism for the global symmetry, top partner masses above 1.5 TeV for a realistic Higgs mass of 125 GeV can be produced without raising the symmetry breaking scale. For a maximally symmetric version of this model, which has also just been proposed, top partner masses above 2 TeV can be realized, while simultaneously a significantly reduced fine-tuning of $\mathcal{O}(10)$ is achieved providing a quantitative proof for the existence of a natural minimal composite Higgs model which is not in tension with current observations. To carry out this analysis, the 4-dimensional effective field theory of the softened symmetry breaking is reviewed and then embedded into a 5-dimensional holographic theory through the AdS/CFT duality. Numerical scans on the resulting particle spectrum and the tuning in the holographic dual are performed including a detailed parameter study of the outcome. A theoretical review of the 4- and 5-dimensional picture as well as their maximally symmetric extensions is also provided.

ABSTRACT

Im Zuge dieser Arbeit wird das Spektrum von Top-Partner Massen im minimalen Composite-Higgs-Modell mit Fermionen in der Fundamental-Darstellung untersucht. Es zeigt sich, dass es über einen erst kürzlich entwickelten Mechanismus zur sanften globalen Symmetrybrechung möglich ist, bei einer Higgs-Masse von 125 GeV Top-Partner-Massen von über 1.5 TeV zu erzeugen ohne dabei die Skala der Symmetriebrechung anzuheben. In einer Version dieses Models, welche maximale Symmetrie berücksichtigt, können, bei gleichzeitig enorm verringerten Feintuning von $\mathcal{O}(10)$, Massen von über 2 TeV erreicht werden, was beweist, dass es möglich ist ein natürliches minimales Composite-Higgs-Modell zu schaffen, welches nicht in Widerspruch zu aktuellen experimentellen Beobachtungen steht. Für diese Analyse wird ein bereits existierender qualitativer Ansatz in 4 Dimensionen mittels der AdS/CFT-Dualität in einer 5-dimensionalen holographischen Theorie realisiert. Es werden numerische Scans des resultierenden Teilchen-Spektrums sowie des Tunings in der 5-dimensionalen holographischen Theorie durchgeführt und die Ergebnisse in einer detaillierten Parameter-Studie festgehalten. Zudem wird eine Zusammenfassung der 4- sowie der 5-dimensionalen Theorie inklusive ihrer maximal symmetrischen Erweiterungen bereitgestellt.

Contents

Acronyms

AdS Anti-de-Sitter space.

BC Boundary Condition.

BR Branching Ratio.

BSM Beyond Standard Model.

CCWZ Callan-Coleman-Wess-Zumino.

CFT Conformal Field Theory.

CHM Composite Higgs Model.

CL Confidence Level.

EFT Effective Field Theory.

EW Electroweak.

EWPO Electroweak Precision Operator.

EWPT Electroweak Precision Tests.

EWSB Electroweak Symmetry Breaking.

FCC Future Circular Collider.

FCNC Flavor Changing Neutral Current.

GUT Grand Unified Theory.

HL-LHC High Luminosity LHC.

IR Infrared.

KK Kaluza-Klein.

LHC Large Hardon Collider.

LO Leading-Order.

MCHM Minimal Composite Higgs Model.

NGB Nambu-Goldstone Boson.

NLO Next-to-Leading-Order.

pNGB pseudo Nambu-Goldstone Boson.

QCD Quantum Chromodynamics.

SM Standard Model.

SSB Spontaneous Symmetry Breaking.

SUSY Supersymmetry.

TC Technicolor.

UV Ultraviolet.

VEV Vacuum Expectation Value.

VLQ Vector-Like Quark.

List of Figures

List of Tables

1 Introduction

The *Standard Model* (SM) has been and still is the best tested and most conclusive description tool particle physicists have to explain the behavior of fundamental particles on small scales. However, it is unable to give answers to many of the most pressing physical questions of our time: *How do neutrinos obtain their masses?* [1–5], *What is Dark Matter?* [6–11], *Why does the Universe expand?* [12–15] or *How does gravitation work on small scales?* [16–18]. Even though the SM might not be wrong, it certainly is incomplete.

Apart from these fundamental questions of particle physics there are also issues within the SM regarding well established physical principles like *Naturalness* [19–21]. Two of the most prominent unanswered questions in this context are the *strong CP problem* [22] and the *flavor puzzle* [23]. These rather "esthetical" problems do not fundamentally question the SM by experimental evidence, but they do give rise to doubts about its validity. Therefore, physicists work on alternatives to the SM which do not incorporate these problems in order to give a more "natural" explanation for our observations and, thereby, even tackle the more fundamental questions by this approach.

The question addressed in this thesis reads: *Why is the weak force of the SM by a factor of 10^{34} stronger than gravity?*[1] This rather generic formulation is linked to what physicists call the *Hierarchy problem* of the SM [24–27].

A hierarchy problem in general occurs when the expected bare value of a particles property (like its coupling or mass) is vastly different from its effective value (which was measured in an experiment) due to renormalization. From a physicists point of view, such behavior is "unnatural" because it implies huge renormalization corrections to cancel each other without having any physical reason to do so. The occurrence of a hierarchy problem is unique to elementary scalars such that in the framework of the SM it can only affect the Higgs boson. The quantum corrections of fermions and bosons are proportional to their own masses such that their loop corrections are suppressed by the size of their tree-level contribution. For both sectors this happens because in the massless limit symmetries are restored, the chiral symmetry in the fermion sector and gauge symmetry in the gauge sector. However, this does not apply for the Higgs boson. At loop level it receives corrections from self interactions, gauge loops and fermion loops (especially from the top quark) which are proportional to the cutoff $\delta_{\mathrm{SM}} m_H^2 \propto \Lambda_{\mathrm{SM}}^2$ of the theory. If the SM is actually valid up to *Planck scale* $\Lambda_{\mathrm{SM}} \lesssim M_{\mathrm{Pl}} = 10^{19}\,\mathrm{GeV}$ and therefore $\Lambda_{\mathrm{SM}} \gg 1\,\mathrm{TeV}$, it can be concluded that $\delta_{\mathrm{SM}} m_H^2 \gg m_H^2$ and the Hierarchy problem arises [28, 29].

In the past there have been many attempts to tackle this problem. Some of them like original *Technicolor* (TC) theories [30–33] have already been ruled out by experiment, others like *Supersymmetry* (SUSY) [34–37] are currently under great tension. One of the most promising attempts for a long time have been *Composite Higgs Models* (CHMs). In these models the Hierarchy problem is naturally solved by treating the SM as an

[1] The factor of 10^{34} yields the ratio between the energy of the weak and gravitational interaction between two core protons at sufficiently small distances.

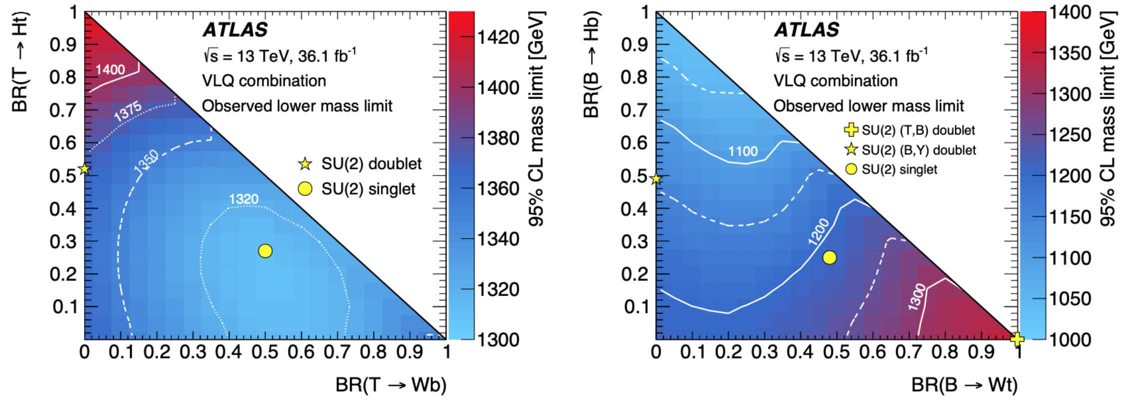

(a) (b)

Figure 1.1: Most recent data on the observed lower exclusion limits at 95% *Confidence Level* (CL) of additional up-type (*a*) and down-type (*b*) *Vector-Like Quarks* (VLQs) as a function of the *Branching Ratios* (BRs) of selected decay channels. The case of an isospin doublet (T, B) is indicated by the yellow star in the left plot and the yellow cross in the right plot, excluding masses below 1.37 TeV. This value will be referenced as a conservative approach to the top partner exclusion limit in the subsequent models. Taken from [38].

effective theory with a cutoff at $\Lambda \sim 1\,\text{TeV}$. This is achieved by introducing an enhanced global symmetry $\mathcal{G}$ of a strongly interacting sector, which is spontaneously broken to a subgroup $\mathcal{H}$ at a scale f by the condensation of a new strong force. Like pions in *Quantum Chromodynamics* (QCD), the Higgs boson emerges as a composite particle corresponding to the *Nambu-Goldstone Bosons* (NGBs) of this *Spontaneous Symmetry Breaking* (SSB). The SM *Electroweak* (EW) symmetry $\mathcal{G}_{\text{EW}} = SU(2)_L \times U(1)_Y \subset \mathcal{H}$ is then broken via the *vacuum misalignment mechanism*. Couplings to SM particles, which do not respect the enhanced global symmetry, explicitly break $\mathcal{G}$ radiatively creating a potential for the Higgs boson which is in fact a composite *pseudo Nambu-Goldstone Boson* (pNGB). With a Higgs created at an $\mathcal{O}(1\,\text{TeV})$ scale, the Hierarchy problem ceases to exist.

The Higgs boson as an essential ingredient for the famous mechanism of *Electroweak Symmetry Breaking* (EWSB) was first proposed in 1964 [39–41]. After its discovery in 2012 [42] physicists at the *Large Hardon Collider* (LHC) made great effort to test its internal structure. Explicitly, they searched for fermionic partners which are predicted from CHMs to have a mass of a few TeV [38, 43]. Especially the *Minimal Composite Higgs Model* (MCHM) - or MCHM$_5$ to be more precise - which is studied throughout this thesis, requires partner masses below 1 TeV at a breaking scale around $f \sim 800\,\text{GeV}$ in order to keep the Higgs boson sufficiently light (see [44, 45] and the references therein). The lack of experimental evidence as displayed in Figure 1.1 stimulated searches for alternative realizations.

One possibility to which this analysis is dedicated to, is to raise the masses of the fermionic partners (especially for the top quark) by softening the breaking of the enhanced global symmetry with new vector-like fermions [46]. This promising novel mechanism has, so far, only been discussed in the framework of an effective 4D theory of the aforementioned model. The unknown nature of the strong force, which causes the symmetry breaking, restricts the predictive power of the effective theory regarding certain model parameters like the coupling constants and the Higgs mass. In this thesis, the new approach is embedded into a 5-dimensional holographic theory through an approximate *AdS/CFT duality*, where AdS stands for an *Anti-de-Sitter space* and CFT denotes a *Conformal Field Theory* of lower dimension. The 5D picture adds structure to the theory improving the predictability of the model. Therefore, it facilitates a more detailed study of the composite Higgs and the new vector-like particles, which will be carried out hereinafter.

The rest of this thesis is structured as follows: Section 2 gives an overview of composite Higgs theory, where also the statements of this introduction are revisited and explained. Starting from a general theory of CHMs in Section 2.1, in Section 2.2 the Lagrangian for the 4D model used in this thesis is derived. Moving on to Section 2.3, the general properties of a 5D holographic view on CHMs are explained and the bridge towards the 4D model is built. The 5D implementation of the model as well as the Higgs potential is derived in Section 2.4. Closing the theory part, Section 2.5 focusses on the fine-tuning issues of this theory and proposes an extended symmetry, which might solve these problems. The numerical analysis is carried out in Section 3. Section 3.1 is used as a consistency check with former studies, which do not incorporate the novel symmetry breaking mechanism, whereas Section 3.2 and Section 3.3 analyze the new model derived in Section 2.4. In Section 3.4 the additional symmetry, which has been discussed in Section 2.5, is added and the analysis is redone. Section 4 summarizes the results of this analysis and gives an outlook on further topics to study.

2 Theory and General Setup

In this section at first the basic principles of Composite Higgs theories in general proceeding will be outlined with topics specific to this setup, taken from [46]. In a second step this 4D setup is mapped onto a 5D compact warped spacetime using AdS/CFT duality and methods are derived to calculate the Higgs mass along with the masses for the previously mentioned fermionic partners with dependency on the new model parameters. Eventually, ways to quantify the naturalness of this approach in terms of fine-tuning are discussed. Throughout the Sections 2.1 and 2.2, the argumentation will mostly follow the one of the 2015 review by G. Panico and A. Wulzer [47]. For 2.3 and 2.4 the 2009 lecture notes by R. Contino [48] accompanied with the 2015 paper by A. Carmona and F. Goertz [45] will be used as guidance. Section 2.5 will seize on ideas from papers by G. Panico et al. [49], C. Csáki et al. [50] and S. Blasi et al. [51].

2.1 The Higgs particle as a composite pNGB

2.1.1 An effective approach to the Hierarchy problem

In order to fully understand the motivation expounded in Section 1, the use of an *Effective Field Theory* (EFT) framework is advantageous. The lack of a fundamental and consistent description of gravity within the SM inevitably leads to its breakdown at the Planck scale $M_{\text{Pl}} = 10^{19}\,\text{GeV}$ when the SM-consistent concept of quantum gravity becomes non-perturbative and non-renormalizable. At the latest at this scale new particles and interactions have to emerge, transforming the SM into an EFT with a cutoff scale Λ_{SM} above which these "new physics" contributions have been integrated out. An effective Lagrangian is then composed of infinitely many gauge and Lorentz invariant operators of arbitrary dimension d and coefficients scaling with $\sim \Lambda_{\text{SM}}^{4-d}$. The operators of dimension $d \leq 4$ represent the renormalizable SM with all its *accidential symmetries* (like Baryon and Lepton number conservation or custodial symmetry) which are useful to explain observations like the smallness of neutrino masses or the metastability of the proton. The non-renormalizable operators of dimension $d > 4$ which violate these symmetries are suppressed by powers of the cutoff scale. If $\Lambda_{\text{SM}} \lesssim M_{\text{Pl}}$, the small symmetry violations observed in nature emerge automatically. If $\Lambda_{\text{SM}} \sim 1\,\text{TeV}$, higher order operators have to be constrained to respect them.

Having set the EFT of the SM, the Hierarchy problem (or equivalently a violation of the principle of Naturalness) occurs due to the single dimension $d = 2$ operator of the SM, which represents the Higgs mass term

$$c_H \Lambda_{\text{SM}}^2 H^\dagger H \tag{2.1.1}$$

scaling quadratically with Λ_{SM}. For a high cutoff scale, the dimensionless coupling constant c_H has to be unnaturally tiny in order to reproduce the observed Higgs mass. In other words, if the effective calculation of the Higgs mass is split into a SM and a *Beyond*

Standard Model (BSM) term

$$
\begin{aligned}
m_H^2 &= \int_0^{\Lambda_{\mathrm{SM}}} \mathrm{d}E \frac{\mathrm{d}m_H^2}{\mathrm{d}E}(E;\zeta_{\mathrm{full}}) + \int_{\Lambda_{\mathrm{SM}}}^{\infty} \mathrm{d}E \frac{\mathrm{d}m_H^2}{\mathrm{d}E}(E;\zeta_{\mathrm{full}}) \\
&= \delta_{\mathrm{SM}} m_H^2 + \delta_{\mathrm{BSM}} m_H^2, \qquad (2.1.2)
\end{aligned}
$$

where the ζ_{full} are the true parameters of the unknown complete theory, it can be seen that $\delta_{\mathrm{SM}} m_H^2 \gg m_H^2$ (as stated in Section 1) demands an extremely fine-tuned cancellation coming from $\delta_{\mathrm{BSM}} m_H^2$. This is very unnatural because these two contributions are theoretically independent.

CHMs solve this problem by considering the Higgs boson to be a bound state of a new unknown strong force (like QCD). Therefore, these models set a new scale $m_* \sim \mathcal{O}(1\,\mathrm{TeV})$ which is inversely proportional to the geometric size l_H of the composite Higgs. Thus, at $E \ll l_H^{-1}$, the spatial extension of the Higgs boson can not be resolved and the Higgs along with the contributions $\mathrm{d}m_H^2/\mathrm{d}E(E;\zeta_{\mathrm{full}})$ to its mass behaves like in the SM. The contributions flatten as $E \sim l_H^{-1}$ due to the finiteness of the Higgs boson and become strongly suppressed for energies above this scale. Therefore, m_* can be viewed as the scale which cuts off the quadratical divergence from the Higgs and is labelled as the *confinement scale* of the theory.

This setup enables the Higgs particle to obtain a mass consistent with its observed range around $m_H = 125\,\mathrm{GeV}$ by simultaneously making it insensitive to contributions from any further particles above the TeV scale. Since one is usually interested in m_* being at $\mathcal{O}(\mathrm{TeV})$ or higher, a small separation of scales $g_* \in (1, 4\pi)$ between the confinement scale m_* and the scale of global symmetry breaking f is introduced

$$
g_* = \frac{m_*}{f} \ll 4\pi. \qquad (2.1.3)
$$

By construction this also means that the scale for new particles m_* emerges before the actual strong coupling scale at $\Lambda \sim 4\pi f$ is met. The factor g_* can thus be seen as the coupling strength of this strongly coupled sector connecting the *Vacuum Expectation Value* (VEV) f of the spontaneously broken global symmetry $\mathcal{G}$ to the confinement scale m_*.

For a loop induced Higgs potential with a coupling $g_* > 1$, a natural CHM would require $f \sim v$. However, experimental bounds from *Electroweak Precision Tests* (EWPT) and couplings of the Higgs demand $f > v$. This tension creates an inevitable fine-tuning in all CHMs which will be discussed in Section 2.5.

2.1.2 General features of Composite Higgs theories

Ideas of intertwining TC theories with the common Higgs model reach back to the mid-eighties [52–58]. Over the years many different CHMs evolved, all trying to tackle the same problem (e.g. [59–65]; see [66] for an overview). Despite their huge variety there are certain characteristics all of them have in common. CHMs are EFTs like the SM which have to be replaced by a more fundamental theory above their cutoff scales. They are usually split into two sectors (see Figure 2.1), a *composite* and an *elementary* one.

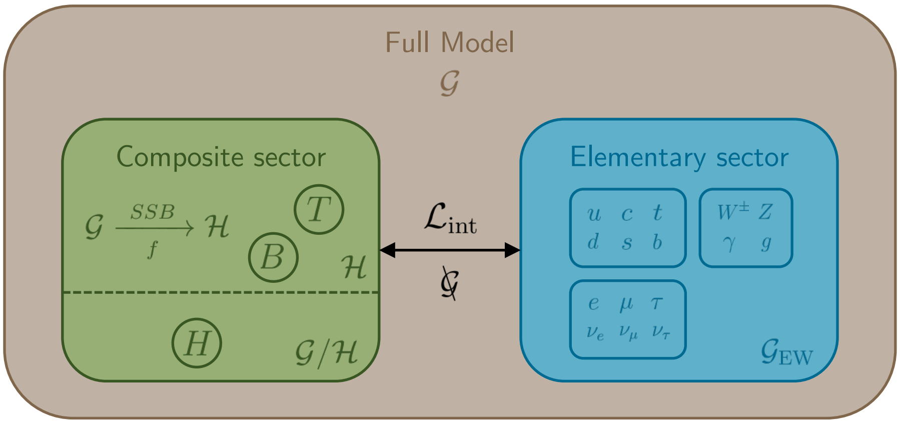

Figure 2.1: Structure of a general Composite Higgs Model.

Emerging from a higher scale $\Lambda_{\text{UV}} \gg 1\,\text{TeV}$, the composite sector initially respects the full Goldstone symmetry group $\mathcal{G}$. Like in QCD (or TC theories) this symmetry is spontaneously broken into a subgroup $\mathcal{H}$ at a confinement scale m_*. Different from earlier attempts [19, 67] the Higgs boson emerges in a CHM as a NGB within the coset $\mathcal{G}/\mathcal{H}$. Therefore, it is massless at tree level.

The elementary sector is weakly coupled and contains all SM particles except the Higgs (and maybe the right-handed top quark t_R). Its symmetry group is $SU(2)_L \times U(1)_Y \equiv \mathcal{G}_{\text{EW}} \subset \mathcal{G}$ which is gauged by the SM vector bosons. Due to the gauging of a subgroup of $\mathcal{G}$, the elementary SM gauge bosons couple to the composite sector forcing it to also respect $\mathcal{G}_{\text{EW}}$ (i.e. $\mathcal{G}_{\text{EW}} \subset \mathcal{H}$) in order to get a viable theory. The elementary sector in general does not respect the full symmetry $\mathcal{G}$ and breaks it explicitly through fermionic and gauge interactions with the composite sector. The former are necessary for the SM fermions to become massive due to the non-existing Yukawa-terms in the elementary sector. The explicit breaking induces a light mass to the now pNGB Higgs allowing for EWSB to take place. The question why a composite Higgs boson couples in almost the same way to fermions and vector bosons as an elementary one (like in the SM) is explained by the *vacuum misalignment mechanism*.

2.1.3 Vacuum Misalignment

Vacuum misalignment explains EWSB in CHMs and is best illustrated in a geometrical sense (see Figure 2.2). To analyze the mechanism, one can start with a parametrization of the symmetry group $\mathcal{G}$ of the composite sector. Due to its spontaneous breaking into a subgroup $\mathcal{H}$, it is sensible to choose a basis which can be divided into unbroken and broken generators, $\langle\{T^a\}\rangle = \mathcal{H}$ and $\langle\{\hat{T}^{\hat{a}}\}\rangle = \mathcal{G}/\mathcal{H}$, respectively, with $a = 1, ..., \dim\mathcal{H}$ and $\hat{a} = 1, ..., \dim\mathcal{G}/\mathcal{H}$.[2] Thus, a generic vacuum $\mathbf{\Sigma_0}$ of the composite sector can be

[2]Of course, the T's are the generators of the Lie algebras corresponding to the groups, but this will be ignored here because it is of no importance for what follows.

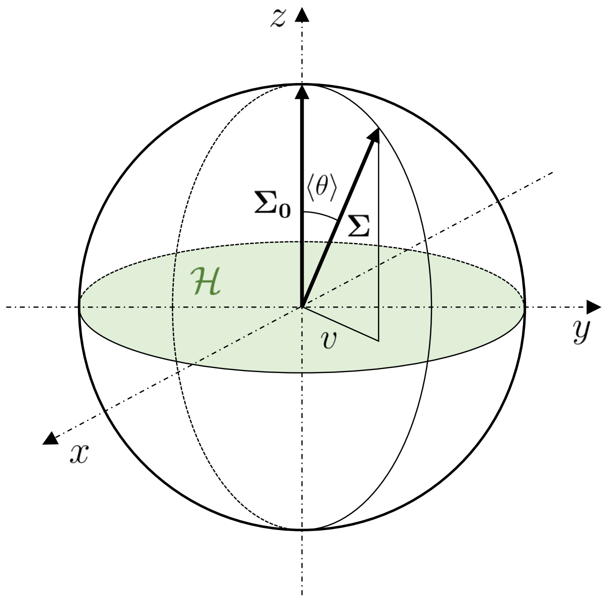

Figure 2.2: The mechanism of vacuum misalignment with $\mathcal{G} = SO(3)$, $\mathcal{H} = SO(2)$ and $\mathbf{\Sigma_0} = (0, 0, f)^T$.

defined, which is characterized by

$$T^a \mathbf{\Sigma_0} = 0, \quad \hat{T}^{\hat{a}} \mathbf{\Sigma_0} \neq 0 \tag{2.1.4}$$

$\forall a, \hat{a}$, such that $\mathbf{\Sigma_0} \perp \mathcal{H} \supset \mathcal{G}_{\mathrm{EW}}$. The NGBs as elements of the coset $\mathcal{G}/\mathcal{H}$ can be defined as transformations along the broken generators $\hat{T}^{\hat{a}}$

$$\mathbf{\Sigma}(x) = e^{i\theta_{\hat{a}}(x)\hat{T}^{\hat{a}}} \mathbf{\Sigma_0}, \tag{2.1.5}$$

where four of the $\theta_{\hat{a}}(x)$ are identified as the real components of the Higgs doublet.

Without explicit breaking of $\mathcal{G}$, the NGB fields do not develop a potential and stay massless. With a redefinition of fields $\mathbf{\Sigma} \to e^{-i\langle\theta_{\hat{a}}\rangle\hat{T}^{\hat{a}}}\mathbf{\Sigma}$ one can, therefore, always set the VEV $\langle\theta\rangle \equiv (\sum_{\hat{a}} \langle\theta_{\hat{a}}\rangle^2)^{1/2}$ of the NGB fields to 0. With the explicit breaking of $\mathcal{G}$ the now pNGBs develop a potential and the VEV cannot be rotated away any more. Thus, $\langle\theta\rangle$ induces EWSB by spontaneously breaking $\mathcal{G}_{\mathrm{EW}} \subset \mathcal{H}$ to $U(1)_{\mathrm{em}}$. Geometrically, this corresponds to the degree of misalignment of the vacuum with respect to $\mathbf{\Sigma_0}$ parametrized by the angle $\langle\theta\rangle$. The scale of EWSB $v = f \sin\langle\theta\rangle$ is then described by the projection of $\mathbf{\Sigma}$ onto $\mathcal{G}_{\mathrm{EW}}$ with $f = |\mathbf{\Sigma}|$ being the breaking scale of $\mathcal{G} \to \mathcal{H}$. Throughout literature, the parameter

$$\xi = \frac{v^2}{f^2} = \sin^2\langle\theta\rangle \tag{2.1.6}$$

is used to describe the deviation of the CHM to the SM. For $\xi \sim 1$ the EWSB is maximal and the CHM effectively describes an TC-like theory. Due to $v \sim f$ this is excluded

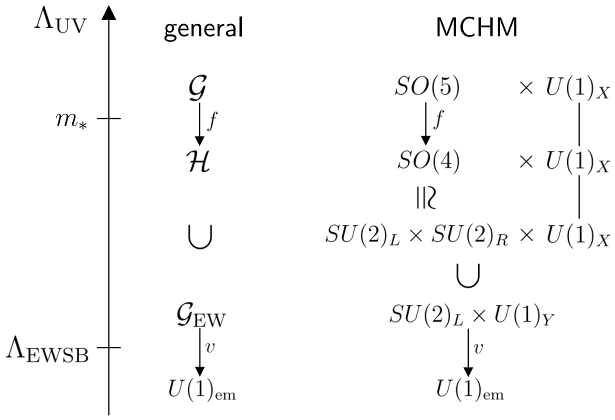

Figure 2.3: Symmetry breaking pattern of a general CHM setup (left) and explicitly of the MCHM (right) with $\mathcal{G} = SO(5) \times U(1)_X$, $\mathcal{H} = SO(4)$ and the EW symmetry $\mathcal{G}_{\mathrm{EW}} = SU(2)_L \times U(1)_Y$.

by experimental constraints as mentioned in Section 2.1.1. For $\xi \to 0$ at fixed v the composite sector is decoupled from the theory since $f \to \infty$ and the SM is recovered. Therefore, the interesting regime for CHMs is when $\xi \ll 1$ but not 0. Here, the vacuum misalignment leads to a sizable separation of scales between v and f. The smallness of ξ introduces a small amount of fine-tuning which has to be accepted for now. Considering current bounds on *Electroweak Precision Operators* (EWPOs) $\xi \lesssim 0.1$ is favored [68] demanding $f \gtrsim 800\,\mathrm{GeV}$.

2.2 The Minimal Composite Higgs Model

Now, the specific model which will be used throughout the rest of this thesis, will be introduced. For a more general approach to the subsequent discussion, the reader is redirected towards the followed review [47].

Amongst various other symmetry group configurations (e.g. [69–73] ; see again [66] for an overview) the MCHM, first introduced by K. Agashe, R. Contino and A. Pomarol [74], is the minimal realization of a CHM featuring custodial symmetry. It resembles a non-linear σ-model of the coset $SO(5)/SO(4)$ (see also [75]) and, as other theories with SSB, its dynamics can be described by the *Callan-Coleman-Wess-Zumino* (CCWZ) construction [76, 77]. The breaking pattern of the theory is visualized in Figure 2.3. Note that an additional $U(1)_X$ symmetry is needed in order to obtain the right quantum numbers for the SM fermions after breaking. However, it does not affect the subsequent discussion and will be omitted for now.

2.2.1 The Higgs of the SO(5)/SO(4) coset

The 10 generators of the fundamental **5** representation of $SO(5)$ can be parametrized in a decomposed way

$$T^a_{L,ij} = -\frac{i}{2}\left[\frac{1}{2}\varepsilon^{abc}(\delta^b_i\delta^c_j - \delta^b_j\delta^c_i) + (\delta^a_i\delta^4_j - \delta^a_j\delta^4_i)\right], \quad a = 1,2,3 \tag{2.2.1}$$

$$T^a_{R,ij} = -\frac{i}{2}\left[\frac{1}{2}\varepsilon^{abc}(\delta^b_i\delta^c_j - \delta^b_j\delta^c_i) - (\delta^a_i\delta^4_j - \delta^a_j\delta^4_i)\right], \quad a = 1,2,3 \tag{2.2.2}$$

$$\hat{T}^{\hat{a}}_{ij} = -\frac{i}{\sqrt{2}}\left[\delta^{\hat{a}}_i\delta^5_j - \delta^{\hat{a}}_j\delta^5_i\right], \quad \hat{a} = 1,2,3,4, \tag{2.2.3}$$

normalized to their Cartan-Killing inner product $\mathrm{tr}(T^\alpha T^\beta) = \delta^{\alpha\beta}$. The 6 generators T^a_L, T^a_R of $SU(2)_L$ and $SU(2)_R$, respectively, generate (reduced to 4×4 matrices) the fundamental **4** representation of the unbroken $SO(4)$ subgroup. This is possible because due to the isomorphism $SO(4) \cong SU(2)_L \times SU(2)_R$, both groups possess the same underlying algebra with the commutation relations $[T^a_L, T^b_R] = 0$, $[T^a_L, T^b_L] = i\varepsilon^{abc}T^c_L$ and $[T^a_R, T^b_R] = i\varepsilon^{abc}T^c_R$. The $\hat{T}^{\hat{a}}$ denote the 4 broken generators of the left coset $SO(5)/SO(4)$. Using

$$\mathbf{\Theta} = \frac{1}{\sqrt{2}}\big(i\sigma_\alpha\Pi^\alpha + \mathbb{1}_2\Pi^4\big), \quad \alpha = 1,2,3, \tag{2.2.4}$$

with σ_α being the Pauli-matrices, a real vector $\mathbf{\Pi}$ in the **4** of $SO(4)$ can be rewritten into a pseudo-real 2×2 matrix and thus into the $(\mathbf{2},\mathbf{2})$ representation of $SU(2)_L \times SU(2)_R$. Identifying the $SU(2)_L$ with the weak SM group and the third generator T^3_R of $SU(2)_R$ with the hypercharge Y of $U(1)_Y$, the SM Higgs doublet with hypercharge 1/2 is created out of the real fields via

$$\boldsymbol{H} = \begin{pmatrix} h_u \\ h_d \end{pmatrix} = \frac{1}{\sqrt{2}}\begin{pmatrix} \Pi^2 + i\Pi^1 \\ \Pi^4 - i\Pi^3 \end{pmatrix} \tag{2.2.5}$$

rewriting $\mathbf{\Theta} = (\boldsymbol{H}^c, \boldsymbol{H})$ with $\boldsymbol{H}^c = i\sigma^2\boldsymbol{H}^*$. As can be seen, the **4** representation of a real field decomposes under $\mathcal{G}_{\mathrm{EW}}$ into $\mathbf{4} = (\mathbf{2},\mathbf{2}) \to \mathbf{2}_{1/2}$ providing the right quantum numbers for the SM Higgs.

For illustration, it is useful to switch to a toy model here, where symmetry breaking is triggered by the VEV of a sigma field $\mathbf{\Phi}$ rather than a vacuum condensate of the composite sector as for realistic CHMs. Note that, although the fundamental mechanism of SSB is vastly different, most of the calculations are indeed similar, such that the presented σ-model can be seen as an analogy to the real CHM which might provide a more intuitive insight for the reader.

The general Lagrangian for a real scalar $SO(5)$ fiveplet $\mathbf{\Phi}$ reads

$$\mathcal{L}_s = \frac{1}{2}\partial_\mu\mathbf{\Phi}^T\partial^\mu\mathbf{\Phi} + \frac{g_*^2 f^2}{4}\mathbf{\Phi}^T\mathbf{\Phi} - \frac{g_*^2}{8}(\mathbf{\Phi}^T\mathbf{\Phi})^2, \tag{2.2.6}$$

with f still being the breaking scale and $g_* \in (1, 4\pi)$ corresponding to the coupling of the strong sector. Choosing a vacuum in agreement with the selection criteria of Eq. 2.1.4

$$\mathbf{\Phi_0} = \begin{pmatrix} \mathbf{0} \\ f \end{pmatrix}, \tag{2.2.7}$$

the fiveplet can be parametrized as

$$\mathbf{\Phi}(x) = e^{i\frac{\sqrt{2}}{f}\Pi_{\hat{a}}(x)\hat{T}^{\hat{a}}} \begin{pmatrix} \mathbf{0} \\ f + \sigma(x) \end{pmatrix} = (f + \sigma(x)) \begin{pmatrix} \sin\frac{\Pi}{f}\frac{\mathbf{\Pi}}{\Pi} \\ \cos\frac{\Pi}{f} \end{pmatrix}, \tag{2.2.8}$$

with $\sigma(x)$ being the radial and $\Pi_{\hat{a}}(x) \equiv \mathbf{\Pi}$ the angular components of an S^4 sphere embedded in a 5-dimensional space (speaking in the geometrical picture of Figure 2.2). The so-called *Goldstone matrix*

$$U[\mathbf{\Pi}] = e^{i\frac{\sqrt{2}}{f}\Pi_{\hat{a}}(x)\hat{T}^{\hat{a}}} = \begin{pmatrix} \mathbb{1}_4 - (1-\cos\frac{\Pi}{f})\frac{\mathbf{\Pi}\mathbf{\Pi}^T}{\Pi^2} & \sin\frac{\Pi}{f}\frac{\mathbf{\Pi}}{\Pi} \\ -\sin\frac{\Pi}{f}\frac{\mathbf{\Pi}^T}{\Pi} & \cos\frac{\Pi}{f} \end{pmatrix}, \tag{2.2.9}$$

with $\Pi = \sqrt{\mathbf{\Pi}^T\mathbf{\Pi}}$ is thereby at first sight a general element of the left-handed $SO(5)/SO(4)$ coset and can be derived for any $\mathcal{G} \to \mathcal{H}$ spontaneous breaking. The Lagrangian in this new parametrization reads

$$\begin{aligned}\mathcal{L}_s =& \frac{1}{2}\partial_\mu\sigma\partial^\mu\sigma - \frac{(g_*f)^2}{2}\sigma^2 - \frac{g_*^2 f}{2}\sigma^3 - \frac{g_*^2}{8}\sigma^4 \\ &+ \frac{1}{2}\left(1+\frac{\sigma}{f}\right)^2\left[\frac{f^2}{\Pi^2}\sin^2\frac{\Pi}{f}\partial_\mu\mathbf{\Pi}^T\partial^\mu\mathbf{\Pi} + \frac{f^2}{4\Pi^4}\left(\frac{\Pi^2}{f^2} - \sin^2\frac{\Pi}{f}\right)\partial_\mu\Pi^2\partial^\mu\Pi^2\right].\end{aligned} \tag{2.2.10}$$

As expected, $\mathcal{L}_s$ contains one massive *resonance* σ with a mass $m_* = g_* f$ corresponding to the confinement scale of the strong sector and four massless NGB fields $\Pi_{\hat{a}}$ which can be written in terms of the SM Higgs field of Eq. 2.2.5

$$\mathbf{\Pi} = \begin{pmatrix} \Pi_1 \\ \Pi_2 \\ \Pi_3 \\ \Pi_4 \end{pmatrix} = \frac{1}{\sqrt{2}} \begin{pmatrix} -i(h_u - h_u^\dagger) \\ h_u + h_u\dagger \\ i(h_d - h_d^\dagger) \\ h_d + h_d^\dagger \end{pmatrix}. \tag{2.2.11}$$

Note here, that the aforementioned field $\mathbf{\Sigma}$ is equivalent to the field $\mathbf{\Phi}$ where the resonance σ has been integrated out.

The Lagrangian is still invariant under $SO(4)$ which can be seen by performing a linear transformation of $\mathbf{\Pi}$ or $\mathbf{\Phi}$ along the unbroken generators of $SO(5)$

$$\mathbf{\Pi} \to e^{i\alpha_a t^a}\mathbf{\Pi} \quad \Leftrightarrow \quad \mathbf{\Phi} \to e^{i\alpha_a T^a}\mathbf{\Phi}, \tag{2.2.12}$$

where t^a are the generators of the fundamental **4** representation of $SO(4)$. Due to the spontaneous nature of the symmetry breaking, the Lagrangian is of course also invariant by transformations along the broken generators, but this invariance (symmetry) is realized in a *non-linear* way

$$\boldsymbol{\Pi} \to \boldsymbol{\Pi} + \Pi \cot \frac{\Pi}{f} \boldsymbol{\alpha} + \left(\frac{f}{\Pi} - \cot \frac{\Pi}{f} \right) (\boldsymbol{\alpha}^T \boldsymbol{\Pi}) \frac{\boldsymbol{\Pi}}{\Pi} \quad \Leftrightarrow \quad \boldsymbol{\Phi} \to \boldsymbol{\Phi} + i \alpha_{\hat{a}} \hat{T}^{\hat{a}} \boldsymbol{\Phi}. \tag{2.2.13}$$

Although phenomenologically different, the mechanism of symmetry breaking in this toy-model is analogous to the mechanism in a real CHM, to which is switched back, now.

2.2.2 Gauge couplings to the Higgs

EW interactions can be added to the theory by gauging the EW subgroup $\mathcal{G}_{\mathrm{EW}}$ of $SO(4)$. As mentioned earlier, the $SU(2)_L$ generators are identified with the SM ones using the third generator of $SU(2)_R$ to generate the hypercharge $U(1)_Y$. While the kinetic terms of the gauge fields are implemented in the usual way

$$\mathcal{L}_{\mathrm{kin}} = -\frac{1}{4} W^a_{\mu\nu} W^{a\mu\nu} - \frac{1}{4} B_{\mu\nu} B^{\mu\nu} \tag{2.2.14}$$

keeping the gauge self interactions SM-like at leading order in ξ, the covariant derivative of the $\boldsymbol{\Phi}$ field becomes

$$D_\mu \boldsymbol{\Phi} = \left(\partial_\mu - i g W^a_\mu T^a_L - i g' B_\mu T^3_R \right) \boldsymbol{\Phi}, \tag{2.2.15}$$

with g and g' labelling the electroweak SM couplings. While ignoring the resonance terms including σ for the moment, the Lagrangian of Eq. 2.2.10 yields

$$\mathcal{L}_s \supset \frac{f^2}{2H^2} \sin^2 \frac{\sqrt{2}H}{f} D_\mu \boldsymbol{H}^\dagger D^\mu \boldsymbol{H} + \frac{f^2}{8H^4} \left(2\frac{H^2}{f^2} - \sin^2 \frac{\sqrt{2}H}{f} \right) (\partial_\mu H^2)^2, \tag{2.2.16}$$

with $H = \sqrt{\boldsymbol{H}^\dagger \boldsymbol{H}}$ and

$$D_\mu \boldsymbol{H} = \left(\partial_\mu - i g W^a_\mu \frac{\sigma^a}{2} - i g' B_\mu \frac{\mathbb{1}}{2} \right) \boldsymbol{H}. \tag{2.2.17}$$

In unitary gauge the Higgs doublet can be rewritten in the usual way as

$$\boldsymbol{H} = \frac{1}{\sqrt{2}} \begin{pmatrix} 0 \\ \tilde{v} + h(x) \end{pmatrix}, \tag{2.2.18}$$

with $h(x)$ being the physical Higgs field and $\tilde{v}$ its VEV.[3] The Lagrangian rewrites into the simple form

$$\mathcal{L}_s \supset \frac{1}{2} (\partial h)^2 + \frac{g^2 f^2}{4} \sin^2 \left(\frac{\tilde{v} + h}{f} \right) \left(W^+_\mu W^{-\mu} + \frac{1}{2 c_W^2} Z_\mu Z^\mu \right), \tag{2.2.19}$$

[3] Note that due to vacuum misalignment, the SM Higgs VEV v is in CHMs just the breaking scale of the EW symmetry. It is connected to the Higgs VEV $\tilde{v}$ in CHMs via the breaking scale f as derived in the following.

with the $W^\pm$ and Z already in their mass eigenstates and $c_W = \cos\theta_W = g/\sqrt{g^2+g'^2}$ the cosine of the Weinberg angle. One can see from this equation that the W and Z already have the right SM masses $m_W = c_W m_Z = \frac{1}{2} g f \sin\frac{\tilde{v}}{f} \equiv \frac{1}{2} g v$, thus leaving the experimentally well tested ρ parameter

$$\rho = \frac{m_W^2}{c_W^2 m_Z^2} = 1 \tag{2.2.20}$$

unaltered at tree level. This does not happen by accident but due to custodial protection within the model. The appearance of the Higgs VEV $\tilde{v}$ breaks the $SO(4)$ spontaneously into the custodial symmetry $SO(3)_{\text{cust}}$ which is sufficient to generate the right ratio between the $W^\pm$ and Z boson masses (see [78] for the general mechanism). The relation between the scales for this model is given by

$$\xi = \frac{v^2}{f^2} = \sin^2\frac{\tilde{v}}{f}. \tag{2.2.21}$$

By performing a Taylor expansion around $h = 0$ in the sine of the Lagrangian one can derive deviations from the gauge boson to Higgs couplings

$$\begin{aligned}\mathcal{L}_s \supset &\left[1 + 2\sqrt{1-\xi}\frac{h}{v} + (1-2\xi)\frac{h^2}{v^2} - \frac{4}{3}\xi\sqrt{1-\xi}\frac{h^3}{v^3} + \ldots\right] \\ &\cdot \left(m_W^2 W_\mu^+ W^{-\mu} + \frac{1}{2} m_Z^2 Z_\mu Z^\mu\right),\end{aligned} \tag{2.2.22}$$

which yield for the one- and two-Higgs couplings

$$\frac{g_{hVV}^{\text{MCHM}}}{g_{hVV}^{\text{SM}}} = \sqrt{1-\xi}, \quad \frac{g_{hhVV}^{\text{MCHM}}}{g_{hhVV}^{\text{SM}}} = 1 - 2\xi. \tag{2.2.23}$$

Unlike in the SM there is also an infinite set of higher order couplings present which is expressed by $d > 4$ operators. The deviations in Eq. 2.2.23 as well as the higher order terms in Eq. 2.2.22 vanish in the SM limit $\xi \to 0$ for fixed v.

2.2.3 Fermionic couplings to the Higgs

Adding SM fermions with realistic coupling strengths to CHMs is realized by a mechanism called *partial compositeness* [79], which also solves the *flavor puzzle* (i.e. the question of large hierarchies between the fermionic Yukawa couplings) in the SM.

Unlike in TC models [30, 67], the elementary fermions in CHMs are coupled linearly to the composite sector

$$\mathcal{L}_{\text{int}} = \frac{\lambda_{t_L}}{\Lambda_{\text{UV}}^{d_L - \frac{5}{2}}} \bar{q}_L \mathcal{O}_F^L + \frac{\lambda_{t_R}}{\Lambda_{\text{UV}}^{d_R - \frac{5}{2}}} \bar{t}_R \mathcal{O}_F^R + \ldots\,, \tag{2.2.24}$$

with $q_L = (t_L, b_L)^T$, t_R being usual SM fermions and $\mathcal{O}_F^{L,R}$ fermionic operators of the composite sector with dim $[\mathcal{O}_F^{L,R}] = d_{L,R}$. As one can see, these interactions are generated

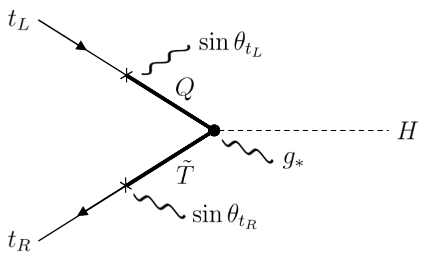

Figure 2.4: Yukawa diagram for a partially composite top-quark mixing with its partners. It is assumed here, that there are no ways for elementary fermions to interact directly with the Higgs particle.

at a high scale Λ_{UV} such that, for following considerations, the full $SO(5)$ theory has to be taken into account. The couplings $\lambda_{t_{L,R}}$ evolve down to the confinement scale via

$$\lambda_{t_{L,R}}(m_*) \simeq \lambda_{t_{L,R}} \left(\frac{m_*}{\Lambda_{\text{UV}}}\right)^{d_{L,R}-\frac{5}{2}} \tag{2.2.25}$$

leading to the low energy Lagrangian

$$\mathcal{L}_{\text{int}} = \lambda_{t_L} \bar{q}_L \mathcal{O}_F^L + \lambda_{t_R} \bar{t}_R \mathcal{O}_F^R + \ldots \,, \tag{2.2.26}$$

where the $\lambda_{t_{L,R}}(m_*) \equiv \lambda_{t_{L,R}}$ are redefined and the dimensional corrections in powers of m_* absorbed into the fermionic operators. As mentioned earlier, this setup has two advantages. Firstly, no hierarchy issue arises, since the $\lambda_{t_{L,R}}$ can be kept at $\mathcal{O}(1)$ with $d_{L,R} \gtrsim 5/2$. Secondly, small deviations of the λ's for the different fermions at $\mathcal{O}(1)$ level at Λ_{UV} scale can lead, due to different operator dimensions in Eq. 2.2.25, to great discrepancies at EW scale, giving a natural explanation for the hierarchies among the fermionic couplings.

Due to the linear couplings in Eq. 2.2.26 there will be mixing between the elementary fields and composite resonances at scale m_*. The resulting physical fermion fields will thus be "partially composite"

$$|\text{Phys.}\rangle_i = \cos\theta_i \,|\text{Elem.}\rangle_i + \sin\theta_i \,|\text{Comp.}\rangle_i \,, \tag{2.2.27}$$

which explains the naming of the mechanism. Note that the composite states are excited by the local gauge invariant operators $\mathcal{O}_F^{L,R}$, each of which is expected to have at least one resonance. Therefore, one can identify fermionic composite fields like Q and $\tilde{T}$ yielding

$$\langle 0|\mathcal{O}_F^L|Q\rangle \neq 0, \quad \langle 0|\mathcal{O}_F^R|\tilde{T}\rangle \neq 0, \tag{2.2.28}$$

with each fermionic operator $\mathcal{O}_F^{L,R}$ for each family. These fields embed resonances with quantum numbers identical to the SM fields, which are called *partners* to the respective SM particles. They are usually embedded in representations of the full group $\mathcal{G}$, have Dirac mass terms (i.e. they are vector-like, because both chiralities have the same quantum numbers) and are charged under the QCD symmetry. The latter is necessary, because otherwise the interaction terms with the SM fermions would break QCD which is contradictory to the observation of an exact global (and local) $SU(3)_c$ symmetry realized in nature. A possible mass Lagrangian for the top-top partner system would look like [47]

$$\mathcal{L}^{t,L}_{\text{Mass}} \simeq -m_* \bar{Q}Q - \frac{\lambda_{t_L} m_*}{g_*}(\bar{q}_L Q + h.c.), \quad \mathcal{L}^{t,R}_{\text{Mass}} \simeq -m_* \bar{\tilde{T}}\tilde{T} - \frac{\lambda_{t_R} m_*}{g_*}(\bar{t}_R \tilde{T} + h.c.). \tag{2.2.29}$$

As pictured in Figure 2.4, the top partners Q and $\tilde{T}$ also couple to the Higgs with coupling strength g_*. The general SM Yukawa coupling for the top-quark thus scales with

$$y_t = g_* \sin\theta_{t_L} \sin\theta_{t_R} \simeq \frac{\lambda_{t_L}\lambda_{t_R}}{g_*}. \tag{2.2.30}$$

Note that Eq. 2.2.29 is a simplicifaction, i.e. m_* should be seen as a scale and e.g. contains Dirac and Yukawa terms of the composite resonances in the first two terms. Furthermore, it is assumed here, that the SM fermions do not directly couple to the Higgs field (i.e. that there are no Yukawa terms present for the elementary particles) in order to prevent possible large *Flavor Changing Neutral Currents* (FCNCs). The full fermionic Lagrangian and, therefore, the modified couplings and masses of the fermions are not only dependent on the general model but also on the embedding of the fermions within the model.

Nevertheless, one can see from this example that the masses of the SM fermions highly depend on the couplings λ_f to their partners. The greater the coupling, i.e. the more "composite" the physical SM fields are, the heavier are they. This also means, that the fermions of the third family will have the greatest impact on the breaking of $SO(5)$. To simplify the calculations it thus makes sense from now on to consider the top quark only, namely q_L and t_R, which give the leading contribution to the Higgs mass.

In $SO(5)$ the most general top mass Lagrangian which can be written down yields [45]

$$\begin{aligned}\mathcal{L}^t_{\text{Mass}} = \text{tr}\Bigg[&- \sum_{r,r'=T,t} m_{r,r'} \bar{\Psi}^r_L \Psi^{r'}_R - f \sum_{i=1}^{n} \sum_{r,r'=T,t} Y_i^{r,r'} \bar{\Psi}^r_L g_i^{r,r'}(\mathbf{\Sigma}/f)\Psi^{r'}_R \\ &- \lambda_{t_L} f \bar{q}_L \Delta_L \Psi^T_R - \lambda_{t_R} f \bar{t}_R \Delta_R \Psi^t_L \Bigg] + h.c., \end{aligned} \tag{2.2.31}$$

where Ψ^T and Ψ^t are the two vector-like resonances which contain the partners for q_L and t_R. They have Dirac masses and possible mixings $m_{r,r'}$. The $\Delta_{L,R}$ are matrices which ensure that the SM fermions couple to their partners with the same SM quantum numbers within the composite resonances, leaving the Lagrangian invariant under $\mathcal{G}_{\text{EW}}$. Finally, the $\bar{\Psi}^r_L g_i^{r,r'}(\mathbf{\Sigma}/f)\Psi^{r'}_R$ term describes all combinations which can be formed out of the bilinear compounds of the resonances $\bar{\Psi}^T_L$ and Ψ^T_R with non-trivial functions of $\mathbf{\Sigma} = fU_{I5}$, $I = 1, ..., 5$. These terms are invariant under $SO(5)$ and depend on the particular representation of this symmetry group. The $Y_i^{r,r'}$ correspond to the Yukawa couplings of the strong sector.

2.2.4 The MCHM$_5$

Throughout this thesis, only the case where the fermions and their partners are embedded in the fundamental **5** representation of $SO(5)$ is considered [80]. This sub-model is labelled MCHM$_5$. Other possible representations are e.g. the spinorial **4**, the **10** or the **14**.

As mentioned earlier in this section, $SO(5)$ as such does not have a representation which decomposes with the right $SU(2)_L \times U(1)_Y$ charges $2_{1/6}$, $1_{2/3}$ and $1_{-1/3}$ under $\mathcal{G}_{\mathrm{EW}}$ in order to form multiplets of the fermionic partners. Therefore one has to add an additional charge $U(1)_X$ as pictured in Figure 2.3. Bosonic fields such as the Higgs and the gauge bosons are neutral under $U(1)_X$. Therefore, their dynamics, discussed in Section 2.2.1 and 2.2.2, do not change. The $U(1)_X$ does affect fermion couplings because it adds a new gauge field X_μ changing the hypercharge to $Y = T^3_R + X$.[4] For the MCHM$_5$, $X = 2/3$ can be chosen under which the fermionic composite multiplets are charged. The decomposition from $SO(5)$ to $SO(4)$ to $\mathcal{G}_{\mathrm{EW}} \equiv SU(2)_L \times U(1)_Y$ yields

$$\mathbf{5}_{2/3} \to \mathbf{4}_{2/3} \oplus \mathbf{1}_{2/3} \to \mathbf{2}_{7/6} \oplus \mathbf{2}_{1/6} \oplus \mathbf{1}_{2/3}, \tag{2.2.32}$$

where the latter two can couple to the left- and right-handed up-type fermions of the SM. To obtain $\mathbf{2}_{1/6} \oplus \mathbf{1}_{-1/3}$ needed to couple to left- and right-handed down-type fermions one would start with $X = -1/3$ instead.

A multiplet in the fundamental **5** representation of $SO(5)$ in the basis of the generators in Eq. 2.2.1 and 2.2.2 can be constructed by summing over the eigenvectors of the $T^3_{L,R}$

$$\mathbf{5} = \frac{1}{\sqrt{2}} \begin{pmatrix} q_{--} - q_{++} \\ -i(q_{--} + q_{++}) \\ q_{+-} + q_{-+} \\ i(q_{+-} - q_{-+}) \\ -i\sqrt{2} q_{00} \end{pmatrix}, \tag{2.2.33}$$

where the $\pm$ denote their eigenvalue/charge under $SU(2)_{L,R}$ ($T^3_{L,R} = \pm 1/2$). The q_{00} remains uncharged. It can be seen, that the **5** consists of a bidoublet $(\mathbf{2}, \mathbf{2})$ and a singlet $(\mathbf{1}, \mathbf{1})$ of $SU(2)_L \times SU(2)_R$.

Following [45], the mass Lagrangian for the MCHM$_5$ is designed as follows. Starting with Eq. 2.2.31 one first decomposes, as pictured in Eq. 2.2.32, the general resonance fields Ψ^T and Ψ^t, which are multiplets of the $\mathbf{5}_{2/3}$ of $SO(5) \times U(1)_X$ into the $\mathbf{4}_{2/3} \oplus \mathbf{1}_{2/3}$ of $SO(4) \times U(1)_X$ by transformation with the Goldstone matrix $U[\Pi]$

$$\Psi^{T,t} = U[\mathbf{\Pi}] \begin{pmatrix} Q^{T,t} \\ \tilde{T}^{T,t} \end{pmatrix}, \quad Q^{T,t} \in \mathbf{4}_{2/3}, \quad \tilde{T}^{T,t} \in \mathbf{1}_{2/3}. \tag{2.2.34}$$

Note that the $U[\Pi]$ is fully determined by the choice of the model (MCHM in this case).

[4] The resulting gauge fields as well as the breaking pattern will be discussed later when dealing with the 5D theory.

In unitary gauge, it yields

$$U[\mathbf{\Pi}] = \begin{pmatrix} 1 & 0 & 0 & 0 & 0 \\ 0 & 1 & 0 & 0 & 0 \\ 0 & 0 & 1 & 0 & 0 \\ 0 & 0 & 0 & \cos\left(\frac{\tilde{v}+h}{f}\right) & \sin\left(\frac{\tilde{v}+h}{f}\right) \\ 0 & 0 & 0 & -\sin\left(\frac{\tilde{v}+h}{f}\right) & \cos\left(\frac{\tilde{v}+h}{f}\right) \end{pmatrix}, \tag{2.2.35}$$

where $\mathbf{\Pi}$ is defined as in Eq. 2.2.11 and $\boldsymbol{H}$ as in Eq. 2.2.18. For the MCHM$_5$ the only bilinear term ($n = 1$) of the resonance fields is

$$\begin{aligned} \bar{\Psi}^r_L g_1^{r,r'} \Psi^{r'}_R &= \bar{\Psi}^r_L \frac{\Sigma\Sigma^T}{f^2} \Psi^{r'}_R = \bar{\Psi}^r_L U_{I5} (U_{I5})^T \Psi^{r'}_R \\ &= \left(\bar{Q}^r, \bar{\tilde{T}}^r\right) \left[U^\dagger (U_{I5}(U_{I5})^T) U\right] \begin{pmatrix} Q^{r'} \\ \tilde{T}^{r'} \end{pmatrix} = \bar{\tilde{T}}^r \tilde{T}^{r'} \end{aligned} \tag{2.2.36}$$

such that the Yukawa couplings of the composite fields can be absorbed into the masses of the singlets $\tilde{m}_{rr'} = m_{rr'} + f\ Y_1^{rr'}$.

The MCHM$_5$ mass Lagrangian becomes

$$\begin{aligned} \mathcal{L}_M^{\mathrm{MCHM}_5} = &- \sum_{r,r'=T,t} \left(m_{rr'} \bar{Q}^r_L Q^{r'}_R + \tilde{m}_{rr'} \bar{\tilde{T}}^r_L \tilde{T}^{r'}_R \right) - \lambda_{t_L} f (\bar{q}_L \Delta_L)_I \Big(U_{Ii} Q^{T\,i}_R \\ &+ U_{I5} \tilde{T}^T_R \Big) - \lambda_{t_R} f (\bar{t}_R \Delta_R)_I \Big(U_{Ii} Q^{t\ i}_L + U_{I5} \tilde{T}^t_L \Big) + h.c.\ , \end{aligned} \tag{2.2.37}$$

where $I = 1, ..., 5,\ i = 1, ..., 4$. The Q^T and $\tilde{T}^t$, which have been introduced in order to map this Lagrangian properly to the 5D theory elucidated in Section 2.3 and 2.4, are now integrated out arriving at the low energy effective Lagrangian for the top mass mixing

$$\begin{aligned} \mathcal{L}_{\mathrm{Mass}}^{\mathrm{MCHM}_5} = &- m_Q \bar{Q}_L Q_R - \tilde{m}_T \bar{\tilde{T}}_L \tilde{T}_R - y_{t_L} f (\bar{q}_L \Delta_L)_I \big(a_L U_{Ii} Q^i_R + b_L U_{I5} \tilde{T}_R \big) \\ &- y_{t_R} f (\bar{t}_R \Delta_R)_I \big(a_R U_{Ii} Q^i_L + b_R U_{I5} \tilde{T}_L \big) + h.c.\ , \end{aligned} \tag{2.2.38}$$

where $m_Q \equiv m_{tt}$, $\tilde{m}_T \equiv \tilde{m}_{TT}$, $\tilde{T} \equiv \tilde{T}^T$ and $Q \equiv Q^t$. By integrating out Q^T ($\tilde{T}^t$) a factor $a_L = -m_{Tt}/m_{TT}\ b_L$ ($b_R = -(\tilde{m}_{Tt}/\tilde{m}_{tt})^*\ a_R$) is introduced as well as a factor b_L (a_R) for convenience by defining $y_{t_L} = \lambda_{t_L}/b_L$ ($y_{t_R} = \lambda_{t_R}/a_R$) [44] (see Appendix A.1 for a full derivation).

In order to define the exact form of the $\Delta_{L,R}$ matrices, one conceives of the resonances Q and $\tilde{T}$ to live in the same multiplet by setting $T = t$.[5] Using Eq. 2.2.33, top partners

[5] If this had been done in the very beginning considering an additional term which can be found in [45], one would have arrived at the very same Eq. 2.2.38. However, the analogy to the 5D picture, which will be discussed in the following, would have been lost.

$(T, B) \leftrightarrow q_L$ and $\tilde{T} \leftrightarrow t_R$ can be identified within the resonances

$$\begin{pmatrix} Q \\ \tilde{T} \end{pmatrix} \equiv \frac{1}{\sqrt{2}} \begin{pmatrix} B - X_{5/3} \\ -i(B + X_{5/3}) \\ T + X_{2/3} \\ i(T - X_{2/3}) \\ -i\sqrt{2}\tilde{T} \end{pmatrix}, \tag{2.2.39}$$

whereas $(X_{5/3}, X_{2/3})$ is another doublet belonging to the $\mathbf{2}_{7/6}$ in the $\mathcal{G}_{\mathrm{EW}}$ decomposition of Eq. 2.2.34 (the subscripts denote their $U(1)_{\mathrm{em}}$ charges). Therefore, the $\Delta_{L,R}$ yield

$$\Delta_L = \frac{1}{\sqrt{2}} \begin{pmatrix} 0 & 0 & 1 & -i & 0 \\ 1 & i & 0 & 0 & 0 \end{pmatrix}, \quad \Delta_R = \begin{pmatrix} 0 & 0 & 0 & 0 & i \end{pmatrix}. \tag{2.2.40}$$

2.2.5 Softened Goldstone symmetry breaking - the sMCHM$_5$

Keeping the mass of the Higgs particle small requires the top partners in minimal models to be light. The reason behind is the proportionality of the Higgs mass to the strength of the Goldstone symmetry breaking parameters $y_{t_{L,R}}$ [80–83]. As estimated before in Eq. 2.2.30, the top Yukawa coupling in the MCHM$_5$ [44, 45]

$$y_t \simeq \frac{\left| b_L^* b_R m_Q^* - a_L^* a_R \tilde{m}_T^* \right|}{2\sqrt{2}|a_L||b_R|f} \sin\theta_{t_L} \sin\theta_{t_R} \simeq \frac{y_{t_L} y_{t_R} f}{m_l} \sim \frac{y^2 f}{m_l} \tag{2.2.41}$$

scales anti-proportionally to the mass of the lightest top partner $m_l = \min\{m_Q, \tilde{m}_T\}$. The first equity just resembles Eq. 2.2.30, where one can assume the a_L, b_R as well as the a_R, b_L parameters to be naturally of $\mathcal{O}(1)$ such that the first term reduces to $g_* \simeq \max\{m_Q, \tilde{m}_T\}/f$. For the second equity, the correlations $\sin\theta_{t_L} = |a_L| y_{t_L} f/m_Q$ and $\sin\theta_{t_R} = |b_R| y_{t_R} f/\tilde{m}_T$, which can be derived from diagonalization of the mass terms, have been used. Moreover, in the last step a similar size for the right- and left-handed mixings $y_{t_L} \sim y_{t_R} \equiv y$ has been assumed.

From Eq. 2.2.41 it is evident that for large top partner masses, one needs large left- and right-handed top-top partner mixings in order to keep the SM top quark $m_t = y_t v$ sufficiently heavy. Since these mixings also encode the explicit symmetry breaking which creates the Higgs mass, a variation of y_{t_L} and y_{t_R} will have an effect on the m_H parameter as well. The correlation between y and m_H can be derived by looking at the characteristic Higgs potential in the MCHM

$$V(h) = -\alpha s_h^2 + \beta s_h^4, \quad s_h^2 \equiv \sin^2\left(\frac{\tilde{v} + h}{f}\right) \tag{2.2.42}$$

which is derived explicitly later for the 5D theory with coefficients $\alpha, \beta > 0$.[6] The Higgs mass corresponds to the second derivative of the potential at $h = 0$. Plugging in the

[6]The constraint $\alpha, \beta > 0$ is necessary to form a SM-like Higgs potential and thereby trigger EWSB.

minimum condition at this point, $\alpha = 2\beta\xi$, with ξ defined in Eq. 2.2.21, one obtains

$$m_H^2 = \frac{8\beta}{f^2}\xi(1-\xi) \propto \frac{\beta}{f^2}\xi \tag{2.2.43}$$

up to leading order in ξ. Performing a "spurion analysis" (which will be explained in more detail later) to estimate the contributions to the Higgs potential, it becomes clear that β scales with $y^4 f^4$ (see again [44] for an explicit calculation). Substituting $\xi = v^2/f^2$ and inserting Eq. 2.2.41 into Eq. 2.2.43, one obtains

$$m_H \propto y^2 v \sim \frac{m_l}{f} m_t. \tag{2.2.44}$$

It is evident from this formula, that for a fixed top mass m_t and breaking scale f, the mass of the Higgs boson is proportional to the mass of the top partners. Therefore, a light Higgs mass around 125 GeV requires also the top partners to be light ($\sim$ 600 GeV for $f \sim$ 800 GeV and $m_t \sim$ 170 GeV). Unfortunately, as already discussed in the beginning (see Figure 1.1), light top partners are in tension with the exclusion limits from the LHC. One possibility to circumvent this difficult situation is by changing the nature of the breaking of the Goldstone symmetry as recently proposed by S. Blasi and F. Goertz [46]. One can easily see from Eq. 2.2.38 that the mixing terms of the elementary particles with their partners break $SO(5)$ symmetry because the former do not fill up a full **5** multiplet of $SO(5)$. This can be changed by introducing new vector-like elementary fermions, namely the two doublets v, w and the singlet s such that

$$\psi_L = \frac{1}{\sqrt{2}}\begin{pmatrix} b_L - w_{L1} \\ -i(b_L + w_{L1}) \\ t_L + w_{L2} \\ i(t_L - w_{L2}) \\ -i\sqrt{2}s_L \end{pmatrix}, \quad \psi_R = \frac{1}{\sqrt{2}}\begin{pmatrix} v_{R2} - w_{R1} \\ -i(v_{R2} + w_{R1}) \\ v_{R1} + w_{R2} \\ i(v_{R1} - w_{R2}) \\ -i\sqrt{2}t_R \end{pmatrix}. \tag{2.2.45}$$

The new mass mixing Lagrangian

$$\begin{aligned}\mathcal{L}_{\text{Mass}}^{\text{sMCHM}_5} =& - m_Q \bar{Q}_L Q_R - \tilde{m}_T \bar{\tilde{T}}_L \tilde{T}_R - y_{t_L} f \bar{\psi}_{LI}\big(a_L U_{Ii} Q_R^i + b_L U_{I5}\tilde{T}_R\big) \\ & - y_{t_R} f \bar{\psi}_{RI}\big(a_R U_{Ii} Q_L^i + b_R U_{I5}\tilde{T}_L\big) + h.c. \end{aligned} \tag{2.2.46}$$

is now invariant under $SO(5)$. Meanwhile, the explicit breaking is shifted towards the elementary sector only by the introduction of vector-like mass terms for the new particles

$$\begin{aligned}\mathcal{L}_{\text{el}}^{\text{sMCHM}_5} =& - m_w(\bar{w}_L w_R + \bar{w}_R w_L) - m_v(\bar{v}_L v_R + \bar{v}_R v_L) - m_s(\bar{s}_L s_R + \bar{s}_R s_L) \\ & - (m_1 \bar{s}_L t_R + m_2 \bar{q}_L v_R + h.c.). \end{aligned} \tag{2.2.47}$$

Note that in general v_R and s_L can mix with the SM fields because they have the same quantum numbers. This is accounted for by the mass mixing parameters m_1 and m_2.[7] It is evident that unlike in Eq. 2.2.38, the mixing terms between the SM fields and the

[7] However, for simplicity it is assumed $m_1 = m_2 = 0$ in the following.

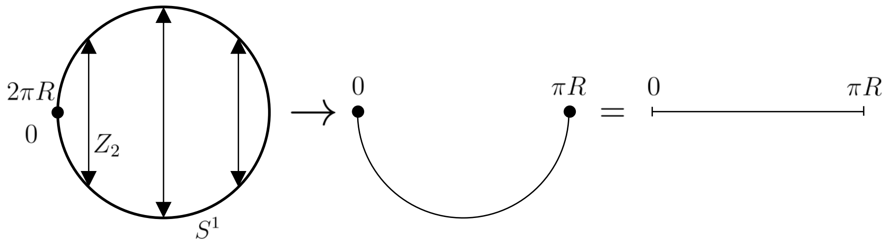

Figure 2.5: Sketch of an orbifold denoted by S^1/Z_2 which can be mapped to a line segment $[0, \pi R]$.

composite resonances in the mass Lagrangian in Eq. 2.2.46 emerging from the UV theory, do not break the $SO(5)$ global symmetry any longer. Instead, the symmetry breaking scales now with the vector-like mass terms of Eq. 2.2.47, a mechanism usually referred to as "soft" breaking. Since the breaking mechanism is changed, the proportionality argument of Eq. 2.2.44 does not hold any longer. As one can see in detail below, it becomes possible to raise the top partner masses while keeping the Higgs light without raising the scale f. Taking $m_s, m_v, m_w \to \infty$ decouples the vector-like particles and recovers the scenario displayed in the MCHM_5.

2.3 The holographic dual in 5 dimensions

The Composite Higgs setup in 4 dimensions works fine in the low energy regime and even calculations of form factors and the Higgs potential become possible by discretizing the spectrum (so-called *multisite-models*; see e.g. [65]). However, a potential shortcoming of Composite Higgs models in 4D is that the UV physics is fully parametrized by free parameters which leads to a reduced predictability.

Another, at first sight completely different approach which contains more of the UV structure are 5D *holographic* models on an AdS space. These are connected to the 4D theory by the famous AdS/CFT duality, first realized by J. Maldacena [84] for symmetry groups of large N, and give explicit, analytical results for the Higgs potential and other observables. In order to embed the 4D sMCHM_5 approach consistently into the 5D framework which will used as the underlying theory for numerical scans later, it is useful to look at general properties of these 5D models first and how they translate through this duality.

2.3.1 Kaluza-Klein decomposition on a flat 5D spacetime

Let us start on a 5D Minkowski spacetime

$$\mathrm{d}s^2 = \eta_{MN} \mathrm{d}x^M \mathrm{d}x^N, \tag{2.3.1}$$

with $\eta_{MN} = (+,-,-,-,-)$ signature and $M, N = \mu, 5$, where the μ describe the normal 4D Minkowski coordinates.[8] The fifth dimension is compact and defined via the *orbifold* S^1/Z_2 illustrated in Figure 2.5. Generally speaking, an orbifold is a circle S^1 with radius R where the opposite ends are identified with each other by a Z_2 symmetry. This can be expressed in terms of x^5 by the mappings

$$x^5 \to 2\pi R + x^5, \quad x^5 \to 2\pi R - x^5. \tag{2.3.2}$$

Only considering the unique physical points, a line segment of length $L = \pi R$ with $x^5 \in [0, L]$ is obtained.

The action for a scalar particle $\Phi(x, x^5)$ with mass m on this manifold would look like

$$S_\Phi = \frac{1}{2} \int \mathrm{d}^4x \int_0^L \mathrm{d}x^5 \Big[\partial_M \Phi(x, x^5) \partial^M \Phi(x, x^5) - m^2 \Phi^2(x, x^5)\Big]. \tag{2.3.3}$$

While trying to derive the equations of motion via the variational principle

$$\delta S_\Phi = \int \mathrm{d}^4x \int_0^L \mathrm{d}x^5 \Big[m^2 \Phi(x, x^5) - \partial_M \partial^M \Phi(x, x^5)\Big] \delta\Phi + \int \mathrm{d}^4x \Big[\partial_5 \Phi \delta\Phi\Big]_0^L, \tag{2.3.4}$$

it is clear that *Boundary Conditions* (BCs) on the fields for $x^5 \in \{0, L\}$ have to be imposed such that the variation of the action also vanishes on these boundaries. The BCs have to be constructed such that the second term in equation 2.3.4 disappears. The easiest options which fulfill this constraint

$$\Phi(x, x^5 \in \{0, L\}) = 0, \quad \partial_5 \Phi(x, x^5 \in \{0, L\}) = 0 \tag{2.3.5}$$

are the well-known Dirichlet and Neumann BCs. In fact, the Dirichlet BCs lead to hard symmetry breaking because $\delta\Phi = 0$ has to be imposed. However, they can be softened by inducing mass terms $M_{1,2}$ on the boundaries, deriving the needed conditions and taking $M_{1,2} \to \infty$ in the end. This will also break the symmetry, but in a smoother way. For an explicit derivation the reader is referred to Section 2.3.4. Note, that these boundary conditions correspond to 2 degrees of freedom for each 5D field which can be chosen freely.

A 5D scalar theory can be mapped onto 4D by a technique introduced by Kaluza [85] and Klein [86] in 1921 (1926). Due to the compactness of the fifth dimension it is possible to decompose the scalar field by a Fourier series

$$\Phi(x, x^5) = \sum_{n=0}^{\infty} \phi_n(x) f_n(x^5), \tag{2.3.6}$$

where the fields f_n form a complete orthonormal set of functions on $[0, L]$ with orthonormalization conditions

$$\int_0^L \mathrm{d}x^5 f_m(x^5) f_n(x^5) = \delta_{mn}. \tag{2.3.7}$$

[8] From now on roman capital letters for 5D coordinates and small greek letters for coordinates in 4D will be used.

Table 2.1: Orthonormal basis $\{f_n\}$ for a single scalar KK theory on the interval $[0, L]$ for different choices of the BCs at $x^5 = 0$ (columns) and $x^5 = L$ (rows). The $(+)/(-)$ denote Neumann/Dirichlet BCs. Note that $n \in \mathbb{N}_0$ for $(+,+)$ and $n \in \mathbb{N}$ for the other combinations of BCs.

BCs	$(+,*)$	$(-,*)$
$(*,+)$	$\sqrt{\frac{2-\delta_{n0}}{L}}\cos\left(\frac{n\pi}{L}x^5\right)$	$\sqrt{\frac{2}{L}}\sin\left((n-\frac{1}{2})\frac{\pi}{L}x^5\right)$
$(*,-)$	$\sqrt{\frac{2}{L}}\cos\left((n-\frac{1}{2})\frac{\pi}{L}x^5\right)$	$\sqrt{\frac{2}{L}}\sin\left(\frac{n\pi}{L}x^5\right)$

A convenient choice for this basis that solves the equations of motion is

$$f_n(x^5) = A_n \cos\big(w_n x^5\big) + B_n \sin\big(w_n x^5\big), \tag{2.3.8}$$

with

$$f_n''(x^5) = -w_n^2 f_n(x^5). \tag{2.3.9}$$

The parameters A_n, B_n and w_n are fixed by Eq. 2.3.7 and the BCs which translate to the f_n fields like

$$f_n'(x_i^5) = 0 \;\; \text{Neumann } (+), \quad f_n(x_i^5) = 0 \;\; \text{Dirichlet } (-), \tag{2.3.10}$$

with $x_i^5 \in \{0, L\}$. The 4 possible solutions are given in Table 2.1 where the $(\pm)$ denote the chosen BCs at $x^5 = 0$ and $x^5 = L$. Inserting Eq. 2.3.6 into S_Φ and using the properties of the f_n one obtains

$$\begin{aligned} S_\Phi =& \frac{1}{2}\int \mathrm{d}^4x \sum_n \Big[\partial_\mu\phi_n(x)\partial^\mu\phi_n(x) - m^2\phi_n^2(x)\Big] \\ &+ \frac{1}{2}\int \mathrm{d}^4x \int_0^L \mathrm{d}x^5 \sum_{m,n} \phi_m(x)\phi_n(x) f_m(x^5) f_n''(x^5) \\ &- \frac{1}{2}\int \mathrm{d}^4x \sum_{m,n} \phi_m(x)\phi_n(x)\Big[f_m(R)f_n'(R) - f_m(0)f_n'(0)\Big] \\ =& \frac{1}{2}\int \mathrm{d}^4x \sum_n \Big[\partial_\mu\phi_n(x)\partial^\mu\phi_n(x) - m_n^2\phi_n^2(x)\Big], \end{aligned} \tag{2.3.11}$$

where $m_n^2 = m^2 + w_n^2$.

As can be seen, the scalar theory of a 5D field $\Phi(x, x^5)$ with mass m has been traded for a 4D theory of infinitely many scalars $\phi_n(x)$ with increasing masses m_n. These 4D scalars ϕ_n are called *Kaluza-Klein* or KK-*modes* and the set of possible masses $\{m_n\}$ is a KK-*tower*. Just considering the $n = 0$ state corresponds to a low energy theory at tree level like the SM Lagrangian. Depending on the 5D fields, the higher order mass terms

$n > 1$ in the model considered below are either "unphysical" and thus can be gauged away (as for the Higgs) or correspond to resonances of a strongly interacting 4D theory (as for the fermion fields).

For a vanishing 5D mass $m = 0$ the m_n are equidistantly distributed. It is evident from Table 2.1 that there exists in this case a massless 4D state ϕ_0 called *zero-mode* only for the $(+,+)$ BCs. This will become very important in the following discussion.

2.3.2 Symmetry reduction on the branes

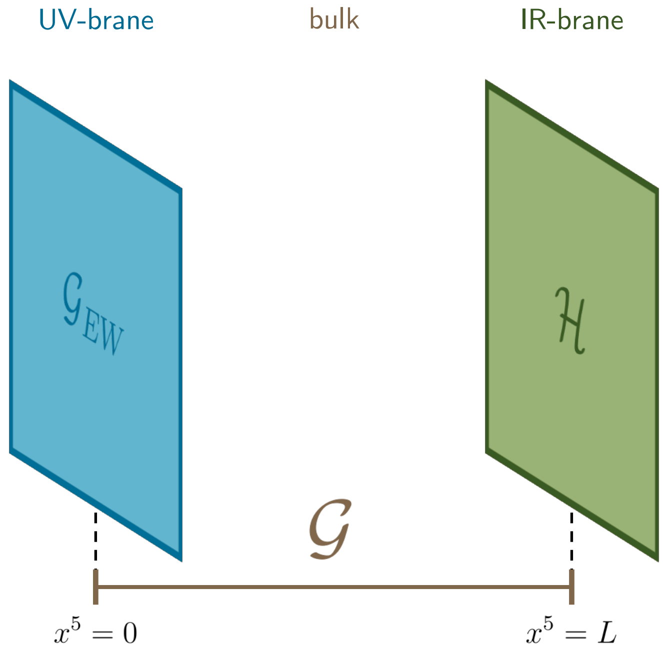

Figure 2.6: Illustration of a compact AdS_5 space with length L. The space on the interval $(0, L)$, called bulk, is 5-dimensional while the two planes, labelled as UV- and IR-brane, represent 4D manifolds at the boundaries of the 5D space. The symmetry $\mathcal{G}$ on the bulk is reduced on the boundaries to $\mathcal{G}_{\mathrm{EW}}$ on the UV-brane and to $\mathcal{H}$ on the IR-brane, respectively.

As pictured in Figure 2.6 the boundaries of the 5D compact space are 4-dimensional manifolds called *branes*.[9] Even though the explicit labelling as UV- and IR-branes becomes much more meaningful once going to a warped space-time, this notation is introduced now for consistency reasons. The space in between, where the fields can propagate within the fifth dimension, is called *bulk*.

Let us impose a gauge symmetry $\mathcal{G}$ on the bulk which comes with gauge fields $A_M = A_M^A T^A$, where the 4D components A_μ^A act like vector fields and the A_5^A like scalars under

[9] The naming is in analogy with models in string theory, which make extensive use of compact extra dimensions.

Lorentz transformation.[10] These gauge fields are not only necessary in order to obtain the SM gauge bosons, they can also be embedded in a way that they reduce the overall symmetry on the boundaries. A general gauge transformation acts on A_M like

$$A_M \to A'_M = \frac{i}{g_5}\Omega D_M \Omega^\dagger \tag{2.3.12}$$
$$\Omega(x, x^5) = \mathcal{P}\exp\big(-ig_5\omega^A(x, x^5)T^A\big), \tag{2.3.13}$$

with $D_M = \partial_M - ig_5 A_M$ being the covariant derivative in presence of $\mathcal{G}$, g_5 the dimensionful coupling (with mass dimension $[g_5] = -1/2$) and $\mathcal{P}$ accounts for the path ordering of the exponential term. A gauge transformation should not change the BCs of the gauge fields. Therefore, the BCs of the gauge parameters ω^A must follow from the BCs of the A_M^A. By assuming Neumann BCs for A_μ^A

$$\partial_5 A_\mu^{A\prime}{}_{|x_i} = \cancel{\partial_5 A_\mu^A{}_{|x_i}} - \partial_5\partial_\mu\omega^A{}_{|x_i} = -\partial_\mu\partial_5\omega^A{}_{|x_i} \stackrel{!}{=} 0 \tag{2.3.14}$$
$$\Rightarrow \partial_5\omega^A{}_{|x_i} = 0, \tag{2.3.15}$$

with $x_i \in \{0, L\}$ and similar for Dirichlet BCs one can see, that the gauge parameters ω^A have to obey the same BCs as the A_μ^A gauge fields. Repeating this calculation for the A_5^A components it is evident, that in this case the BCs for the ω^A have to be opposite to the BCs of A_5^A.[11] This means, that the fifth component of the gauge fields A_5^A always has BCs opposite to the BCs of the 4D components A_μ^A.

A convenient choice for a set of BCs for the gauge fields is

$$\begin{aligned} &A_\mu^a(+,+), \quad A_5^a(-,-) && T^a \in \mathcal{H}_0 \\ &A_\mu^{\dot a}(-,+), \quad A_5^{\dot a}(+,-) && T^{\dot a} \in \mathcal{H}/\mathcal{H}_0 \\ &A_\mu^{\hat a}(-,-), \quad A_5^{\hat a}(+,+) && \hat{T}^{\hat a} \in \mathcal{G}/\mathcal{H}, \end{aligned} \tag{2.3.16}$$

where $\mathcal{H} \subset \mathcal{G}$ and $\mathcal{H}_0 \equiv \mathcal{G}_{\text{EW}} \subset \mathcal{H}$.[12] At $x^5 = 0$ only the gauge fields A_μ^a are non-vanishing, reducing the global symmetry $\mathcal{G}$ to $\mathcal{G}_{\text{EW}}$ on the UV-brane. At $x^5 = L$, the same happens due to the presence of the A_μ^a, $A_\mu^{\dot a}$ leading to the effective symmetry $\mathcal{H}$ on the IR-brane. Furthermore, one can see, that for low energies ($n = 0$) the overall gauge symmetry reduces to $\mathcal{G}_{\text{EW}}$ because only the $A_\mu^a(+,+)$ zero-modes are present together with the zero-modes of $A_5^{\hat a}(+,+)$.

Apart from the zero-modes $A_\mu^{a(0)}(x)$, $A_5^{\hat a(0)}(x^5)$ which correspond to massless gauge and scalar fields in the 4D, KK-towers of massive spin-1 fields $A_\mu^{A(n)}(x)$ are remaining.

[10] The T^A are the generators of the symmetry group $\mathcal{G}$. For $SO(5)$ these will be the matrices defined in Eq. 2.2.1, 2.2.2 and 2.2.3.

[11] Due to KK-decomposition and the compactness of the fifth dimension $\partial_5^2\omega^A \propto \omega^A$ can be assumed in this calculation.

[12] $\mathcal{H}_0 \equiv \mathcal{G}_{\text{EW}}$ and $\mathcal{H}_0 \subset \mathcal{H}$ are the same assumptions made for simplicity as in Section 2.1.3. A more generic approach can be found in [48].

The modes of the A_5^a and $A_5^{\dot{a}}$ fields can be gauged away by an axial gauge transformation

$$\Omega(x,x^5) = \mathcal{P}\exp\left(-ig_5\int_0^{x^5} \mathrm{d}y A_5(x,y)\right), \tag{2.3.17}$$

with $\omega^A(x,x^5) = \int_0^{x^5} \mathrm{d}y A_5^A(x,y)$ yielding $A_5 = 0$ for the corresponding A_M. This is effectively a Higgs-mechanism where level by level each $A_5^{(n)}(x^5)$ mode gets eaten by the corresponding $A_\mu^{(n)}(x)$ gauge boson mode. Unfortunately, this does not work for the $A_5^{\hat{a}}$ because of their zero-modes which spoil the BCs of the $\omega^{\hat{a}}$. However, by subtracting the zero-mode for each field

$$\Omega(x,x^5) = \mathcal{P}\exp\left(-ig_5\int_0^{x^5} \mathrm{d}y A_5(x,y)\right)\exp\left(ig_5\frac{x^5}{\sqrt{L}}A_5^{\hat{a}(0)}(x)\hat{T}^{\hat{a}}\right) \tag{2.3.18}$$

an almost axial gauge with $A_5^{\hat{a}}(x,x^5) = A_5^{\hat{a}(0)}(x)/\sqrt{L}$ [62] constant in x^5 can be achieved using $f_0^{(+,+)} = 1/\sqrt{L}$ from Table 2.1. The remaining $A_5^{\hat{a}(0)}(x)$ are physical massless 4D fields at tree level. It is shown in the following, that one can actually identify four of these zero-modes with the composite NGB Higgs of a spontaneously broken symmetry.

2.3.3 The holographic idea

How does the 5D model look like to a 4D observer on one of the branes? This is the most important question to raise if one wants to truly understand the mapping between these two models. To answer it, one can consider the partition function for the bulk fields $\Phi(x,0) \equiv \Phi_0$ at $x^5 = 0$ [48]

$$\begin{aligned} Z &= \int \mathrm{d}\Phi e^{iS[\Phi]+iS_0[\Phi]} = \int \mathrm{d}\Phi_0 e^{iS_0[\Phi_0]}\int_{\Phi_0}\mathrm{d}\Phi e^{iS[\Phi]} \\ &= \int \mathrm{d}\Phi_0 e^{iS_0[\Phi_0]+iS_{\text{eff}}[\Phi_0]}, \end{aligned} \tag{2.3.19}$$

where S_0 denotes the 5D action at $x^5 = 0$. A 4D observer on the UV-brane would feel the 5D action on the bulk and at $x^5 = L$ as a strong force defined by an effective action

$$iS_{\text{eff}}[\Phi_0] \equiv \ln\left[\int_{\Phi_0}\mathrm{d}\Phi e^{iS[\Phi]}\right] \tag{2.3.20}$$

at $x^5 = 0$. This picture allows to separate the total 5D action into an “elementary” sector S_0 which contains the degrees of freedom on the boundary $x^5 = 0$ and a “composite” one, S_{eff}, incorporating the field dynamics on the bulk and on the boundary $x^5 = L$ as illustrated in Figure 2.7. This is now in complete analogy to the CHMs discussed in Section 2.1 and 2.2. The KK-modes on the UV-brane then correspond to the elementary fields of a CHM and, turning around the argument (i.e. stating a 4D observer at x^5=L), the KK-modes on the IR-brane correspond to the composite fields. Moreover, staying in this picture it can be argued, that the KK-modes of the 5D fields can now be seen as mass eigenstates of the mixing between fields of the composite and the elementary sector. Therefore, the 5D approach automatically includes partial compositeness (see Section 2.2.3).

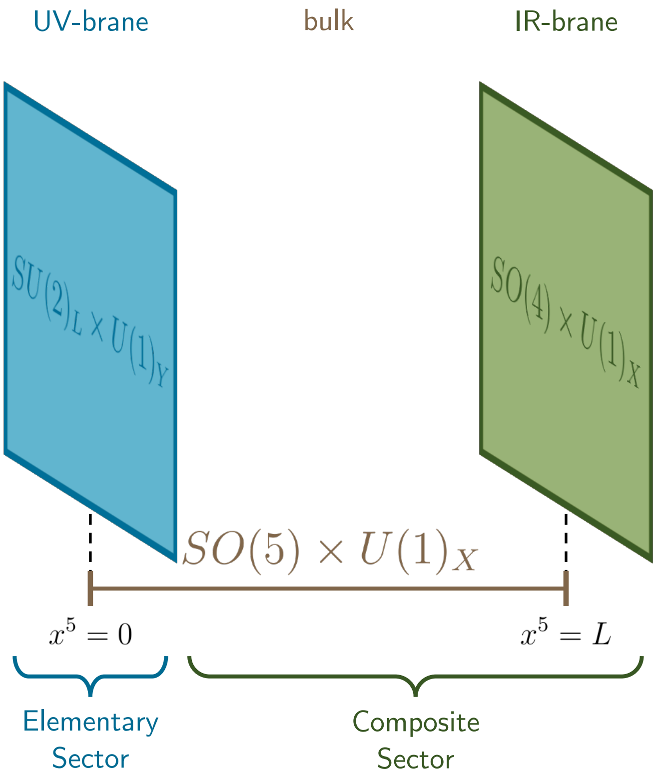

Figure 2.7: The same picture as in Figure 2.6 with the explicit symmetries $\mathcal{G} = SO(5) \times U(1)_X$, $\mathcal{H} = SO(4) \times U(1)_X$ and $\mathcal{G}_{\text{EW}} = SU(2)_Y \times U(1)_Y$. Also pictured are the two sectors of the 4D CHM from a holographic 5D standpoint. The elementary sector can be identified with the UV-brane while the composite sector is settled in the bulk and on the IR-brane.

Explicitly, by setting $\mathcal{G} = SO(5) \times U(1)_X$ which reduces to $\mathcal{H} = SO(4) \times U(1)_X$ on the boundary $x^5 = L$, one can assume S_{eff} to be locally invariant at least under $\mathcal{H}$ (i.e. $S_{\text{eff}}[h(x)\Phi_0] = S_{\text{eff}}[\Phi_0]$ for $h \in \mathcal{H}$).[13] Starting from an axial gauge one can redefine the fields $\Phi \to \tilde{\Omega}\Phi$ in the bulk with the transformation

$$\tilde{\Omega}(x, x^5) = \exp\left(-ig_5 \int_L^{x^5} \mathrm{d}y A_5^{\hat{a}}(x, x^5)\hat{T}^{\hat{a}}\right) = \exp\left(-i\frac{g_5}{\sqrt{L}}(x^5 - L)A_5^{\hat{a}(0)}(x)\hat{T}^{\hat{a}}\right) \tag{2.3.21}$$

with $A_5^{\hat{a}}(x, x^5)$ defined as in Eq. 2.3.18. As an effect of this redefinition, the zero-modes of the A_5 components of the gauge fields, which transform accordingly via Eq. 2.3.12,

[13]Again, this discussion can be set up to be more general but is reduced and thus simplified to the case which is relevant for the further discussion.

vanish everywhere except at $x^5 = 0$.[14] At this point, $\tilde{\Omega}(x, 0)$ can be identified with a non-local operator in almost axial gauge, the *Wilson line* towards the UV-brane

$$W_{\mathrm{UV}}(x) = \exp\left(ig_5 \int_0^L \mathrm{d}x^5 A_5(x, x^5)\right) \tag{2.3.22}$$

$$\rightarrow \exp\left(ig_5 \sqrt{L} A_5^{\hat{a}(0)}(x) \hat{T}^{\hat{a}}\right) \equiv \exp\left(i\theta(x)\right), \tag{2.3.23}$$

which is in this parametrization equivalent to the exponent of the zero-modes of the $A_5^{\hat{a}}$ ($\Omega(x, x^5)$ is then called *Wilson line transformation*).[15] Using this parametrization, the redefinition induces a shift in the BCs of the bulk fields at $x^5 = 0$

$$\Phi_0 \rightarrow \Phi_0' = e^{i\theta(x)} \Phi_0. \tag{2.3.24}$$

If S_{eff} should stay invariant under $\mathcal{G}$, the Wilson line has to transform as a NGB field

$$e^{-i\theta(x)} \rightarrow e^{-i\theta'(x)} = g e^{-i\theta(x)} h^{-1}(\theta(x), g), \tag{2.3.25}$$

with $g \in \mathcal{G}$, $h \in \mathcal{H}$ truly classifying it to be the 5D complement to the Goldstone matrix in CHMs. With S_{eff} being invariant under $\mathcal{H}$

$$S_{\mathrm{eff}}\left[\Phi_0'\right] \rightarrow S_{\mathrm{eff}}\left[h(\theta, g) e^{i\theta} g^{-1} g \Phi_0\right] = S_{\mathrm{eff}}\left[h(\theta, g)\Phi_0'\right] = S_{\mathrm{eff}}\left[\Phi_0'\right] \tag{2.3.26}$$

it is evident, that the $\mathcal{G}$ symmetry of the composite sector at $x^5 = 0$ is just non-linearly realized. This corresponds to a SSB of $SO(5) \times U(1)_X \rightarrow SO(4) \times U(1)_X$ releasing four NGBs which become the composite Higgs of the model.

In order to reach full consistency with a viable theory of a composite Higgs model, one has to ensure that the elementary sector is weakly coupled. The most convenient way to do this is by warping the extra dimension.

2.3.4 Warped extra dimensions and AdS/CFT duality

The problem raised at the end of the previous section is related to the question, how one can restrict the coupling to the elementary sector to the zero-modes of the introduced gauge fields only. One possibility is to introduce large kinetic terms which make all non-zero-modes very heavy because they raise the masses m_n of the KK-towers. Therefore, they would effectively decouple in the 4D holography. Another much more practical idea is realized by introducing a warping factor to the metric

$$\mathrm{d}s^2 = e^{-2ky} \eta_{\mu\nu} \mathrm{d}x^\mu \mathrm{d}x^\nu - \mathrm{d}y^2, \tag{2.3.27}$$

[14] This redefinition is not a gauge transformation, because $\Omega(x, 0) \neq 1$, but on the bulk and at $x^5 = L$ it acts like one, thus leaving S_{eff} invariant.

[15] The Wilson line transformation can be defined generally in both ways shifting the Higgs either to the UV- or IR-brane. The resulting Wilson lines differ by a minus sign in the exponent.

with $y \equiv x^5$ and curvature $k > 0$ making AdS$_5$ metric non-trivial.[16] A completely equivalent metric which will be much more useful to the following discussion is

$$ds^2 = a^2(z)(\eta_{\mu\nu}dx^\mu dx^\nu - dz^2), \tag{2.3.28}$$

with a(z)=R/z and z being the radial AdS$_5$ coordinate (for an explicit mapping between these two metrics, see Appendix B.1). From here, it is evident that this metric is conformal, i.e. invariant under simultaneous rescaling $z \to cz$ and $x^\mu \to cx^\mu$. Thus, a rescaling of z corresponds to a change in energy in the 4D theory with $z \to 0 \Leftrightarrow E \to \infty$ and vice versa. If the interval of the z parameter is truncated, the conformality is of course broken through the boundaries whose labelling becomes now much more meaningful. Introducing a boundary on the left at $z = R$ now corresponds to a UV-cutoff $\Lambda_{\text{UV}} \sim 1/R$ of the CFT. Usually, this cutoff is chosen to be at the Planck scale such that $R \sim 1/M_{\text{Pl}} \sim 10^{-16}\,\text{TeV}^{-1}$. A boundary on the right at $z = R' \gg R$ would then correspond to an IR-cutoff at $\Lambda_{\text{IR}} \sim 1/R'$ or, as derived in the previous section, to a spontaneously broken CFT at low energies (see Figure 2.8 for an illustration; see also [60, 87]).[17] Furthermore, an IR-brane introduces discrete KK-modes which become strongly interacting after the breaking of conformality. Keeping in mind the analogy between z and the energy scale of a 4D theory, this behavior corresponds to a QCD-like theory (like a CHM) which produces bound states like composite fields or the composite Higgs at low energies which could then induce EWSB as usual. In order to be consistent with the 4D approach, one usually sets $R' \sim \mathcal{O}(1\,\text{TeV}^{-1})$.

Since the bulk of the AdS$_5$ corresponds to a CFT in 4D, a local gauge symmetry $\mathcal{G}$ induced on it will also be present as a global symmetry in the 4D approach. Vice versa, the symmetry breaking in the MCHM must be mimicked by the 5D theory. As shown in Section 2.3.2, symmetry breaking on 5D is induced by boundary conditions on the branes. Looking back to Eq. 2.3.16 one can see, that the boundary conditions are already set in a way, that the right symmetry breaking pattern in 4D is obtained. As mentioned in Section 2.3.1, Dirichlet BCs break symmetries at a boundary and can also be used to get rid of non-needed gauge fields. If a gauge field has $(-)$ BCs on the UV-brane, its KK-masses will scale with $m_n \sim 1/R$ and it will decouple from the low energy theory. In order to break a symmetry in a specific way, one can introduce a "boundary Higgs" with the right quantum numbers to realize the breaking pattern in the desired way and then take its VEV to infinity. Starting, e.g., with fields R^a_μ of $SU(2)_R$ and B_μ of $U(1)_X$ a boundary Higgs doublet in a $(\mathbf{1},\mathbf{2})_{1/2}$ representation of $SU(2)_L \times SU(2)_R \times U(1)_X$ can be introduced, which breaks $SU(2)_R \times U(1)_X \to U(1)_Y$ as needed for the MCHM. The same holds using a bidoublet $(\mathbf{2},\mathbf{2})_0$ to break $SO(5) \times U(1)_X \to SO(4) \times U(1)_X$ on the IR-brane (see [89] for more information). The latter breaking will also induce the same SSB pattern as in the 4D theory.

It can be concluded that fields which break the bulk gauge symmetry on the UV-brane will not gauge the global 4D symmetry. Fields which leave the bulk symmetry

[16] The Minkowski metric used so far is the trivial AdS metric with $k = 0$.

[17] Note, that such warped extradimensional models solve the Hierarchy problem also without the need of a Composite Higgs setup (see [88]). In these cases, the Higgs is assumed to be a scalar field in the bulk rather than a pNGB of a spontaneously broken theory.

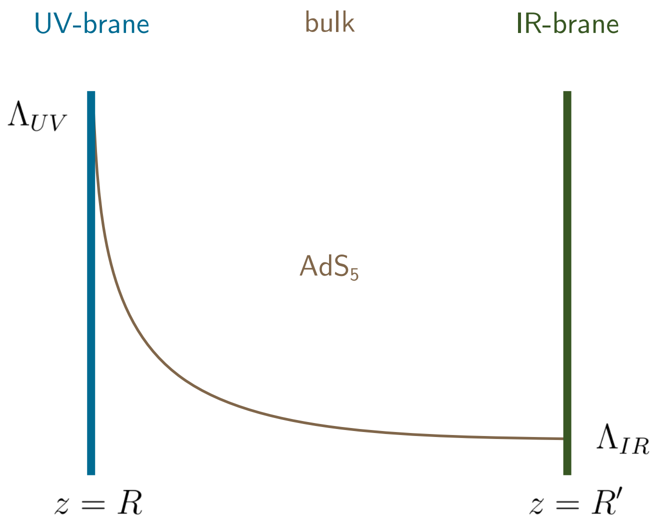

Figure 2.8: Illustration of a warped AdS$_5$ space following the metric of Eq. 2.3.28 with boundaries at R and R'. Also displayed are the corresponding energy scales of the 4D theory on the boundaries.

unbroken on the UV-brane because of (+) BCs will, however, lead to a weak gauging of the global 4D symmetry, ensuring a weakly coupled elementary sector. This is realized by their zero-modes corresponding to the weak gauge fields of the SM. The massive modes of their KK-tower will again scale with $m_n \sim 1/R$ and effectively decouple.

In order to get a better overview of the AdS/CFT duality, the main points of the preceding discussion are summarized in Table 2.2.

2.3.5 Boundary conditions of fermions in flat space

So far a lot of effort has been made to display the general duality between a 5D holographic theory on a warped AdS space and a 4D CHM. Before moving on and mapping the sMCHM$_5$ setup onto a 5D extra-dimensional theory, it is necessary to discuss one additional thing: fermions. In the 4D approach it has been shown that the mixing of elementary fermions with composite resonances explicitly breaks the global symmetry $\mathcal{G}$. Through this mechanism, the Higgs obtains a light mass as a pNGB of the theory. In the holographic approach this mixing happens at the UV-brane, such that it can be concluded that (−) BCs of the fermions at $z = R$ are the source of the explicit breaking in the 5D theory. In the sMCHM$_5$ it was possible to soften this breaking by introducing new massive vector-like elementary fields. This can also be done in the 5D theory. The softening is now achieved by the introduction of mixing terms of the corresponding fields on the UV-brane with their localized 4D chiral partners. This is needed to make the vector-like fermions massive and will also shift the BCs away from Dirichlet conditions which will be seen in the following. The masses of the zero-modes of the (partially composite) fermion fields in the bulk, which correspond to the SM fields in the 4D theory,

Table 2.2: Equivalent statements in terms of the AdS/CFT duality. Content taken from [89].

AdS_5	(S)CFT
Bulk of AdS	CFT
Coordinate z along AdS	Energy scale of CFT
Appearance of UV-brane at $z = R$	CFT has UV-cutoff at $\Lambda \sim 1/R$
Appearance of IR-brane at $z = R'$	CFT has IR-cutoff at $\Lambda \sim 1/R'$
KK-modes on UV-brane	elementary fields coupled to CFT
KK-modes on IR-brane	composite fields of CFT
Fermion overlap with IR-brane	partial composite fermions in CFT
gauge fields in the bulk	CFT has global symmetry $\mathcal{G}$
Bulk gauge symmetry broken on UV-brane	global symmetry not gauged
Bulk gauge symmetry unbroken on UV-brane	global symmetry weakly gauged
Bulk gauge symmetry broken on IR-brane	SSB of CFT at $\Lambda \sim 1/R'$
Higgs on IR-brane	CFT confines at low energy produces composite Higgs

originate from couplings with the Higgs boson on the IR-brane.

The action of a fermion field Ψ in flat space yields

$$S_\Psi^{\text{bulk}} = \int \mathrm{d}^4x \int_0^L \mathrm{d}x^5 \left[\frac{i}{2}\left(\bar\Psi \partial_M \Gamma^M \Psi - \partial_M \bar\Psi \Gamma^M \Psi\right) - m_\psi \bar\Psi\Psi\right], \tag{2.3.29}$$

with m_ψ being the mass of the field and Γ^M the 5D gamma matrices

$$\Gamma^M = \left\{\gamma^\mu, i\gamma^5\right\}, \quad \left\{\Gamma^M, \Gamma^N\right\} = 2\eta^{MN}, \tag{2.3.30}$$

with γ^μ the usual 4D gamma matrices in a chiral basis (see Appendix B.2). Note that the covariant terms in the derivative are neglected for simplicity. The bulk fermion can be split into its left and right-handed chiral components

$$\Psi = \begin{pmatrix} \Psi_L(x, x^5) \\ \Psi_R(x, x^5) \end{pmatrix} \equiv \begin{pmatrix} s_{L\alpha} \\ \bar\psi^{\dot\alpha} \end{pmatrix}, \quad \bar\Psi = -\begin{pmatrix} \Psi_R^\dagger(x, x^5) \\ \Psi_L^\dagger(x, x^5) \end{pmatrix}^T \equiv -\left(\psi^\alpha, \bar s_{L\dot\alpha}\right) \tag{2.3.31}$$

denoted in SUSY-notation (see also Appendix B.2).[18] Plugging this into the action, one

[18] The s_L will be identified as the left-handed singlet of the new vector-like fermions, later, and ψ labels his chiral partner.

obtains

$$S_\Psi^{\text{bulk}} = \int \mathrm{d}^4x \int_0^L \mathrm{d}x^5 \Big[-i\bar{s}_L\bar{\sigma}^\mu\partial_\mu s_L - i\psi\sigma^\mu\partial_\mu\bar{\psi} + \frac{1}{2}\left(\psi\overleftrightarrow{\partial_5}s_L - \bar{s}_L\overleftrightarrow{\partial_5}\bar{\psi}\right) + m_\psi(\psi s_L + \bar{s}_L\bar{\psi})\Big], \tag{2.3.32}$$

where $\overleftrightarrow{\partial_5} = \overrightarrow{\partial_5} - \overleftarrow{\partial_5}$ denotes the partial derivative of x^5 in both directions. By varying the action with respect to $\bar{s}_L$ and ψ which comprise the two chiral degrees of freedom the equations of motion yield

$$-i\bar{\sigma}^\mu\partial_\mu s_L - \partial_5\bar{\psi} + m_\psi\bar{\psi} = 0 \tag{2.3.33}$$
$$-i\sigma^\mu\partial_\mu\bar{\psi} + \partial_5 s_L + m_\psi s_L = 0. \tag{2.3.34}$$

This expression can be simplified even further by the performance of a KK-decomposition for the fields

$$s_L = \sum_n s_n(x^5)\chi_n(x), \quad \bar{\psi} = \sum_n f_n(x^5)\bar{\psi}_n(x), \tag{2.3.35}$$

where the $\{\chi_n\}$, $\{\bar{\psi}_n\}$ are the chiral bases for the left- and right-handed fields. Together they form 4D Dirac spinors with masses m_n being the mass eigenstates of the (partial) composite fermions in the 4D theory. Therefore, they have to obey the Dirac equations

$$-i\bar{\sigma}^\mu\partial_\mu\chi_n + m_n\bar{\psi}_n = 0 \tag{2.3.36}$$
$$-i\sigma^\mu\partial_\mu\bar{\psi}_n + m_n\chi_n = 0 \tag{2.3.37}$$

which simplifies the equations of motion drastically

$$s_n' + m_\psi s_n - m_n f_n = 0 \tag{2.3.38}$$
$$f_n' - m_\psi s_n + m_n s_n = 0. \tag{2.3.39}$$

Because of the linear independence of the basis elements χ_n and $\bar{\psi}_n$ this has to be true for every n. In fact, Eq. 2.3.38 and 2.3.39 can even be decoupled by recombination

$$s_n'' + (m_n^2 - m_\psi^2)s_n = 0 \tag{2.3.40}$$
$$f_n'' + (m_n^2 - m_\psi^2)f_n = 0, \tag{2.3.41}$$

leaving two harmonic differential equations (see Appendix B.3 for the exact calculations). Depending on the sign of $m_n^2 - m_\psi^2$ the s_n and f_n can be written in terms of trigonometric or hyperbolic functions. Sticking to $k_n \equiv m_n^2 - m_\psi^2 > 0 \; \forall n$ one obtains

$$s_n(x^5) = A_n\cos\big(k_n x^5\big) + B_n\sin\big(k_n x^5\big) \tag{2.3.42}$$
$$f_n(x^5) = C_n\cos\big(k_n x^5\big) + D_n\sin\big(k_n x^5\big). \tag{2.3.43}$$

In order to set the correct boundary conditions, one has to look at the boundary term of the variation of the action

$$\delta S_\Psi^{\text{bound}} = \frac{1}{2}\int \mathrm{d}^4x \Big[\delta\bar{s}_L\bar{\psi} - \delta\bar{\psi}\bar{s}_L - \delta\psi s_L + \delta s_L\psi\Big]_0^L \stackrel{!}{=} 0. \tag{2.3.44}$$

Since this term has to vanish, the most simple BCs which can be written down are introduced which correspond to the Dirichlet conditions in Eq. 2.3.10 for s_L or $\bar{\psi}$. The solutions to the corresponding s_n and f_n are then equivalent to the ones in Table 2.1. Note that only two of the four BCs can be chosen freely. The other two are fixed by Eq. 2.3.33 and 2.3.34

$$s_L|_{x_i^5} = 0 \qquad \Rightarrow \qquad \partial_5\bar{\psi}|_{x_i^5} = +m_\psi\bar{\psi}|_{x_i^5} \tag{2.3.45}$$

$$\bar{\psi}|_{x_i^5} = 0 \qquad \Rightarrow \qquad \partial_5 s_L|_{x_i^5} = -m_\psi s_L|_{x_i^5} \tag{2.3.46}$$

for $x_i^5 \in \{0, L\}$. In the limit $m_\psi \to 0$, the boundary conditions between the two chiral states are always opposite.

Generally speaking, the action of a particle on an AdS_5 can be described by the sum over the action in the bulk and on the boundaries

$$S_\Psi = S_\Psi^{\text{bulk}} + S_\Psi^{\text{UV}} + S_\Psi^{\text{IR}} \tag{2.3.47}$$

where the latter two terms were not present in the previous discussion. Adding e.g. a localized right-handed particle s_R on the UV-brane, which interacts with the s_L, changes the UV action to

$$S_\Psi^{\text{UV}} = \int \mathrm{d}^4x \left[-i s_R\sigma^\mu\partial_\mu\bar{s}_R + \frac{c_s}{\sqrt{L}}(s_R s_L + \bar{s}_L\bar{s}_R)\right]_{x^5=0}, \tag{2.3.48}$$

with c_s being the dimensionless coupling constant and L the scale. The latter accounts for the fact that s_L has as a spinor of a 5D field has mass dimension $[s_L] = 2$ and s_R as a localized 4D field has mass dimension $[s_R] = 3/2$. Note that the UV action leaves the equations of motions in the bulk unchanged. The decomposition of the s_R looks like

$$\bar{s}_R = \sum_n E_n\bar{\psi}_n(x), \tag{2.3.49}$$

with the E_n being constants in x^5. Note that s_R as a right-handed field has to be expressed in the same chiral basis as ψ.

The s_R field can be used to substitute the $(-)$ BC on the UV-brane with a BC depending on the coupling constant c_s which can be associated with a vector-like mass term. This will soften the symmetry breaking of $\mathcal{G}$ analogously to the 4D theory. However, finding the exact BC from the variational principle is rather difficult. Luckily, this task can be simplified by the following mechanism: One first takes $\bar{\psi}_{|0} = 0$ to be the BC on the UV-brane and pushes in a second step the localization of s_R a factor of ε away from the brane. Leaving Eq. 2.3.34 unaltered, this ε shift changes equation 2.3.33 in the bulk and adds another one by variation of s_R

$$-i\bar{\sigma}^{\mu}\partial_{\mu}s_L - \partial_5\bar{\psi} + m_{\psi}\bar{\psi} + \frac{c_s}{\sqrt{L}}\bar{s}_R\,\delta\big(x^5-\varepsilon\big) = 0 \tag{2.3.50}$$

$$\left\{-i\sigma^{\mu}\partial_{\mu}\bar{s}_R + \frac{c_s}{\sqrt{L}}s_L\right\}\delta\big(x^5-\varepsilon\big) = 0. \tag{2.3.51}$$

Integrating Eq. 2.3.50 from 0 to ε and taking the limit $\varepsilon \to 0^+$, one is left with

$$\bar{\psi}_{|0^+} = \frac{c_s}{\sqrt{L}}\bar{s}_R \neq 0 \tag{2.3.52}$$

where the kinetic as well as the bulk mass term vanish due to the smoothness of the antiderivative of s_L and $\bar{\psi}$ with respect to x^5. Repeating the same procedure with Eq. 2.3.51 yields

$$s_{L|_{0^+}} = \frac{\sqrt{L}}{c_s}i\sigma^{\mu}\partial_{\mu}\bar{s}_R. \tag{2.3.53}$$

One can check that Eq. 2.3.52 and 2.3.53 which both depend on c_s acutally provide valid BCs at $x^5 = 0$ for $\bar{\psi}$ and s_L by inserting them into Eq. 2.3.44.[19]

What has just been shown, can be interpreted as a transformation. The vector-like mass term with a free parameter c_s resulting from an interaction of a bulk field s_L with a localized boundary field s_R has been translated into a c_s-dependent BC for s_L. This allows to retreat from Dirichlet BCs and soften the symmetry breaking. By decoupling the $\bar{s}_R$ setting $c_s \to \infty$, the Dirichlet BC is restored.

Having fixed the BCs, they can be used to determine the coefficients $A_n - E_n$ of Eq. 2.3.42, 2.3.43, and 2.3.49 in order to obtain solutions for the KK-tower $\{m_n\}$ corresponding to the mass eigenstates of the system. In terms of the x^5 dependent KK-fields, the BCs translate to

$$f_n(0) = C_n = \frac{c_s}{\sqrt{L}}E_n \tag{2.3.54}$$

$$s_n(0) = A_n = \frac{\sqrt{L}}{c_s}m_nE_n = \frac{m_nL}{c_s^2}C_n \tag{2.3.55}$$

$$s_n(L) = A_n\cos(k_nL) + B_n\sin(k_nL) = 0, \tag{2.3.56}$$

where for the second equity in the second equation the relation 2.3.36 has been used. The BC $s_{L|_L} = 0$ (and therefore also $\bar{\psi}_{|_L}$) is left unaltered. Since the two fields have been decoupled at some point, which was useful to solve the differential equations, the information about their relation has not been included yet. Therefore, the mixed equations of motion 2.3.38 and 2.3.39 evaluated an $x^5 = 0$ provide two additional constraints

$$k_nB_n + m_{\psi}A_n - m_nC_n = 0 \tag{2.3.57}$$

$$k_nD_n - m_{\psi}C_n + m_nA_n = 0. \tag{2.3.58}$$

[19] For more information on the general process, see [90].

Setting $m_\psi \to 0$ ($k_n \to |m_n|$) for a pure simplification purpose, one is left to solve a system of linear differential equations

$$\begin{pmatrix} \cos(|m_n|L) & \sin(|m_n|L) & 0 & 0 \\ 1 & 0 & -\frac{m_n L}{c_s^2} & 0 \\ 0 & |m_n| & -m_n & 0 \\ m_n & 0 & 0 & |m_n| \end{pmatrix} \begin{pmatrix} A_n \\ B_n \\ C_n \\ D_n \end{pmatrix} = 0, \tag{2.3.59}$$

which is equivalent to solve

$$\det M_t = |m_n| m_n \sin(|m_n|L) + \frac{L}{c_s^2} |m_n|^2 m_n \cos(|m_n|L) \stackrel{!}{=} 0. \tag{2.3.60}$$

Apart from a zero-mode $m_n = 0$, a spectrum for m_n is obtained corresponding to the solutions to the transcendent equation

$$|m_n| = -\frac{c_s^2}{L} \tan(|m_n|L). \tag{2.3.61}$$

To calculate the coefficients $A_n - E_n$, one can take one of the possible solutions for m_n, insert it back into the Eq. 2.3.59 and rewrite the coefficients in terms of e.g. A_n. The last coefficient is then fixed using one of the normalization conditions

$$\int_0^L \mathrm{d}y \big(f_n(y) f_m(y) + e_n e_m \delta(y) \big) = \delta_{mn} \tag{2.3.62}$$

$$\text{or} \qquad \int_0^L \mathrm{d}y s_n(y) s_m(y) = \delta_{mn}. \tag{2.3.63}$$

2.3.6 Fermion fields on a warped AdS$_5$ space

Having seen this example on a flat Minkowski space, the reader is now familiar with the general procedure. The next step will be a more elaborated case on a warped AdS space which is also going to be considered for the setup relevant for the numerical analysis in Section 2.4.

For this purpose, $\Psi \equiv \Psi_1$ is relabelled and another 5D Dirac spinor

$$\Psi_2 = \begin{pmatrix} \chi_\alpha \\ \bar{t}_R{}^{\dot\alpha} \end{pmatrix}, \quad \bar\Psi_2 = -\left(t_R^\alpha, \bar\chi_{\dot\alpha} \right), \tag{2.3.64}$$

with KK-decompositions

$$\chi = \sum_n g_n(z) \chi_n(x), \quad \bar{t}_R = \sum_n t_n(z) \bar\psi_n(x) \tag{2.3.65}$$

is added to the theory.[20] Considering an AdS$_5$ space with a metric displayed in Eq. 2.3.28, one arrives at the bulk action

$$S_{\text{bulk}} = \sum_{k=1,2} \int \mathrm{d}^5 x \sqrt{G} \Big\{ \frac{i}{2} E_a^M (\bar\Psi_k \Gamma^a D_M \Psi_k - D_M \bar\Psi_k \Gamma^a \Psi_k) - m_k \bar\Psi_k \Psi_k \Big\}, \tag{2.3.66}$$

[20] The t_R component will later be identified with the right-handed top quark.

with $\sqrt{G} = (\det g_{MN})^{1/2} = a(z)^5$ the square-root of the metric determinant with $g_{MN} = a(z)\eta_{MN}$ and $E_a^M = a^{-1}(z)\delta_a^M$ the inverse 5D vielbein used in differential geometry to correctly map the gamma matrices to the covariant derivative. The latter is generally defined as $E_M^a \eta_{ab} E_N^b = g_{MN}$. The $m_k \in \{m_\psi, m_\chi\}$ denote the bulk masses of the two fields. Again, the gauge field contributions will be ignored, i.e. $D_M \equiv \partial_M$. Inserting Ψ_1 and Ψ_2, S_{bulk} is rewritten in its spinor components

$$\begin{aligned} S_{\text{bulk}} = \int \mathrm{d}^5x \left(\frac{R}{z}\right)^4 \Big[& - i\bar{s}_L\bar{\sigma}^\mu\partial_\mu s_L - i\psi\sigma^\mu\partial_\mu\bar{\psi} - i\bar{\chi}\bar{\sigma}^\mu\partial_\mu\chi - it_R\sigma^\mu\partial_\mu\bar{t}_R \\ & + \frac{1}{2}(\psi\overleftrightarrow{\partial_5}s_L - \bar{s}_L\overleftrightarrow{\partial_5}\bar{\psi}) + \frac{1}{2}(t_R\overleftrightarrow{\partial_5}\chi - \bar{\chi}\overleftrightarrow{\partial_5}\bar{t}_R) \\ & + \frac{c_\psi}{z}(\psi s_L + \bar{s}_L\bar{\psi}) + \frac{c_\chi}{z}(t_R\chi + \bar{\chi}\bar{t}_R)\Big], \end{aligned} \tag{2.3.67}$$

with $c_k = m_k R$ being the dimensionless bulk masses. By variation of $\bar{s}_L$, ψ, $\bar{\chi}$ and t_R the bulk equations of motion are obtained

$$-i\bar{\sigma}^\mu\partial_\mu s_L - \partial_5\bar{\psi} + \frac{c_\psi+2}{z}\bar{\psi} = 0 \tag{2.3.68}$$

$$-i\sigma^\mu\partial_\mu\bar{\psi} + \partial_5 s_L + \frac{c_\psi-2}{z}s_L = 0 \tag{2.3.69}$$

$$-i\bar{\sigma}^\mu\partial_\mu\chi - \partial_5\bar{t}_R + \frac{c_\chi+2}{z}\bar{t}_R = 0 \tag{2.3.70}$$

$$-i\sigma^\mu\partial_\mu\bar{t}_R + \partial_5\chi + \frac{c_\chi-2}{z}\chi = 0, \tag{2.3.71}$$

with

$$\delta S_{\text{bound}} = \int \mathrm{d}^4x \left[\left(\frac{R}{z}\right)^4 \left(\bar{\psi}\delta\bar{s}_L - s_L\delta\psi + \bar{t}_R\delta\bar{\chi} - \chi\delta t_R\right)\right]_R^{R'}. \tag{2.3.72}$$

Note, that here the four additional contributions to the boundary action are suppressed, because they do not add more information to the system and vanish if the displayed four do. Again, these four equations of motion are rewritten in terms of the KK-fields using Eq. 2.3.36 and 2.3.37

$$s_n' + \frac{c_\psi-2}{z}s_n - m_n f_n = 0 \qquad f_n' - \frac{c_\psi+2}{z}f_n + m_n s_n = 0 \tag{2.3.73}$$

$$g_n' + \frac{c_\chi-2}{z}g_n - m_n t_n = 0 \qquad t_n' - \frac{c_\chi+2}{z}t_n + m_n g_n = 0. \tag{2.3.74}$$

As in the flat case, these equations can be decoupled (see also Appendix B.3) arriving at

$$f_n'' - \frac{4}{z}f_n' + \left(m_n^2 - \frac{c_\psi^2 - c_\psi - 6}{z^2}\right)f_n = 0 \tag{2.3.75}$$

and similar for the other fields. Performing some modifications, one can actually see, that these differential equations equal Bessel equations and that solutions for the KK-fields can generally be expressed in terms of Bessel functions. However, for a better handling these fields are defined in terms of sine- and cosine-like functions which are a combination of these Bessel functions. They read [91]

$$C_c(z) \equiv \frac{\pi}{2} m_n R \left(\frac{z}{R}\right)^{c+\frac{1}{2}} \left(Y_{c-\frac{1}{2}}(m_n R) J_{c+\frac{1}{2}}(m_n z) - J_{c-\frac{1}{2}}(m_n R) Y_{c+\frac{1}{2}}(m_n z)\right) \quad (2.3.76)$$

$$S_c(z) \equiv \frac{\pi}{2} m_n R \left(\frac{z}{R}\right)^{c+\frac{1}{2}} \left(J_{c+\frac{1}{2}}(m_n R) Y_{c+\frac{1}{2}}(m_n z) - Y_{c+\frac{1}{2}}(m_n R) J_{c+\frac{1}{2}}(m_n z)\right), \quad (2.3.77)$$

with J and Y being Bessel functions of the first and second kind. The most important properties of these functions are $S_c(R) = 0$, $C_c(R) = 1$, $S'_c(R) = m_n$ and $C'_c(R) = 0$, which will become very useful in the following. The KK-modes in this basis yield

$$s_n(z) = \left(\frac{R}{z}\right)^{c_\psi - 2} \left(A_n C_{c_\psi}(z) + B_n S_{c_\psi}(z)\right) \quad (2.3.78)$$

$$f_n(z) = \left(\frac{R}{z}\right)^{-c_\psi - 2} \left(C_n C_{-c_\psi}(z) + D_n S_{-c_\psi}(z)\right) \quad (2.3.79)$$

$$g_n(z) = \left(\frac{R}{z}\right)^{c_\chi - 2} \left(F_n C_{c_\chi}(z) + G_n S_{c_\chi}(z)\right) \quad (2.3.80)$$

$$t_n(z) = \left(\frac{R}{z}\right)^{-c_\chi - 2} \left(H_n C_{-c_\chi}(z) + I_n S_{-c_\chi}(z)\right). \quad (2.3.81)$$

For a detailed derivation the reader is referred to Appendix B.4. From the mixed differential equations 2.3.73 and 2.3.74 evaluated at the UV-brane $z = R$, the 4 constraints

$$A_n = -D_n \qquad B_n = C_n \qquad F_n = -I_n \qquad G_n = H_n \quad (2.3.82)$$

are obtained, whereas for the other four one again has to look at the modified boundary conditions. This, however, will be delayed until the full sMCHM$_5$ setup has been realized.

For now, it is interesting to investigate how SM candidates like the t_R can be identified in general . To do so, $(-,-)$ BCs are chosen for its spinor partner (i.e. $\chi_{|_{R,R'}} = 0$) which leads to the conditions $F_n = 0$ and $S_{c_\chi}(R') = 0$. The latter constraint is fulfilled initially at $m_0 = 0$, inducing a zero-mode for t_n and not for the $g_0 = 0$ (since $S_{c_\chi}(z)_{|_{m_n=0}} = 0 \ \forall z, c_\chi$). This is expected since t_R now has $(+,+)$ BCs. With $C_{-c_\chi}(z)_{|_{m_n=0}} = 1 \ \forall z, c_\chi$ this zero-mode is then given by

$$t_0(z) = H_0 \left(\frac{R}{z}\right)^{-c_\chi - 2} \quad (2.3.83)$$

and can be identified with the t_R SM particle of the 4D theory. If one had chosen $(\pm,\mp)$ BCs, there would not have been a zero-mode for either of the two spinors. The H_0 can be determined by canonical normalization

$$\int_R^{R'} \mathrm{d}z \left(\frac{R}{z}\right)^5 \frac{z}{R} H_0^2 \left(\frac{R}{z}\right)^{-2c_\chi - 4} \stackrel{!}{=} 1, \quad (2.3.84)$$

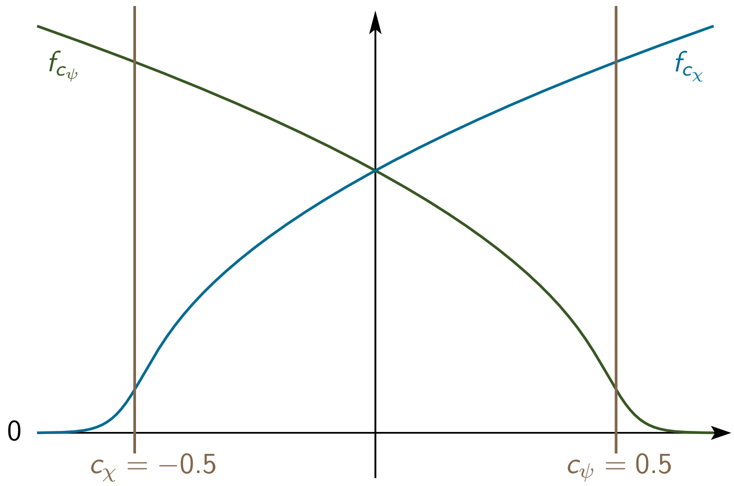

Figure 2.9: Illustration of the behavior of the f_{c_χ} (blue) and f_{c_ψ} (green) for different bulk mass parameters c_χ and c_ψ. Also displayed are the boundaries (brown) which discriminate between UV- and IR-localized fermions for both cases. The range $c_\chi, c_\psi \in [-0.5, 0.5]$ defines the region, where both, left- and right-handed fermion fields ar IR-localized. For $R = 10^{-16}\,\mathrm{TeV}^{-1}$ and $R' = \mathcal{O}\big(1\,\mathrm{TeV}^{-1}\big)$ the f_{c_ψ}, f_{c_χ} parameters are of $\mathcal{O}(1)$ in the presumed range.

where the first term is just the square root of the gamma matrix, the second denotes the vielbein and the last one is t_0^2. The solution is given by

$$H_0 = \frac{\sqrt{1+2c_\chi}}{\sqrt{R}\sqrt{\left(\frac{R}{R'}\right)^{1+2c_\chi} - 1}}, \tag{2.3.85}$$

which makes it possible to rewrite the zero mode for the t_R in a more convenient way

$$t_0(z) = \frac{f_{c_\chi}}{\sqrt{R'}}\left(\frac{z}{R}\right)^2\left(\frac{z}{R'}\right)^{c_\chi}, \tag{2.3.86}$$

with [81]

$$f_{c_\chi} \equiv \sqrt{\frac{1+2c_\chi}{1-\left(\frac{R}{R'}\right)^{1+2c_\chi}}}. \tag{2.3.87}$$

What can be seen from this equation and will generally be true for all fermions, is that the localization of the fermions in the bulk is dependent on the parameter c_k of their bulk mass. Right-handed particles like the t_R are localized near the UV-brane if $c_\chi < -1/2$ and near the IR-brane for $c_\chi > -1/2$. This can be made transparent by removing either of the branes and see for which values of c_χ the zero-mode remains normalizable. After removal of the IR-brane by taking $R' \to \infty$, H_0 stays finite for $c_\chi < -1/2$ and is thus UV-localized. The opposite is true if the UV-brane is removed by taking $R \to 0$. For left-handed particles the same is true for $c_\psi > 1/2$ (UV) and $c_\psi < 1/2$ (IR). This becomes evident by switching the boundary conditions and repeating the calculation.[21]

Since UV-localized fermions correspond to elementary (and therefore light) particles in the 4D theory, which implies that they do not contribute much to the Higgs mass, the bulk mass parameter range will be constraint to $-1/2 < c < 1/2$ for all fermions in the following discussion. As can be seen from Figure 2.9, the f_{c_χ} and f_{c_ψ} parameters control the localization of the fermions within the bulk defining their degree of compositeness in the 4D analogon. Therefore, it makes sense to identify them with the mixing angles $\sin\theta_{t_R}$, $\sin\theta_{t_L}$ of the fermions with their partners.

2.4 The sMCHM$_5$ setup on an AdS$_5$ space

After discussing general features of extra-dimensional models along with AdS/CFT duality it is time to map the sMCHM$_5$ in 4 dimensions onto an AdS$_5$ setup with the previously used metric

$$\mathrm{d}s^2 = \left(\frac{R}{z}\right)^2 (\eta_{\mu\nu}\mathrm{d}x^\mu \mathrm{d}x^\nu - \mathrm{d}z^2). \tag{2.4.1}$$

Starting with the gauge sector, it is convenient to continue implementing the new vector-like fermions and the top quark. Finally, the potential for a radiatively generated Higgs boson, used to calculate the new fermionic contributions to the Higgs mass, is discussed.

2.4.1 Symmetry breaking via SM gauge fields

A bulk symmetry $\mathcal{G} = SO(5)\times U(1)_X$ is broken to $\mathcal{G}_{\mathrm{EW}} = SU(2)_R \times U(1)_Y$ on the UV-brane and to $\mathcal{H} = SO(4)\times U(1)_X$ on the IR-brane. The breaking happens through BCs of the corresponding gauge fields. Due to the isomorphism $SO(4) \cong SU(2)_L \times SU(2)_R$, the L^a_μ and R^a_μ, $a = 1,2,3$, will be denoted as the gauge fields of $SU(2)_L$ and $SU(2)_R$, respectively. The $C^{\hat{a}}_\mu$, $\hat{a} = 1,2,3,4$, are the gauge fields of the coset $SO(5)/SO(4)$ and X_μ the one of the $U(1)_X$ symmetry. In order to break the symmetries in a correct manner, the boundary conditions are chosen to be

$$L^a_\mu(+,+) \quad R^b_\mu(-,+) \quad B_\mu(+,+) \quad Z'_\mu(-,+) \quad C^{\hat{a}}_\mu(-,-) \tag{2.4.2}$$

$b = 1,2$, with generators as in Eq. 2.3.16.[22] The B_μ and the Z'_μ are linear combinations of

$$B_\mu = s_\phi R^3_\mu + c_\phi X_\mu \qquad Z'_\mu = c_\phi R^3_\mu - s_\phi X_\mu, \tag{2.4.3}$$

with

$$c_\phi = \frac{g_5}{\sqrt{g_5^2 + g_X^2}} \qquad s_\phi = \frac{g_X}{\sqrt{g_5^2+g_X^2}}, \tag{2.4.4}$$

[21] The zero mode for the s_L is similar and can be obtained by replacing c_χ with $-c_\psi$ (especially $f_{c_\psi} = f_{-c_\chi}$).

[22] The same setup as in [45] is used here.

where the g_5 and g_X are the dimensionful couplings of the forces associated with the $SO(5)$ and $U(1)_X$ symmetries. The covariant derivative can, therefore, be written as

$$D_M = \partial_M - ig_5 T_L^a L_M^a - ig_5 T_R^b R_M^b - ig_Y Y B_M - i\frac{g_Y}{c_\phi s_\phi}(T_R^3 - s_\phi^2 Y) Z'_M - ig_5 \hat{T}^{\hat{a}} C_M^{\hat{a}}, \quad (2.4.5)$$

with $g_Y = g_5 s_\phi$ the reduced coupling strength of B_M through mixing. As in the 4D model $Y = T_R^3 + X$ denotes the SM hypercharge.

It can be observed that at low energies only the zero-modes of the L_μ^a, B_μ and $C_5^{\hat{a}}$ are present, which can be identified with the SM $W_\mu^{1,2,3}$ and B_μ fields as well as the complex Higgs doublet $\boldsymbol{H}$. EWSB then happens like in the SM at scale v giving rise to the massive $W^\pm$ and Z vector bosons, the massless A_μ photon field and the physical Higgs boson h. Fixing $1/R \sim 10^{16}\,\text{TeV} = M_{\text{Pl}}$ as a Λ_{UV} cut-off at the Planck scale and keeping $1/R' \sim \mathcal{O}(1\,\text{TeV})$, the parameters s_ϕ, g_5 and $\tilde{v}$ as the VEV of the fourth component of $\boldsymbol{\Pi}$ are determined by the well-measured parameters α_{QED}, $\sin^2\theta_W$ and m_W. The remaining free parameter R' sets the scale f of the CHM.

To see how these parameters are related, one can look at the Goldstone matrix which has been identified with the Wilson line in Section 2.3.3. Using the vacuum choice of Section 2.2.2, the 4D Goldstone matrix looks like

$$U^\dagger[\boldsymbol{\Pi}] = e^{-i\frac{\sqrt{2}}{f}\Pi_{\hat{a}}(x)\hat{T}^{\hat{a}}} = e^{-i\frac{\sqrt{2}}{f}(\tilde{v}+h(x))\hat{T}^{\hat{4}}}, \quad (2.4.6)$$

with $T^{\hat{4}}$ the broken generator defined in 2.2.3. Setting $C_5^{\hat{a}(0)}(x,z) = f_h^{\hat{a}}(z)\Pi^{\hat{a}}(x)$, this can be compared to the Wilson line of Eq. 2.3.22 in almost axial gauge in warped space

$$\begin{aligned} W_{\text{IR}}(x) &= \exp\left(-ig_5 \int_R^{R'} \mathrm{d}z\, C_5^{\hat{a}(0)}(x,z)\hat{T}^{\hat{a}}\right) = \exp\left(-ig_5 \Pi_{\hat{a}}(x)\hat{T}^{\hat{a}} \int_R^{R'} \mathrm{d}z\, f_h^{\hat{a}}(z)\right) \\ &= \exp\left(-ig_5(\tilde{v}+h(x))\hat{T}^{\hat{4}} \int_R^{R'} \mathrm{d}z\, f_h^{\hat{4}}(z)\right) \stackrel{!}{=} e^{-i\frac{\sqrt{2}}{f}(v+h(x))\hat{T}^{\hat{4}}} \end{aligned} \quad (2.4.7)$$

identifying

$$f \equiv \left[\frac{g_5}{\sqrt{2}} \int_R^{R'} \mathrm{d}z\, f_h^{\hat{4}}(z)\right]^{-1}. \quad (2.4.8)$$

In order to calculate $f_h^{\hat{4}}(z)$ it is necessary to look at the action for the gauge bosons in general, given by

$$S_A = -\frac{1}{4}\int \mathrm{d}^5x\sqrt{G}g^{MR}g^{NS}F_{MN}F_{RS}, \quad (2.4.9)$$

with $F_{MN} = \partial_M A_N - \partial_N A_M$ neglecting the self interactions.[23] By performing a KK-decomposition of the fields

$$A_\mu(x,z) = \sum_n A_\mu^{(n)}(x)\zeta_n(z), \quad A_5(x,z) = \sum_n A_5^{(n)}(x)\vartheta_n(z), \quad (2.4.10)$$

[23] The A_M^A are as before the 5D gauge fields of $SO(5)$ whose indices $A = 1, ..., 10$ are suppressed.

the fifth dimension can be integrated out to obtain the equations of motion as well as the required relations between the 5D base functions ζ_n and ϑ_n. The decomposed action yields

$$\begin{aligned}
S_A =& -\frac{1}{4}\int \mathrm{d}^5x \frac{R}{z}\Big[F_{\mu\nu}F^{\mu\nu} - 2F_{\nu 5}F^{\nu}{}_5\Big] \\
=& -\frac{1}{4}\sum_{n,m}\int \mathrm{d}^5x\frac{R}{z}\Big(\partial_\mu A_\nu^{(n)} - \partial_\nu A_\mu^{(n)}\Big)\Big(\partial^\mu A^{(m)\nu} - \partial^\nu A^{(m)\mu}\Big)\zeta_n\zeta_m \\
&+ \frac{1}{2}\sum_{n,m}\int \mathrm{d}^5x\frac{R}{z}\Big(\vartheta_n\partial_\mu A_5^{(n)} - A_\mu^{(n)}\partial_5\zeta_n\Big)\Big(\vartheta_m\partial^\mu A_5^{(m)} - A^{(m)\mu}\partial_5\zeta_m\Big) \\
=& -\frac{1}{4}\sum_{n,m}\int \mathrm{d}^4x\left(\int_R^{R'}\mathrm{d}z\frac{R}{z}\zeta_n\zeta_m\right)F_{\mu\nu}^{(n)}F^{(m)\mu\nu} && (2.4.11)\\
&+ \frac{1}{2}\sum_{n,m}\int \mathrm{d}^4x\left(\int_R^{R'}\mathrm{d}z\big(-\partial_5\big(R/z\partial_5\big)\zeta_n\big)\zeta_m\right)A_\mu^{(n)}A^{(m)\mu} && (2.4.12)\\
&- \frac{1}{2}\sum_{n,m}\int \mathrm{d}^4x\left(\int_R^{R'}\mathrm{d}z\big(-\partial_5(R/z\vartheta_n)\big)\zeta_m\right)2\partial_\mu A_5^{(n)}A^{(m)\mu} && (2.4.13)\\
&+ \frac{1}{2}\sum_{n,m}\int \mathrm{d}^4x\left(\int_R^{R'}\mathrm{d}z\frac{R}{z}\vartheta_n\vartheta_m\right)\partial_\mu A_5^{(n)}\partial^\mu A_5^{(m)} && (2.4.14)\\
&+ \frac{1}{2}\sum_{n,m}\int \mathrm{d}^4x\left[\frac{R}{z}\Big(\partial_5\zeta_n\zeta_m A_\mu^{(n)} + 2\vartheta_n\zeta_m A_5^{(n)}\partial_\mu\Big)A^{(m)\mu}\right]_R^{R'} && (2.4.15)\\
\stackrel{!}{=}& \sum_n\int \mathrm{d}^4x\Big(-\frac{1}{4}F_{\mu\nu}^{(n)}F^{(n)\mu\nu} + \frac{1}{2}m_n^2A_\mu^{(n)}A^{(n)\mu} - m_n\partial_\mu A_5^{(n)}A^{(n)\mu} \\
&\qquad + \frac{1}{2}\partial_\mu A_5^{(n)}\partial^\mu A_5^{(n)}\Big), && (2.4.16)
\end{aligned}$$

where the terms 2.4.12 and 2.4.13 have been partially integrated, resulting in the boundary action term 2.4.15. This can be identified with a tower of 4D gauge field theories as displayed in Eq. 2.4.16 given the following properties of the basis functions.[24] The first requirement from the A_μ kinetic term 2.4.11 is the usual orthonormalization requirement for the ζ_n

$$\int_R^{R'}\mathrm{d}z\frac{R}{z}\zeta_n(z)\zeta_m(z) = \delta_{mn}. \tag{2.4.17}$$

The second requirement coming from the A_μ mass term 2.4.12

$$-\frac{z}{R}\partial_5\left(\frac{R}{z}\partial_5\right)\zeta_n = -\partial_5^2\zeta_n + \frac{1}{z}\partial_5\zeta_n = m_n^2\zeta_n \tag{2.4.18}$$

[24] These requirements can be also derived via the variational principle (see Appendix B.6) as for the fermionic fields.

provides the equation of motion for the ζ_n with the solutions

$$\zeta_n(z) = A_n C(z) + B_n S(z), \tag{2.4.19}$$

where the $C(z)$ and $S(z)$ are the warped trigonometric functions defined in Eq. 2.3.76 and 2.3.77 with $c = 1/2$ (see Appendix B.5 for the derivation). It has been shown in Section 2.3.2 that the A_μ and A_5 components of A_M are linked through the gauge parameter α. Therefore, the ζ_n and ϑ_n are expected to be dependent on each other. In order for the mode-mixing term 2.4.13 to look like 4D gauge fields the relation between these modes takes its standard form

$$-\frac{z}{R}\partial_5\left(\frac{R}{z}\vartheta_n\right) = -\partial_5\vartheta_n + \frac{1}{z}\vartheta_n = m_n\zeta_n. \tag{2.4.20}$$

Using equation 2.4.18 it can be seen that this is fulfilled for

$$\vartheta_n(z) = \frac{1}{m_n}\partial_5\zeta_n(z). \tag{2.4.21}$$

The orthonormalization requirement for the ϑ in term 2.4.14

$$\int_R^{R'} \mathrm{d}z \frac{R}{z}\vartheta_n(z)\vartheta_m(z) = \delta_{mn} \tag{2.4.22}$$

is then fulfilled automatically with the previous relations 2.4.17, 2.4.18 and 2.4.21.

The boundary action simply vanishes for $(+)$ or $(-)$ BCs conditions for the A_μ (also fixing the BCs for A_5). Imposing $(+,+)$ BCs as for the unbroken L^a_μ and B_μ fields induces $(-,-)$ BCs for the L^a_5 and B_5 fields. The KK-decomposition for e.g. L^a_M then looks like

$$L^a_\mu(x,z) = \sum_n L^{a(n)}_\mu(x) l^a_n(z), \quad L^a_5(x,z) = \sum_n L^{a(n)}_5(x)\frac{\partial_5 l^a_n(z)}{m_n}, \tag{2.4.23}$$

where all $L^{a(n)}_5$ modes can be gauged away due to the lack of a zero-mode ($\vartheta_0 = 0$ in this case). For the spontaneously broken generators $C^{\hat a}_M$, the BCs are turned around. This time the $C^{\hat a}_5$ acquire zero-modes which cannot be gauged away as discussed earlier and which will be identified with the components of a 4D composite pNGB Higgs. In the KK-decomposition

$$C^{\hat a}_\mu(x,z) = \sum_n C^{\hat a(n)}_\mu(x) c^{\hat a}_n(z), \quad C^{\hat a}_5(x,z) = f^{\hat a}_h(z)\Pi^{\hat a}(x) + \sum_n C^{\hat a(n)}_5(x)\frac{\partial_5 c^{\hat a}_n(z)}{m_n} \tag{2.4.24}$$

these zero-modes $C^{\hat a(0)}_5(x,z) = f^{\hat a}_h(z)\Pi^{\hat a}(x)$ have been singled out. The $f^{\hat a}_h(z)$ components can now be calculated via Eq. 2.4.20 with $\zeta_0 = 0$

$$\partial_5 f^{\hat a}_h(z) = \frac{1}{z} f^{\hat a}_h(z) \quad \Rightarrow \quad f^{\hat a}_h(z) = c^{\hat a}_h\frac{z}{R}, \tag{2.4.25}$$

where the $c_h^{\hat{a}}$ can be fixed by Eq. 2.4.22 yielding

$$c_h^{\hat{a}} = \left[\int_R^{R'} \mathrm{d}z \frac{z}{R}\right]^{-1/2} = \frac{\sqrt{2R}}{\sqrt{R'^2 - R^2}}. \tag{2.4.26}$$

This makes it possible to derive the desired relation between the breaking scale f and R' by inserting $f_h^{\hat{4}}(z)$ into Eq. 2.4.8. In terms of the dimensionless coupling $g_* = g_5/\sqrt{R}$

$$f \equiv \frac{2\sqrt{R}}{g_5\sqrt{R'^2 - R^2}} \approx \frac{2}{g_* R'} \tag{2.4.27}$$

is obtained, where $R' \gg R$. The prior constant g_*, which corresponds to the number of colors

$$N_{\mathrm{CFT}} = \frac{16\pi^2}{g_*^2} \tag{2.4.28}$$

of the UV-theory in the 4D CFT, is thus fixed for a fixed scale f and AdS expansion parameter R'. Since the AdS/CFT duality only holds for large N_{CFT}, g_* has to be chosen accordingly.

The next task is to match the coupling strengths of the SM to the g_5 and g_X of the 5D theory. As can be seen from the covariant derivative in Eq. 2.4.5, the elementary fermions couple on the UV-brane with strength g_5 to the W_μ^a and with reduced strength g_Y to the B_μ field. For a 4D observer on the IR-brane this coupling strength appears to be suppressed by the length of the extra-dimension, e.g. $g_{4\mathrm{D}}^2 = g_{5\mathrm{D}}^2/L$ which is defined in Eq. B.1.5 for a warped AdS_5 space. Therefore, at leading order

$$g^2 \equiv \frac{g_5^2}{R\ln\frac{R'}{R}}, \quad g'^2 \equiv \frac{g_Y^2}{R\ln\frac{R'}{R}} \tag{2.4.29}$$

can be identified as the SM gauge couplings.[25] Making use of the SM relations $g^2 = e^2/\sin^2\theta_W$, $g'^2 = e^2/\cos^2\theta_W$ and $e^2 = 4\pi\alpha_{\mathrm{QED}}$, this of course also fixes g_* which means that R' and f are now in one-to-one correspondence. Fortunately, one can soften this relation by introducing kinetic boundary terms for the SM gauge fields

$$S_{\mathrm{A}}^{\mathrm{UV}} = \int \mathrm{d}^4x \left[-\frac{1}{4}\kappa^2 R\ln\frac{R'}{R} L_{\mu\nu}^a L^{a\mu\nu} - \frac{1}{4}\kappa'^2 R\ln\frac{R'}{R} B_{\mu\nu}B^{\mu\nu}\right], \tag{2.4.30}$$

with κ, κ' being dimensionless parameters which alter the coupling strengths [45] (see also [92]). To good approximation it can be concluded

$$g_5^2 \approx \frac{e^2}{\sin^2\theta_W} R\ln\frac{R'}{R}(1+\kappa^2), \quad g_Y^2 \approx \frac{e^2}{\cos^2\theta_W} R\ln\frac{R'}{R}(1+\kappa'^2) \tag{2.4.31}$$

as well as

$$s_\phi^2 = \frac{g_Y^2}{g_5^2} \approx \tan^2\theta_W \frac{1+\kappa'^2}{1+\kappa^2}. \tag{2.4.32}$$

[25] See also [89] for a more quantitative approach.

The Higgs VEV $\langle\Pi\rangle = \tilde{v}$ can be obtained as in the 4D theory through the breaking scale f via Eq. 2.2.21

$$m_W^2 \approx \frac{v^2 g^2}{4} = \frac{e^2 f^2}{4\sin^2\theta_W}\sin^2\left(\frac{\tilde{v}}{f}\right) \quad \Leftrightarrow \quad \sin^2\left(\frac{\tilde{v}}{f}\right) \approx \frac{4\sin^2\theta_W}{e^2}\frac{m_W^2}{f^2}. \tag{2.4.33}$$

The κ and κ' do also alter the boundary conditions of the corresponding gauge fields and thus the gauge contribution to the Higgs potential, which will be seen later.

2.4.2 Fermions in the 5D sMCHM$_5$

It is convenient to introduce full $SO(5)\times U(1)_X$ multiplets for the top quark and the new vector-like f 5D fields in fundamental $\mathbf{5}_{2/3}$ representation. The embedding is the same in Eq. 2.2.45, rotated into a basis where the T_R^3 and T_L^3 generators are diagonal.[26] This has the benefit that the fermions do not mix within the multiplet and can be achieved by using the unitary matrix

$$A = \frac{1}{\sqrt{2}}\begin{pmatrix} 1 & -i & 0 & 0 & 0 \\ 0 & 0 & -i & 1 & 0 \\ 0 & 0 & i & 1 & 0 \\ -1 & -i & 0 & 0 & 0 \\ 0 & 0 & 0 & 0 & \sqrt{2} \end{pmatrix} \tag{2.4.34}$$

transforming

$$\tilde{T} \to T = A\cdot\tilde{T}\cdot A^\dagger, \quad \tilde{T} \in \{T_L^a, T_R^a, \hat{T}^{\hat{a}}\} \tag{2.4.35}$$

$$\tilde{\psi} \to \psi = A\tilde{\psi}, \quad \tilde{\psi} \in \{\psi_L, \psi_R\}. \tag{2.4.36}$$

The incomplete $SO(5)$ multiplets in the 4D MCHM$_5$ correspond in the 5D to different BCs on the components of the multiplet, projecting out unwanted zero modes

$$\textbf{MCHM}_5\textbf{:} \qquad \psi_L = \begin{pmatrix} w_L[-,+] \\ q_L[+,+] \\ s_L[-,+] \end{pmatrix}, \quad \psi_R = \begin{pmatrix} w_R[-,+] \\ v_R[-,+] \\ t_R[+,+] \end{pmatrix}. \tag{2.4.37}$$

In fact, the BCs are chosen such that only the q_L and t_R have zero-modes which can be identified with the SM particles. In the sMCHM$_5$ the BCs become univeral

$$\textbf{sMCHM}_5\textbf{:} \qquad \psi_L = \begin{pmatrix} w_L[+,+] \\ q_L[+,+] \\ s_L[+,+] \end{pmatrix}, \quad \psi_R = \begin{pmatrix} w_R[+,+] \\ v_R[+,+] \\ t_R[+,+] \end{pmatrix}. \tag{2.4.38}$$

Here, the additional fields s, v and w which, so far, have not been observed in nature, are uplifted via UV boundary masses. Like in Section 2.3.6, the fields are embedded into 5D Dirac spinors

$$\Psi_1 = \begin{pmatrix} \psi_L \\ \bar{\psi} \end{pmatrix}, \quad \Psi_2 = \begin{pmatrix} \chi \\ \bar{\psi}_R \end{pmatrix}. \tag{2.4.39}$$

[26] This can be done simultaneously because the operators commute $[T_L^3, T_R^3] = 0$.

with the difference that each constituent of the spinors is now a full multiplet.[27] The action is the same as in Eq. 2.3.66, such that the solutions to the bulk equations of motion are also equivalent to the ones in Eq. 2.3.78-2.3.81 for all $\bar{\psi}^i_L$, ψ^i_R pairs, $i = 1, ..., 5$. In general, this statement does not hold since the presence of the Higgs would mix the particles in the bulk. However, as derived in Section 2.3.3, one can remove the Higgs from the bulk by performing a Wilson line transformation towards the IR-brane

$$\Omega(x,z) = \exp\left(-ig_5 \int_R^z \mathrm{d}z' C_5^{\hat{4}(0)}(x,z')\hat{T}^{\hat{4}}\right) = \exp\left(-i\frac{\sqrt{2}}{f(z)}(\tilde{v}+h(x))\hat{T}^{\hat{4}}\right), \quad (2.4.40)$$

with

$$f(z) = \frac{2\sqrt{R}}{g_5}\frac{\sqrt{R'^2-R^2}}{z^2-R^2} = \begin{cases} \frac{2}{g_* R'} \equiv f & \text{for} \quad z \to R' \\ \infty & \text{for} \quad z \to R \end{cases}. \quad (2.4.41)$$

The IR-localized Higgs only imposes changes to the BCs of the fermions via interaction terms at $z = R'$

$$S_{\mathrm{IR}} = \int \mathrm{d}^4x \sqrt{-g_{\mathrm{IR}}} \left[\bar{\Psi}_1 \begin{pmatrix} C_{12} & 0 \\ 0 & C_{12} \end{pmatrix} \Psi_2 + \bar{\Psi}_2 \begin{pmatrix} C_{12} & 0 \\ 0 & C_{12} \end{pmatrix} \Psi_1 \right]_{z=R'}, \quad (2.4.42)$$

where $\sqrt{-g_{\mathrm{IR}}} = (R/R')^4$ is the 4D squared metric determinant and $C_{12} = \mathrm{diag}(c_1, c_1, c_1, c_1, c_2)$ parametrizes the interaction terms between the left- and right-handed fermion fields $\psi = W^\dagger_{\mathrm{IR}}(x)\psi'$ which have to be transformed by the Wilson line $W_{\mathrm{IR}}(x) \equiv \Omega(x, R')$ into the h-independent bulk fields. For $c_1 = c_2$ the Higgs effectively decouples. With the KK-decompositions

$$\psi^i_L = \sum_n t^i_{\mathrm{L},n}(z)\chi^i_n(x) \qquad \bar{\psi}^i = \sum_n f^i_n(z)\bar{\psi}^i_n(x) \quad (2.4.43)$$

$$\chi^i = \sum_n g^i_n(z)\chi^i_n(x) \qquad \bar{\psi}^i_R = \sum_n t^i_{\mathrm{R},n}(z)\bar{\psi}^i_n(x) \quad (2.4.44)$$

$i = 1, ..., 5$, the new boundary conditions on the IR-brane yield

$$W^\dagger_{\mathrm{IR}}(x)G_n(z)_{|R'} = +C_{12}W^\dagger_{\mathrm{IR}}(x)T_{L,n}(z)_{|R'} \quad (2.4.45)$$

$$W^\dagger_{\mathrm{IR}}(x)F_n(z)_{|R'} = -C_{12}W^\dagger_{\mathrm{IR}}(x)T_{R,n}(z)_{|R'}, \quad (2.4.46)$$

where $G_n(z) = (g^1_n(z), g^2_n(z), g^3_n(z), g^4_n(z), g^5_n(z))^T$ and equivalent for the other functions.[28] Note that the Wilson line $W_{\mathrm{IR}}(x)$ equals the Goldstone matrix $U[\mathbf{\Pi}]$ in Eq. 2.2.35 rotated by the unitary matrix A of Eq. 2.4.34.

Because of $\Omega(x, R) = 1$, the Wilson line transformation does not effect the UV-brane. Therefore, the imposed BCs at $z = R$ still read

$$f^i_{n|R} = 0 \quad \text{for} \quad i = 3, 4 \qquad g^i_{n|R} = 0 \quad \text{for} \quad i = 5 \quad (2.4.47)$$

$$t^i_{\mathrm{L},n|R} = 0 \quad \text{for} \quad i \neq 3, 4 \qquad t^i_{\mathrm{R},n|R} = 0 \quad \text{for} \quad i \neq 5. \quad (2.4.48)$$

[27] The resulting lack of localization parameters which leads to conflicts with experimental constraints makes it unfavorable to embed ψ_L and ψ_R into a single spinor.

[28] For a derivation of the BCs for just one fermion pair, see Appendix C.2 in [90].

This can be changed by introducing vector-like mass terms for the new 5D fermions via interactions of the w_L, v_R, and s_L with their chiral partners on the UV-brane. While the w_L and w_R just mix at $z = R$, the v_L doublet as well as the s_R singlet have to be induced as UV-localized 4D particles since they are not part of the multiplets. Therefore, the UV action reads

$$S_{\text{UV}} = \int \mathrm{d}^4x \Big[- i s_R \sigma^\mu \partial_\mu \bar{s}_R - i \bar{v}_L \bar{\sigma}^\mu \partial_\mu v_L + \frac{c_s}{\sqrt{R}} (s_R s_L + \bar{s}_L \bar{s}_R) \\ + \frac{c_v}{\sqrt{R}} (v_R^T v_L + \bar{v}_L \bar{v}_R^T) + c_w (w_R^T w_L + \bar{w}_L \bar{w}_R^T) + h.c. \Big]_{z=R}, \tag{2.4.49}$$

with c_s, c_v and c_w being the dimensionless mass parameters of the new fermions. Note that the first two interaction terms have to be scaled with $R^{-1/2}$ because of the lower mass dimension of the localized 4D particles ($[s_R] = [v_L] = 3/2$ and $[s_L] = [v_R] = [w_L] = [w_R] = 2$). Including the new BCs which can be derived for each pair like in Section 2.3.5, the free parameters of the solutions in Eq. 2.3.78-2.3.81 for each pair read

$$\begin{aligned} A_n^{1,2} &= -\frac{1}{c_w} F_n^{1,2} & G_n^{1,2} &= \frac{1}{c_w} B_n^{1,2} \\ B_n^{3,4} &= 0 & G_n^{3,4} &= -\frac{m_n R}{c_v^2} F_n^{3,4} \\ A_n^5 &= \frac{m_n R}{c_s^2} B_n^5 & F_n^5 &= 0, \end{aligned} \tag{2.4.50}$$

with the relations to C_n^i, D_n^i, H_n^i and I_n^i given in Eq. 2.3.82. Using the BCs in Eq. 2.4.45 and 2.4.46, the system of linear equations consisting of the remaining parameters $B_n^{1,2,5}$, $A_n^{3,4}$, $F_n^{1,2,3,4}$ and G_n^5 can be solved for m_n by looking at the roots of the matrix determinant $\det M_t = 0$ as in Eq. 2.3.59 and 2.3.60. The lightest of these roots can be identified with the top mass $m_0 \equiv m_t$ at $h = 0$.[29] The subsequent m_n, $n \geq 1$ represent the masses of the top partners in the 4D model.

2.4.3 The Higgs Potential

Knowing how to obtain the masses for the top as well as its partners in the 5D model, the final step of the analysis is to calculate the Higgs potential and, thereover, the mass of the Higgs boson in the sMCHM$_5$ model. In the extra-dimensional model, there is no Higgs potential present at tree level. This effect also explains its light mass in these models compared to the physical scale. The Higgs is introduced radiatively via the non-local Wilson line operator. Thus, the potential can be approximated by a mechanism first discovered by S. Coleman and E. Weinberg [93]. The so-called *Coleman-Weinberg potential* for a KK-tower looks like

$$V(h) \supset \frac{N_r}{2} \sum_{n=1}^{\infty} \int \frac{\mathrm{d}^4 p}{(2\pi)^4} \ln \left(p^2 + m_n^2(h)\right), \tag{2.4.51}$$

[29] The b quark remains massless, because a multiplet containing b_R has not been introduced, which would allow for Yukawa terms after mixing with the Higgs on the IR-brane.

with N_r corresponding to the degrees of freedom of the resonance ($N_r = +3$ for gauge fields and $N_r = -4$ for fermion fields). The full expression can be rewritten (see e.g. [91, 94, 95]) in terms of a sum over different KK-towers

$$V(h) = \sum_r \frac{N_r N_c}{(4\pi)^2} \int_0^\infty \mathrm{d}p\, p^3 \ln \rho_r(-p^2), \tag{2.4.52}$$

with N_c the number of colors ($N_c = 3$ for quarks and $N_c = 1$ for all other particles) and $\rho_r(-p^2)$ being the spectral functions of the resonances with roots at $m_{n;r}^2(h)$. They can be expressed through the coefficient matrices M_r of the gauge and fermion fields

$$\rho(m_{n;r}^2(h)) = \frac{\det M_r(h)}{\det M_r(-\tilde{v})} \overset{!}{=} 0 \quad \forall\, n \in \mathbb{N}, \tag{2.4.53}$$

where $\det M_r(-\tilde{v})$ denotes the Higgs independent term over which is normalized. The Coleman-Weinberg potential for this case yields

$$V(h) = V_g(h) + \sum_f V_f(h) \approx V_g(h) + V_t(h), \tag{2.4.54}$$

where the top quark KK-tower is expected to have the dominant contribution such that all other fermions can be neglected. The gauge potential is defined as

$$V_g(h) = \frac{3}{(4\pi)^2} \int \mathrm{d}p\, p^3 \left[2 \ln \rho_W(-p^2) + \ln \rho_Z(-p^2)\right]. \tag{2.4.55}$$

For the $W^\pm$ and Z bosons, the spectral functions look like

$$\rho_{W,Z}(-p^2) = 1 + f_{W,Z}(-p^2) s_h^2, \tag{2.4.56}$$

with $s_h^2 \equiv \sin^2((\tilde{v} + h)/f)$ and coefficients

$$f_W(-p^2) = \frac{ip}{2}\frac{R'}{R}\frac{1}{S(R')(C'(R') - ipR\ln(R'/R)\kappa^2 S'(R'))} \tag{2.4.57}$$

$$\begin{aligned} f_Z(-p^2) =& \frac{ip}{2}\frac{R'}{R}\left[\frac{1}{S(R')(C'(R') - ipR\ln(R'/R)\kappa^2 S'(R'))}\right. \\ &\left. + \frac{s_\phi^2}{S(R')(C'(R') - ipR\ln(R'/R)\kappa'^2 S'(R'))}\right], \end{aligned} \tag{2.4.58}$$

where κ, κ' are the kinetic boundary parameters of the gauge contribution and the $S(R'), C(R')$ defined in Appendix B.5 are rewritten into functions of p (see Appendix B.6 for a full derivation of the gauge coefficients).[30] In the sMCHM$_5$ the top contribution yields

$$V_t(h) = -\frac{3}{4\pi^2} \int \mathrm{d}p\, p^3 \ln \rho_t(-p^2), \tag{2.4.59}$$

[30] Check also [96, 97] for more details.

Table 2.3: Overview of the properties between the 4D and the 5D sMCHM$_5$ model, which can be related to each other. The last two relations are evident from Eq. 2.2.38. The c_1, c_2 couple between different (5D) Dirac spinors which is also the the purpose of the a_L, b_R in the 4D which relate q_L to Q_R^t and t_R to $\tilde{T}_L^T$. The C_5 couples particles within the same multiplet as for the a_R, b_L coupling q_L to $\tilde{T}_R^T$ and t_R to Q_L^t.Taken from [45] and extended.

5D	4D
fermionic bulk fields	partial composite fermionic mass eigenstates
zero-modes of fermionic and bosonic fields	SM fermions and bosons
Length R' of the interval	breaking scale f
Higgs as the zero-mode of the fifth component of a 5D gauge field	Higgs as composite pNGB of a SSB at scale f
symmetry reduction via $(-)$ BCs of the gauge fields	symmetry reduction via partial gauging the $SO(5)$ fields
softening via changes in BCs on the UV-brane	softening via completion of the $SO(5)$ multiplet
explicit symmetry breaking via dynamical BCs	explicit symmetry breaking via vector-like mass terms
Wilson line $W_{\mathrm{IR}}(x)$	Goldstone matrix $U[\mathbf{\Pi}]$
KK-masses m_n for $n \geq 1$	m_Q, $\tilde{m}_T$
f_{c_ψ}	$y_{t_L} f/m_Q \approx \sin\theta_{t_L}$
f_{c_χ}	$y_{t_R} f/\tilde{m}_T \approx \sin\theta_{t_R}$
fermion-mass mixings on the IR-brane c_1, c_2	a_L, b_R
fixed Higgs couplings (via C_5 mode)	b_L, a_R

with

$$\rho_t(-p^2) = 1 + f_2(-p^2)s_h^2 + f_4(-p^2)s_h^4. \tag{2.4.60}$$

The $f_{2,4}(-p^2)$ coefficients are quite complicated momentum/mass dependent functions of the input parameters c_ψ, c_χ, c_1, c_2, c_s, c_v and c_w. It is, however, possible to obtain numerical solutions for the Higgs mass, which is just the second derivative of the potential evaluated at $h = 0$

$$\left.\frac{\partial^2 V(h)}{\partial h^2}\right|_{h=0} = m_H^2. \tag{2.4.61}$$

By approximation of $V(h)$ and expanding around $h = 0$ up to linear order

$$V(h) \approx -\alpha s_h^2 + \beta s_h^4 \cong -\mu^2 \boldsymbol{H}^\dagger \boldsymbol{H} + \lambda \left(\boldsymbol{H}^\dagger \boldsymbol{H}\right)^2 \tag{2.4.62}$$

it is evident, that the Coleman Weinberg potential approximately takes the SM form of the Higgs potential for appropriate values of α and β. Furthermore, one can use the observational constraints

$$m_t \sim 150\,\mathrm{GeV}, \qquad \left.\frac{\partial V(h)}{\partial h}\right|_{h=0} = 0 \tag{2.4.63}$$

to fix two of the input parameters. By doing this, it is possible to figure out how the presence of the new particles change the phase space for m_H and the top partner masses. All calculations will be performed numerically using expressions derived in Appendix B.7.

At the end of the explications regarding these two theoretical concepts, the similarities and identifications between the 4D and the 5D theory have been collected and displayed in Table 2.3. This comparison might help the reader to obtain a better overview of the recent discussion. The theoretical findings elaborated in this section will be essential for the numerical scans performed in section 3.

2.5 Solutions to fine-tuning problems in CHMs

Before starting with the mostly numerical analysis of the sMCHM$_5$, it is beneficial to look back on the motivation of its implementation first. As stated in Section 1, CHMs aim to solve the Hierarchy problem of the SM through a different view on the Higgs boson. This, however, comes at the price of (modest) fine-tuning by misaligned vacuum states. Due to the direct link between fine-tuning, naturalness and the Hierarchy problem, it is very important for CHMs to keep this inevitable fine-tuning as low as possible in order to be an attractive alternative to the SM.[31] Therefore, it is necessary to ensure first that the modifications to the MCHM$_5$ do not worsen the fine-tuning by an unacceptable amount before thinking of possibilities which might even cure it.

2.5.1 Fine-tuning in the sMCHM$_5$

The Higgs potential for CHMs can in general be written as

$$V(h) = -\alpha s_h^2 + \beta s_h^4 \tag{2.5.1}$$

[31] Too strong fine-tuning reintroduces a naturalness problem and just shifts the Hierarchy problem instead of solving it.

with $\alpha, \beta > 0$ being the parameters which control EWSB and are dependent on the specific input parameters as well as the structure of the model. The minimum condition of the potential at $h = 0$ leads to a constraint for these two contributions

$$\left.\frac{\partial V(h)}{\partial h}\right|_{h=0} = 0 \quad \Rightarrow \quad \xi = \frac{v^2}{f^2} = \frac{\alpha}{2\beta}. \tag{2.5.2}$$

As pointed out in Section 2.1.3, a separation between the EWSB scale v and the breaking scale f quantified by the parameter ξ is necessary to keep CHMs within the current experimental constraints. This separation can be achieved by introducing a *minimal* fine-tuning on the α and β parameters in order to yield Eq. 2.5.2. The amount of fine-tuning needed, is expressed by the inverse of the ratio which shall be tuned

$$\Delta_{\text{min}} = \frac{1}{\xi} = \frac{f^2}{v^2} \tag{2.5.3}$$

and present in all CHMs. Usually, a tuning of 10% corresponding to $f \sim 800\,\text{GeV}$ is sufficient for this purpose. However, in most CHMs it has been shown (explicitly in 5D holographic approaches) that the fine-tuning is actually much larger (see e.g. [45, 49, 98]). Especially the MCHM$_5$ suffers from an extended, so-called *double-tuning* [44, 99], which arises due to a hierarchy of contributions in the Higgs potential, i.e. the s_h^2 is the leading term in the potential and the s_h^4 term sub-leading. In order to obtain the desired ξ in the MCHM$_5$ one must, therefore, first tune α to be of the same order as β and in a second step tune α to be $2\xi\beta$. In this sense, one has to tune twice.

To explain why the s_h^4 term is actually sub-leading, it is useful to make a *spurion analysis* of the Higgs potential. Spurions are purely mathematical objects like numbers or matrices which are uplifted to physical fields transforming under the symmetries of the theory. Depending on their explicit form, they encode the breaking mechanism of the symmetry and thereby the mass of the Higgs particle as a pNGB of this breaking. In the following, the $\Delta_{L,R}$ matrices first encountered in Eq. 2.2.31 are used as spurions which shall transform under $SO(5)$. The trick of the analysis is to treat the spurions as full multiplets, such that the Higgs potential must be $SO(5)$ invariant under transformations including the spurions. This constraints the number of contributions consisting of spurions and the Higgs fields one can build. After writing down all possible terms which could appear in the potential, the definitions of the spurions given in Eq. 2.2.40 for the MCHM$_5$ are inserted, obtaining an estimate for $V_t(h)$.

Starting with the spurions only, it can easily be seen that only combinations of spurions can also transform under the remnant SM gauge group $\mathcal{G}_{\text{EW}}$, namely

$$(\Gamma_L)_{IJ} = (\Delta_L^*)_I^\gamma (\Delta_L)_{\gamma J}, \quad (\Gamma_R)_{IJ} = (\Delta_R^*)_I (\Delta_R)_J, \tag{2.5.4}$$

with $\gamma = 1, 2$ and $I, J = 1, ..., 5$ the $SO(5)$ indices. These Γ-spurions have the linear transformation properties

$$\Gamma_{L,R} \to g \Gamma_{L,R} g^\dagger, \quad g \in SO(5). \tag{2.5.5}$$

The Higgs in CHMs is, as shown earlier, always encoded in the Goldstone matrix $U[\mathbf{\Pi}]$, defined in Eq. 2.2.9, which transforms non-linearly under $SO(5)$ (see also Eq. 2.3.25)

$$U[\mathbf{\Pi}] \to gU[\mathbf{\Pi}]h^\dagger(\mathbf{\Pi}, g), \quad g \in SO(5), \quad h \in SO(4). \tag{2.5.6}$$

However, this can be changed by introducing the automorphism V defined by $VT^AV^\dagger = \pm T^A$ with $+$ $(-)$ for the unbroken (broken) generators T^a $(T^{\hat{a}})$.[32] Via V it is possible to construct an operator which transforms linearly under $SO(5)$

$$\Sigma \equiv U^\dagger UV \to g\Sigma g^\dagger, \quad g \in SO(5). \tag{2.5.7}$$

Larger Γ-spurion numbers correspond to higher orders in perturbation theory. Therefore, the leading term for the MCHM$_5$ will be given by insertions of only one Γ-spurion, which leaves two terms at *Leading-Order* (LO) [51]

$$V_f^{\mathrm{LO}}(h) = c_L \,\mathrm{tr}(\Sigma\Gamma_L) + c_R \,\mathrm{tr}(\Sigma\Gamma_R) = (2c_R - c_L)s_h^2. \tag{2.5.8}$$

This potential has only trivial minima, such that also the *Next-to-Leading-Order* (NLO) s_h^4 term has to be taken into account. In order to be significant in the potential, it has to have a similar size than $V_f^{\mathrm{LO}}(h)$ leading to the aforementioned double-tuning.

For the MCHM$_5$ the tuning can be estimated to [51]

$$\Delta_5 \simeq \frac{1}{\xi} \cdot 20 \left(\frac{g_\psi}{5}\right)^2, \tag{2.5.9}$$

where the 4D fermionic and bosonic mass scales translate to g_* via $g_\rho = g_\psi \approx 1.2024 g_*$ [45].[33] In order to fulfill constraints coming from the EWPOs

$$S \approx 6\pi\xi g_*^{-2} \qquad T = 0 \qquad U = 0, \tag{2.5.10}$$

it is necessary to keep $g_* \gtrsim 3.6$ making the tuning even larger for reasonable Higgs masses.[34] Taking $m_H = 105\,\mathrm{GeV}$ and $f \simeq 0.79 m_l$, which is derived from the Higgs top partner relation [44]

$$m_H \simeq \frac{\sqrt{N_c}}{\pi} \frac{m_l m_t}{f} \tag{2.5.11}$$

at $m_t = 150\,\mathrm{GeV}$, the relation between the tuning and the top partner mass is given by

$$\Delta_5 \simeq 100 \cdot \left(\frac{m_l}{1\,\mathrm{TeV}}\right)^2. \tag{2.5.12}$$

In the sMCHM$_5$, the double-tuning problem manifested in Eq. 2.5.8 is not resolved but not worsened either. Therefore, it can be concluded that for these parameters at $\xi \simeq 0.1$

[32] V is also called Higgs parity.

[33] For a more general overview on fine-tuning in CHMs, see [99].

[34] Ref [100] claims $S_{|U=0} = 0.05 \pm 0.09$ and $T_{|U=0} = 0.08 \pm 0.07$ at 95% CL, but since the analysis performed above is quite limited, some non-negligible contributions to the T parameter could have been ignored.

(i.e. $f \sim 800\,\text{GeV}$), the tuning in the novel sMCHM$_5$ is similar to the tuning for the MCHM$_5$. This is a very encouraging result, because it means that the tuning is not likely to increase much, if this model actually manages to achieve higher top partner masses for a light Higgs. If the tuning had exploded, one could have just risen f in the MCHM$_5$ and would have obtained a similar result with significantly less effort. The recalculation of the EWPOs is beyond the scale of this thesis such that the parameter constraints for the usual MCHM$_5$ model are taken.

To compute the fine-tuning in the 5D holographic model, the Barbieri-Giudice measure [101]

$$\Delta_{\text{BG}} = \max_{x_i} \left| \frac{\partial \ln \mathcal{O}}{\partial \ln x_i} \right| = \max_{x_i} \left| \frac{x_i}{\mathcal{O}} \frac{\partial \mathcal{O}}{\partial x_i} \right| \tag{2.5.13}$$

is used, with $\mathcal{O}$ being an observable which is dependent on the model parameters x_i ($x_i \in \{\xi, c_\psi, c_\chi, c_1, c_2, c_s, c_v, c_w, \kappa^2, \kappa'^2\}$ for the sMCHM$_5$). Note that this measure is always meant to be a lower bound for the actual fine-tuning since it can only account for the effects which influence the chosen operator. A common choice for $\mathcal{O}$ is the mass of the Z boson m_Z^2 which is at leading order related to the Higgs via

$$m_Z^2(h) = \frac{g^2 v(h)^2}{4\cos^2\theta_W} = \frac{g^2 f^2}{4\cos^2\theta_W} s_h^2 \quad \Rightarrow \quad \Delta_{\text{BG}}^Z = \max_{x_i} \left| \frac{x_i}{s_h^2} \frac{\partial s_h^2}{\partial x_i} \right| , \tag{2.5.14}$$

where the following h denotes the background value of the Higgs field. Since it is much easier to work with the Higgs potential, this equation will again be rewritten, starting with an expansion of the derivative of the potential around ξ (see Appendix B.7 for similar calculations)

$$\begin{aligned} \frac{\partial V(s_h^2)}{\partial s_h^2} &= \cancel{\left.\frac{\partial V(s_h^2)}{\partial s_h^2}\right|_{s_h^2=\xi}} + (s_h^2 - \xi) \left.\frac{\partial^2 V(s_h^2)}{(\partial s_h^2)^2}\right|_{s_h^2=\xi} + \mathcal{O}\big(s_h^4\big) \\ &= (s_h^2 - \xi) \frac{f^2}{4\xi(1-\xi)} m_H^2 + \mathcal{O}\big(s_h^4\big) \end{aligned} \tag{2.5.15}$$

such that

$$\frac{\partial s_h^2}{\partial x_i} = \frac{4\xi(1-\xi)}{f^2 m_H^2} \frac{\partial^2 V(h)}{\partial x_i \partial s_h^2} . \tag{2.5.16}$$

Evaluating the fine-tuning by variation of the minimum yields

$$\Delta_{BG}^Z = \max_{x_i} \left| \frac{4x_i(1-s_h^2)}{f^2 m_H^2} \frac{\partial}{\partial x_i} \left(\frac{\partial V(s_h^2)}{\partial s_h^2} \right) \right|_{s_h^2=\xi} \tag{2.5.17}$$

for this analysis.[35] Another possible observable is the Higgs mass m_H^2, from which the fine-tuning measure

$$\Delta_{\text{BG}}^H = \max_{x_i} \left| \frac{x_i}{m_H^2} \frac{\partial m_H^2}{\partial x_i} \right|_{h=0} = \max_{x_i} \left| \frac{x_i}{m_H^2} \frac{\partial}{\partial x_i} \left(\frac{\partial^2 V(h)}{\partial h^2} \right) \right|_{h=0} \tag{2.5.18}$$

is obtained. For the subsequent analysis both values will be derived taking the higher one as the proper fine-tuning measure for each point in the analysis.

[35] One could have also started with the W mass $m_W^2(h)$ and would arrive at the same result.

2.5.2 The maximally symmetric sMCHM$_5$

In a second step, it is reasonable to think about ways to use the sMCHM$_5$ in order to actually reduce fine-tuning. One promising approach which can easily be included into this model is the concept of *maximal symmetry* [50, 102]. The idea of this approach is to start with an enhanced chiral symmetry for the fermions $SO(5)_L \times SO(5)_R$. This higher symmetry is then broken into a remaining, so-called maximal symmetry $SO(5)'$, which does not contain the Goldstone shift symmetry any more and thus creates a potential for the Higgs.

To achieve this, this concept also requires complete **5** multiplets of $SO(5)_{L,R}$ in the sector of composite resonances. The maximal symmetry group $SO(5)'$ is defined via the previously introduced automorphism V, being the subgroup of $SO(5)_L \times SO(5)_R$ that satisfies

$$g_L V g_R^\dagger = V, \quad g_L \in SO(5)_L, \quad g_R \in SO(5)_R. \tag{2.5.19}$$

The spurions as well as the Goldstone operator transform under this new symmetry as

$$\Gamma_L \to g_R \Gamma_L g_R^\dagger, \quad \Gamma_R \to g_L \Gamma_R g_L^\dagger, \quad \Sigma \to g_L \Sigma g_R^\dagger. \tag{2.5.20}$$

If one requires $SO(5)'$ to be the global symmetry of the model, the first possible invariant combination of operators, which correspond to the leading contribution of the potential, yields [51]

$$V_f^{\mathrm{LO}}(h) = c_{LR}\,\mathrm{tr}(\Sigma\Gamma_L\Sigma^\dagger\Gamma_R) = 2c_{LR}s_h^2c_h^2 = -\alpha_f s_h^2 + \beta_f s_h^4. \tag{2.5.21}$$

Evidently, the maximally symmetric approach avoids double-tuning because the necessary structure for a non-trivial minimum of the potential is already given at leading order. Indeed, the tuning is estimated to be [50]

$$\Delta_5^{\mathrm{MS}} \simeq \frac{1}{\xi} - 2. \tag{2.5.22}$$

Using the same quantities as for Eq. 2.5.12, the relation between the tuning and the mass of the lightest top partner yields

$$\Delta_5^{\mathrm{MS}} \simeq 10 \cdot \left(\frac{m_l}{1\,\mathrm{TeV}}\right)^2 \tag{2.5.23}$$

which is roughly a factor of 10 lower than in the (s)MCHM$_5$.

Unfortunately, by just looking at the fermionic potential, the contributions are not only similar but equal $\alpha_f = \beta_f$, which results in $\xi = 0.5$, a value well excluded by EWPTs [68]. To cure this problem, one usually reintroduces some amount of fine-tuning to let the gauge contribution α_g shift the potential to the desired ξ. This means that the α contributions, which are of similar order have to cancel sufficiently, in order to obtain $\xi = (\alpha_g + \alpha_f)/(2\beta_f) \sim 0.1$.

A combination with the sMCHM$_5$ has been (qualitatively) shown to actually solve this problem without an additional fine-tuning, because it can break *trigonometric parity*, which is the underlying reason for the equal contributions, while preserving the structure of the potential in the maximally symmetric setup.[36] The implementation of maximal symmetry into the sMCHM$_5$ is simple but not trivial. If one would e.g. naively set $m_Q \equiv -\tilde{m}_T$, $a_L = b_L$ and $a_R = b_R$ (corresponding to $c_1 = -c_2$ in the 5D model), the w contribution would introduce a single s_h^2 term at leading order (see [51] for a full derivation) which maximally breaks the trigonometric parity and reintroduces double-tuning. This contribution can be avoided by requiring that the chiral w_L, w_R components in Eq. 2.4.38 to have different chiral partners denoted as $\tilde{w}_R$ and $\tilde{w}_L$ accompanied with a Z_2 symmetry (see below). For a derivation in 4D, the reader is referred to the original paper [51]. In 5D, one first has to set $c_1 = -c_2$ as a fixed constraint for the model. Secondly, the w_L and w_R have to be coupled to brane localized fields, denoted as $\tilde{w}_R$ and $\tilde{w}_L$, on the UV-brane. This alters the UV action to be

$$S_{\mathrm{UV}} = \int \mathrm{d}^4x \Bigg[-is_R\sigma^\mu\partial_\mu\bar{s}_R - i\bar{v}_L\bar{\sigma}^\mu\partial_\mu v_L - i\tilde{w}_R^T\sigma^\mu\partial_\mu\bar{\tilde{w}}_R^T - i\bar{\tilde{w}}_L\bar{\sigma}^\mu\partial_\mu\tilde{w}_L \\ + \frac{c_s}{\sqrt{R}}(s_Rs_L + \bar{s}_L\bar{s}_R) + \frac{c_v}{\sqrt{R}}(v_R^Tv_L + \bar{v}_L\bar{v}_R^T) \\ + \frac{c_{w_R}}{\sqrt{R}}(w_R^T\tilde{w}_L + \bar{\tilde{w}}_L\bar{w}_R^T) + \frac{c_{w_L}}{\sqrt{R}}(\tilde{w}_R^Tw_L + \bar{w}_L\bar{\tilde{w}}_R^T) + h.c.\Bigg]_{z=R}, \tag{2.5.24}$$

with c_{w_L}, c_{w_R} as new free dimensionless parameters of the model. By doing this, of course also the BCs on the UV-brane for the first two pairs are changed, now yielding

$$A_n^{1,2} = \frac{m_nR}{c_{w_L}^2}B_n^{1,2} \qquad G_n^{1,2} = -\frac{m_nR}{c_{w_R}^2}F_n^{1,2}. \tag{2.5.25}$$

Additionally, a Z_2 symmetry is introduced, under which the Ψ_1 and the right-handed UV-localized fields have negative and the Ψ_2 along with the left-handed UV-localized fields have positive parity. This forbids unwanted trigonometric parity breaking terms if it is imposed everywhere, except on the IR-brane, where the symmetry is broken in order to give mass to the SM fermions. The fine-tuning for the soft maximally symmetric model is expected to be described by Eq. 2.5.22 because it follows the same argumentation as for the simple maximally symmetric case. Moreover, since it is not necessary to raise $f \sim 800\,\mathrm{GeV}$ in order to obtain higher top partner masses, one can even assume the tuning in the maximally symmetric sMCHM$_5$ to be constant $\Delta_5^{\mathrm{sMS}} \simeq 8$ over large mass range of m_l. For regions above $m_l \gtrsim 2\,\mathrm{TeV}$ this argumentation does not hold any longer because the vector-like masses are pushed towards more tuned regions in the parameter space. From here on, quadratic growth in the tuning starts again as described by equation 2.5.23 (see [51] for a more detailed discussion).

[36] Trigonometric parity is a discrete symmetry, which leaves the system invariant under the exchange $s_h \leftrightarrow -c_h$. It arises from the Higgs parity V.

3 Analysis and Discussion

The necessary background knowledge as well as the theoretical setup have been laid out paving the way for a numerical analysis of the model properties. Particular emphasis will be laid on the question, if the sMCHM$_5$ is able to produce heavy top partners while keeping the Higgs light. Moreover, fine-tuning studies will be performed for each case.

At first, the general features of this analysis will be explained starting from the MCHM$_5$, where the new fermions are effectively decoupled. As a next step, in the spirit of the original paper [46], only the s_R will be included, investigating how the model changes if the c_s parameter is varied. Eventually, the full sMCHM$_5$ setup with all parameters in play will be tested. Here, focus will also be laid on the question how natural these new parameters are. In a final step, the model will be transformed in order to respect maximal symmetry. This provides an opportunity to test if the fine-tuning can be further reduced while obtaining similar results for the relation of the Higgs to the top partners.

In the following analysis, if not stated otherwise, $f \equiv 800\,\text{GeV}$, $R \equiv 10^{-16}\,\text{TeV}^{-1}$ and $m_t \equiv 150\,\text{GeV}$ are fixed. The R', g_* and s_ϕ parameters will then arise naturally from the Eq. 2.4.8, 2.4.31 and 2.4.32, depending only on the brane kinetic terms κ, κ'. For $\kappa = \kappa' = 0$ they yield $R' \approx 0.625\,\text{TeV}^{-1}$, $g_* \approx 4$ and $s_\phi^2 \approx 0.287$. Furthermore, the VEV of EWSB $v = 246.2\,\text{GeV}$, the fine-structure constant $\alpha_{\text{QED}} = 1/128$ as well as the sine squared of the Weinberg angle $\sin^2\theta_W = 0.223$, remain constant throughout the analysis [103].

3.1 General features of the analysis - The MCHM$_5$

The MCHM$_5$ can be considered as a special case of the sMCHM$_5$ with all localized fermions on the UV-brane decoupled. This is achieved by taking c_s, c_v, $c_w \to \infty$ in the UV BCs of Eq. 2.4.50 which will effectively recover the original BCs for all fermions in the MCHM$_5$ as stated in Eq. 2.4.37. The remaining parameters are c_ψ, c_χ, c_1 and c_2, two of which can be fixed by the constraints in Eq. 2.4.63. The parameter space is scanned over the remaining two free parameters in the range $c_\psi, c_\chi \in [-0.5, 0.5]$ and $c_1, c_2 \in [-1.4, 1.4]$, respectively. Note that if not stated otherwise, these ranges are used as a default.[37]

The relation between the Higgs mass and the lightest of the top partner states in the MCHM$_5$ model is displayed in Figure 3.1. For this purpose, parameter scans have been carried out varying both, the bulk mass parameters c_ψ, c_χ and the brane mass terms c_1, c_2, combining the results in the end. This procedure has been chosen due to degenerate solutions, because varying different parameters eases the access to different regions of the parameter space in the plot shown.

[37] The reasoning for the range of the fermionic bulk mass parameters c_ψ and c_χ has been displayed in the end of Section 2.3.6. The boundaries for the IR-coupling terms c_1 and c_2 have been chosen somewhat more arbitrary, although, higher values would correspond to higher Yukawa couplings and therefore higher Higgs masses, which is contrary to the aim of keeping the Higgs light.

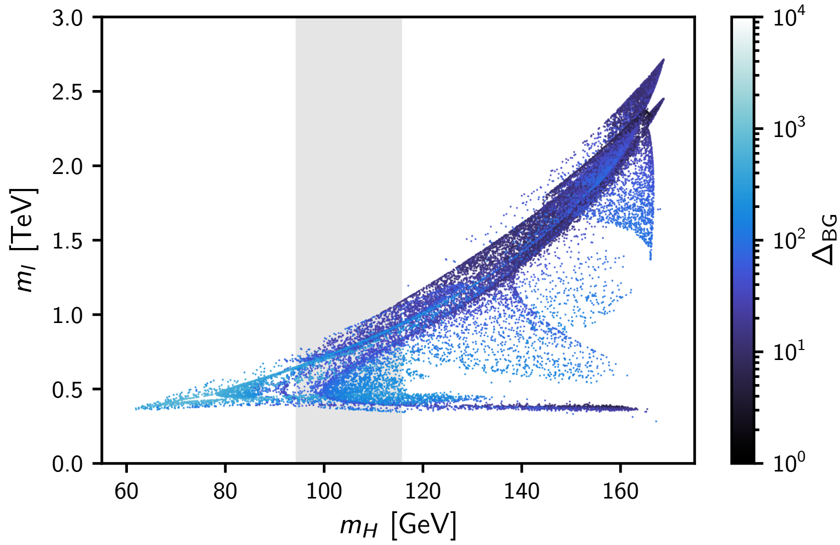

Figure 3.1: Shown is the mass of the lightest top partner state in dependence of the Higgs mass for $c_\psi, c_\chi \in [-0.5, 0.5]$, $c_1, c_2 \in [-1.4, 1.4]$ and $\kappa = \kappa' = 0$ in the MCHM_5. While scanning over c_ψ, c_χ, the other two parameters where fixed by the constraints placed in Eq. 2.4.63 and vice versa. The grey band denotes a variation of $\pm 10\,\%$ around a Higgs mass of $m_H(f) = 105\,\mathrm{GeV}$. The fine-tuning Δ_{BG} for each valid point is color-coded.

It can be seen that the lack of sufficiently high top partner masses in the region of a valid Higgs mass indicated by the grey band restates the initial problem. Moreover, it is beneficial at this point, to discuss other features of the plot which will remain while going to the sMCHM_5 model.

Firstly, one might wonder about the general form of the plot. From Eq. 2.2.44 at fixed m_t and f, an almost linear relation between m_H and m_l is expected. However, it can happen that the lightest top partner has actually different quantum numbers than the top quark itself, such that it cannot mix with it. In consequence, its lightness does not help to reduce the Higgs mass at constant m_t, which explains the parameter points with smaller m_l at fixed m_H.

The bounds on the Higgs mass are dependent on the top quark mass, which in turn is dependent on the f_ψ and f_χ corresponding to the mixing strengths $\sin\theta_{t_L}$, $\sin\theta_{t_R}$ with the top partners in the 4D model. Therefore, the range for possible m_H is dictated by the chosen range for the c_ψ, c_χ (see also Figure 2.9). In principle, this range can be enlarged by allowing for brane kinetic terms (especially with $\kappa^2 \neq 0$) because they alter the coupling strength g_* in 5D as well as in 4D and thus the relation between the masses. Of course, the fixed top mass m_t trivially also provides a lower bound for the top partner mass m_l.

Also displayed in Figure 3.1 is the fine-tuning for each valid point. As expected, the

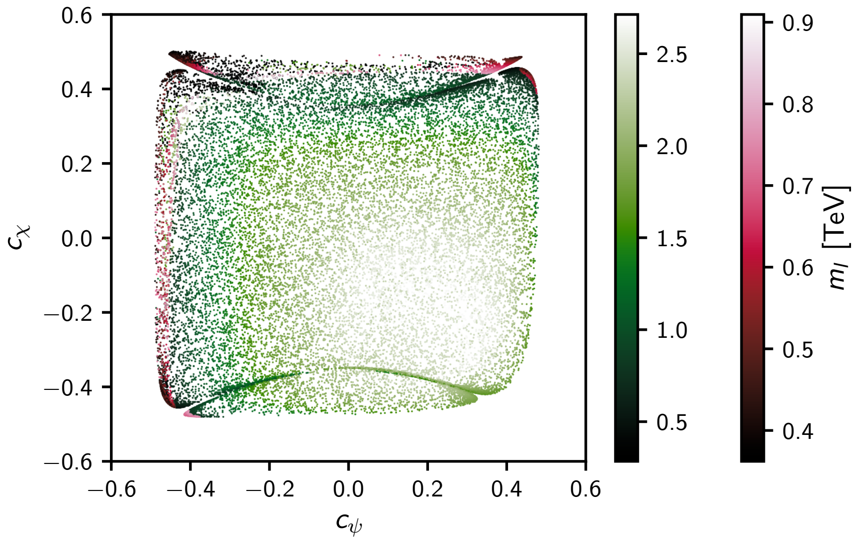

Figure 3.2: Correlation between the bulk mass parameters c_ψ and c_χ in the MCHM$_5$ for the same data set as in Figure 3.1, plotted against the lightest top partner mass m_l for Higgs masses above (green color-bar) and below (pink color-bar) $m_H(f) = 105\,\mathrm{GeV}$.

fine-tuning increases for lower Higgs masses. Most of the points within the grey band yield a tuning between 20 and 200, which is consistent with the expectations stated in Eq. 2.5.9 and 2.5.12.

As can be seen from Figure 2.9 and Table 2.3, the more IR-localized the fermions are ($c_\psi \to -0.5$ and $c_\chi \to 0.5$), the greater are the amplitudes of the top quark f_{c_ψ,c_χ} and, thus, the mixing $\sin\theta_{t_L,t_R}$ of the top with its partners in the 4D model. For a fixed m_t, Eq. 2.2.41 can be used in order to explain the trend towards lower top partner masses for more IR-localized fields in Figure 3.2, where the same set of data points as in Figure 3.1 has been plotted, now with respect to c_ψ, c_χ and m_l. By looking at the first equity in this equation, one can see that for a fixed top mass at higher $\sin\theta_{t_L,t_R}$ the presumed $\mathcal{O}(1)$ couplings have to be adjusted because the overall mass scale of the top partners in the model has been fixed, too. Since the a_L, b_R parameters correspond to the strength of the mixings c_1, c_2 on the IR-brane in the 5D model, it makes sense that in order to keep the m_t fixed one has to adjust the IR-coupling if the fields become more IR-localized. From the second equity in Eq. 2.2.41 it is evident that an increase in $y_{t_{L,R}}$ would only lead to an increase in m_l such that the $\sin\theta_{t_L,t_R}$ would not change much. Therefore, the only feasible way to enlarge $\sin\theta_{t_L,t_R}$ is to reduce m_l which is also observed in Figure 3.2. Note, that Eq. 2.2.41 is still an approximation which, e.g., does not account for cancellations due to accidentally tuned a_L, b_R. Therefore, in Figure 3.2 one can also observe points which do not follow the trend explained above. One can also see here that small Higgs masses, indicated by the pink points, also demand an IR-localization of at least one of the chiral bulk fermions. From a theoretical point of view, this is clear

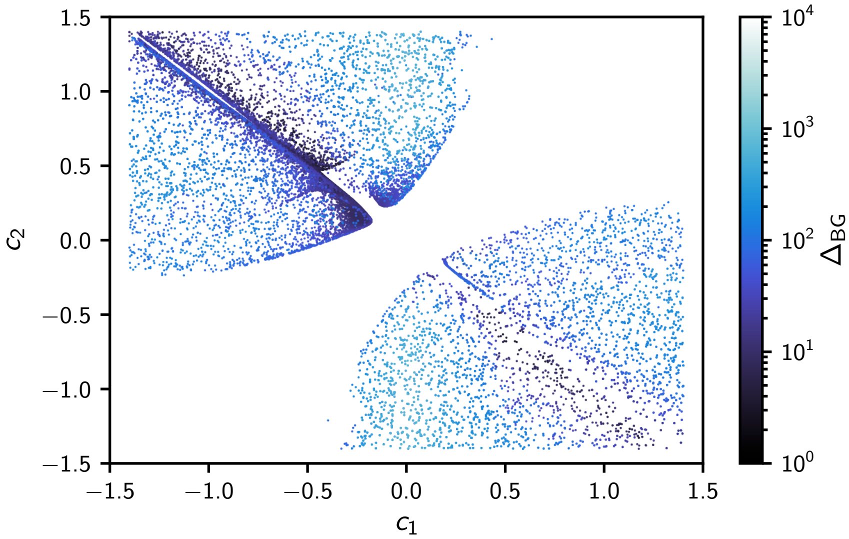

Figure 3.3: Correlation between the bulk brane mixing parameters c_1 and c_2 in the MCHM$_5$ for the same data set as in Figure 3.1. The fine-tuning of each point is indicated by different shades of blue.

because the Higgs mass scales with the mass of the top partner.

In order to investigate the parameter space for the brane mixing terms, the correlations between the c_1 and c_2 parameter for this data set has been displayed in Figure 3.3. The lack of data points for $c_1 \sim c_2$ can be explained best by looking at the top mass

$$m_t^2 \approx \frac{\xi(c_1 - c_2)^2 f_{c_\psi}^2 f_{c_\chi}^2}{2R'^2 \left(1 + c_1^2 \frac{f_{c_\psi}^2}{f_{-c_\chi}^2}\right)\left(1 + c_2^2 \frac{f_{c_\chi}^2}{f_{-c_\psi}^2}\right)}, \tag{3.1.1}$$

where the Bessel functions within $\rho(m_{0;t}^2(\tilde{v})) \equiv \rho(m_t^2)$ have been approximated up to linear order in m_n (see Appendix B.4) and every term beyond s_h^2 has been neglected. It can be easily seen, that the difference between the two input parameters has to overcome a certain limit such that a top mass of 150 GeV can be generated and that $m_t \to 0$ for $c_1 \to c_2$ and vice versa, when the Higgs effectively decouples. Figure 3.3 also suggests that the fine-tuning is reduced for points where $c_1 \approx -c_2$. This is sensible because these points describe a maximally symmetric MCHM$_5$ scenario as pointed out in Section 2.5.2.

Before going to the sMCHM$_5$ it is interesting to study other possibilities to enhance the top partner masses in order to compare them with the new approach. Naively, there are two possible ways to achieve this: increasing f and varying g_*. Both are displayed in Figure 3.4. In the upper two plots, where f has been varied, it is evident, that a higher value of f leads to higher masses of the top partner states. This follows from Eq. 2.2.44. Also evident form Eq. 2.5.3 is that increasing f increases the inevitable tuning of the model, as can be seen in the upper right plot. Varying g_* (by varying the κ's) does

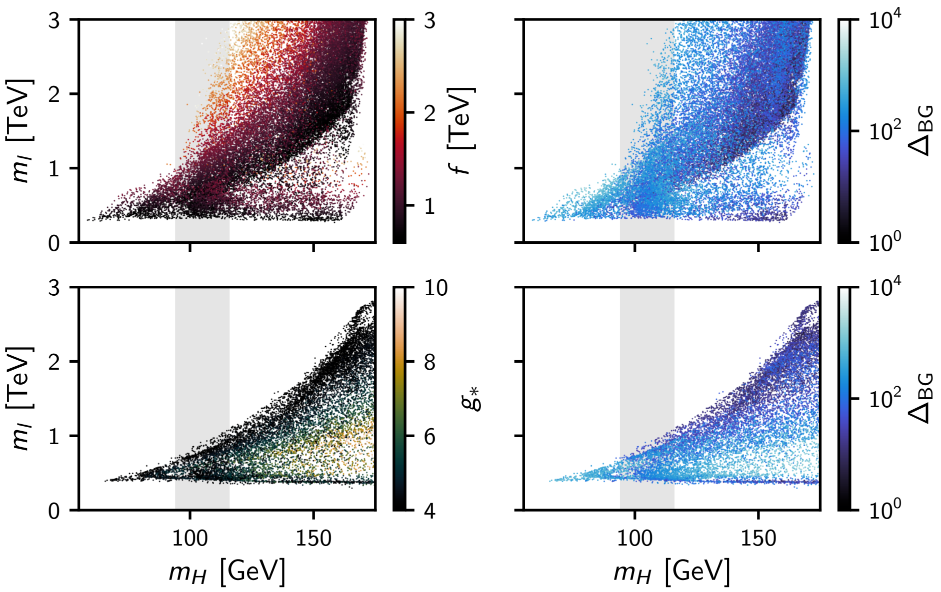

Figure 3.4: Shown is the distribution of m_H and m_l in the MCHM$_5$ while varying certain parameters within the usual bounds. In the upper two plots, the breaking scale f has been varied in the range between 0.6 TeV and 3 TeV at $\kappa = \kappa' = 0$. In the lower two plots, varying g_* between 4 and 10 has been achieved by a variation of $\kappa^2, \kappa'^2 \in [0, 5.25]$ at $f = 800$ GeV. In both cases the varied parameters have been color-coded on the left side where the fine-tuning for each of the two cases is displayed on the right side.

raise top partner masses but only for very high Higgs masses (which are cut off in the plot) and at the price of a much higher tuning for large g_*. Therefore, this possibility is not useful in order to obtain large m_l for a light Higgs. In principle one could think of values $g_* < 4$ by setting $\kappa, \kappa' < 0$. However, this approach has two major flaws. Firstly, smaller g_* are in conflict with EWPOs as stated in Section 2.5.1. Secondly, the negative κ^2 parameter can lead to an unstable potential $V(h)$ which makes it hard to trust these points.

3.2 Adding a vector-like singlet - The sMCHM$_5$ toy model

Before looking at the full sMCHM$_5$, it is useful to first only couple one of the new vector-like fermions to the MCHM$_5$ in order to explore which changes such particles induce. The singlet s seems to be a sensible choice for this purpose. While s_L is already included in the bulk fermionic multiplet ψ_L, the s_R is introduced as a localized 4D fermion living on the UV-brane. Starting from the full model, in this case only the c_v and c_w are taken to infinity, while keeping the c_s, which controls the singlet mass, finite.

As also described in the original paper [46], by simply looking at the approximated

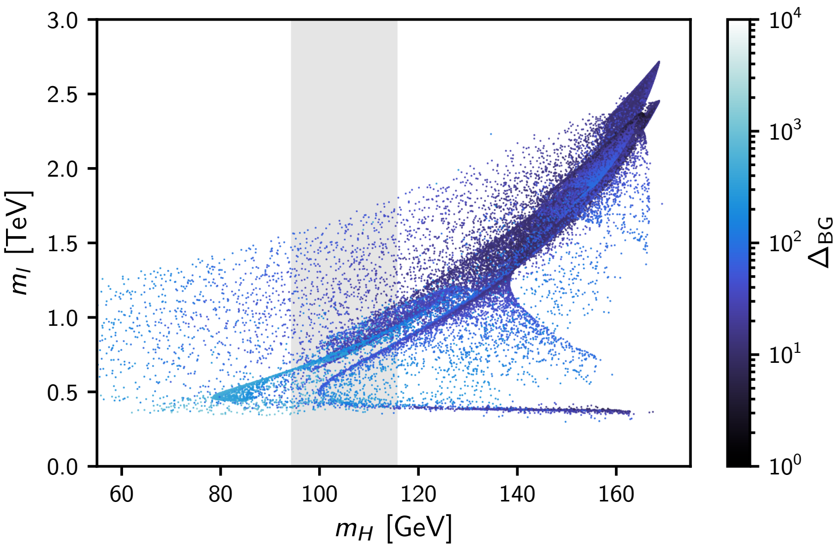

Figure 3.5: Displayed is the lightest top partner state in dependence of the Higgs mass for $c_\psi, c_\chi \in [-0.5, 0.5]$, $c_1, c_2 \in [-1.4, 1.4]$, $c_s \in [10^{-10}, 1]$ and $\kappa = \kappa' = 0$ in the MCHM$_5$ with an additional vector-like singlet s. The grey band denotes a variation of $\pm 10\,\%$ around a Higgs mass of $m_H(f) = 105\,\text{GeV}$. The fine-tuning Δ_{BG} for each valid point is color-coded.

top mass

$$m_t^2 \approx \frac{\xi (c_1 - c_2)^2 f_{c_\psi}^2 f_{c_\chi}^2}{2R'^2 \left(1 + c_1^2 \frac{f_{c_\psi}^2}{f_{-c_\chi}^2}\right)\left(1 + c_2^2 \frac{f_{c_\chi}^2}{f_{-c_\psi}^2} + \frac{c_2^2}{c_s^2}\left(\frac{R}{R'}\right)^{1+2c_\psi} f_{c_\chi}^2\right)}, \tag{3.2.1}$$

which has been derived in the same way as in the simple MCHM$_5$ case, it can be observed that the c_s lowers m_t because it adds a non-negative term in the denominator. Therefore, the top partners should be even lighter as in the MCHM$_5$, which is, by looking at Figure 3.5, certainly a perfectly good argument, why the overall maximum of the top partner mass does not increase. Fortunately, the mechanism also decreases the Higgs mass in a stronger way, such that for a light Higgs points with a larger top partner mass m_l remain. The reason for this is that the new fermion fundamentally changes the Higgs potential such that the previous estimates are no longer valid. This change allows for higher top partner masses even for a light Higgs. Moreover, Figure 3.5 also displays that one of the three proposed particles is apparently already sufficient to raise the masses of the top partners in the critical region to an acceptable amount.[38] The fine-tuning, as estimated in Eq. 2.5.12, does not change too much for higher values of m_l.

But what actually happens to the different parameters with the introduction of s? To investigate this, it is useful to look at Figure 3.6, where the c_ψ parameter is plotted

[38] Note that the s particle itself cannot be the lightest state, because this would violate the EW minimum constraint (see [46] for a more elaborated explanation).

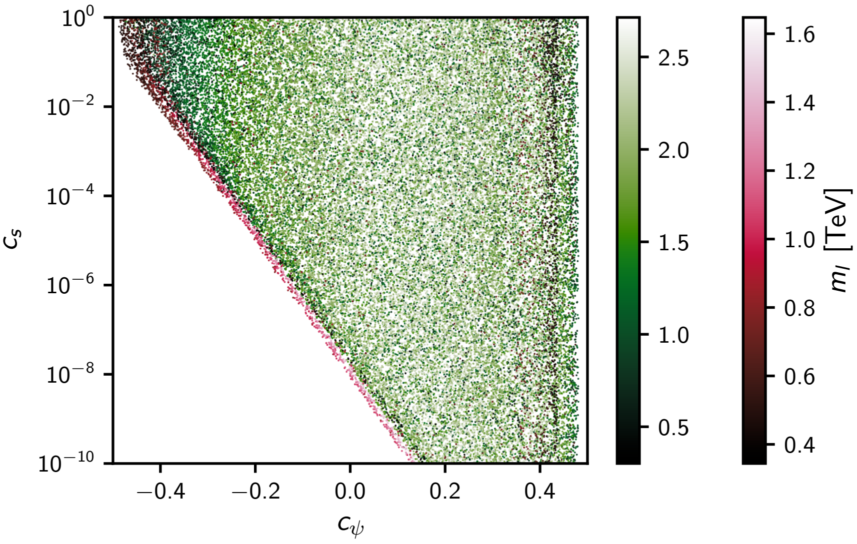

Figure 3.6: Correlation between the bulk mass c_ψ and the c_s parameter in the sMCHM$_5$ toy model for the same data set as in Figure 3.5 plotted against the lightest top partner mass m_l for Higgs masses above (green color-bar) and below (pink color-bar) $m_H(f) = 105\,\text{GeV}$.

against c_s. Unlike for the c_χ, where the full displayed region would be populated, the allowed region for c_ψ shrinks with decreasing singlet mass c_s. The reason for this is the fixed top mass. As displayed in Eq. 3.2.1, it is necessary to keep the new term in the denominator small in order to fulfill this constraint. Keeping $c_2 \sim \mathcal{O}(1)$, this is satisfied for $(R/R')^{1-2c_\chi} \ll c_s^2$, which means that smaller masses for vector-like fermions push the localization of the left-handed bulk fermion towards the UV-brane. Note that the same would have happened for the right-handed bulk fermions, if a new 5D field to the right-handed multiplet had been introduced.[39] However, it is also evident from Figure 3.6, that, while constraining the parameter space for the bulk mass fermions, smaller c_s also cure the demand for an IR-localized c_ψ in order to keep the Higgs light. For less IR-localized c_ψ the top partners are, thus, allowed to be heavier as in the MCHM$_5$ case for the same Higgs mass. On the other hand, the color gradient in the pink dots shows clearly, that smaller c_s lead to higher top partner masses for a light Higgs.

Unfortunately, the toy model has one major drawback. As evident from Figure 3.7 very small s masses are generally needed for a sufficient m_l to arise. Obviously, a value of $c_s \sim 10^{-10}$ is not desirable if one wants to cure the naturalness problem of the SM by switching to a "better" theory. Despite the fact that there are indeed very few points which yield $m_l > 1.5\,\text{GeV}$ with a "moderately small" $c_s \sim 10^{-5}$, they all have (as expected) quite a large tuning of $\Delta_{\text{BG}} > 250$ similar to the MCHM$_5$. Therefore, it will be

[39] In fact, for the full model in Section 3.3 the same behavior between the c_χ parameter and c_v of the v_R fermion can be observed.

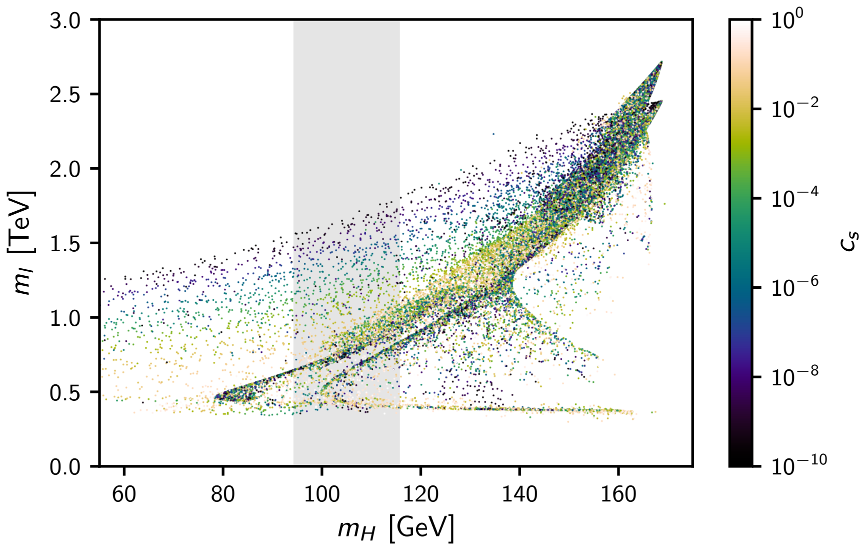

Figure 3.7: Same plot as in Figure 3.5 where the c_s parameter is color-coded for each valid point in the sMCHM$_5$ toy model. A smaller c_s corresponds to a smaller mass for the new vector-like s fermion.

interesting to see if setting up the full model cures this problem of the toy model and if brane kinetic terms help to broaden the parameter space.

3.3 Filling up the multiplet - The complete sMCHM$_5$

Finally, the whole sMCHM$_5$ is taken into account. Differently from Section 3.2, now all vector-like fermions have a finite mass. This changes the estimation of the top mass to

$$m_t^2 \approx \frac{\xi (c_1 - c_2)^2 f_{c_\psi}^2 f_{c_\chi}^2}{2R'^2 \left(1 + c_1^2 \frac{f_{c_\psi}^2}{f_{-c_\chi}^2} + \frac{c_1^2}{c_v^2}\left(\frac{R}{R'}\right)^{1-2c_\chi} f_{c_\psi}^2\right)\left(1 + c_2^2 \frac{f_{c_\chi}^2}{f_{-c_\psi}^2} + \frac{c_2^2}{c_s^2}\left(\frac{R}{R'}\right)^{1+2c_\psi} f_{c_\chi}^2\right)}, \quad (3.3.1)$$

where the c_w parameter first enters in the subdominant terms of this expansion. As explained earlier, the c_w does enter in the leading contribution of the Higgs potential. It is evident from Figure 3.8a that the two additional c_v and c_w, which have also been varied over several scales, are not sufficient to raise the top partner mass that easily. In fact, one sees the same behavior as in Figure 3.5 for the c_s parameter alone. The only difference here is that it is now in general possible to populate more states. If one takes a closer look, there are indeed very few points at top partner masses above $\gtrsim 2\,\text{TeV}$ which are not too far from the grey band of viable Higgs masses. These points suggest that this desired region is actually accessible. However, as transparent from the figure, it involves an extended amount of fine-tuning to reach it.

An easier way at this stage is to vary g_*, which has been done in Figure 3.8b. As before, the strength of the localized kinetic terms for the gauge fields have been varied

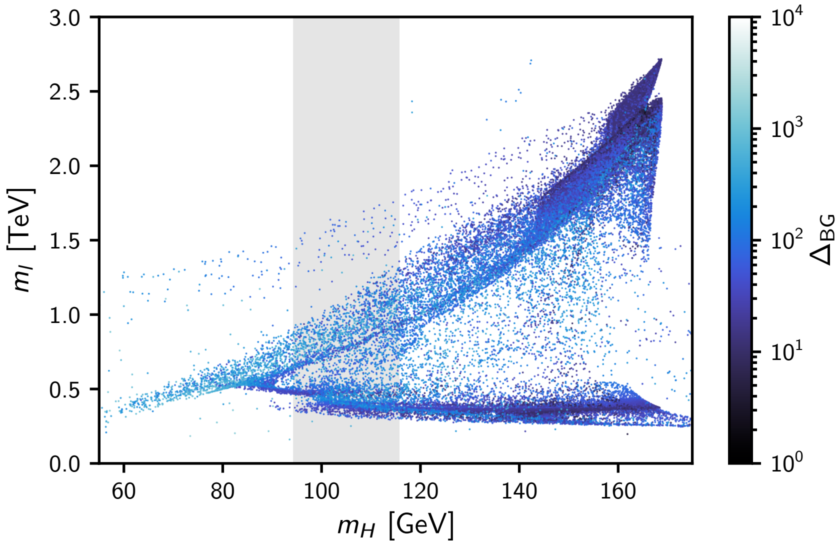

(a) Scatter plot for $\kappa = \kappa' = 0$ where the fine-tuning Δ_{BG} for each valid point is color-coded.

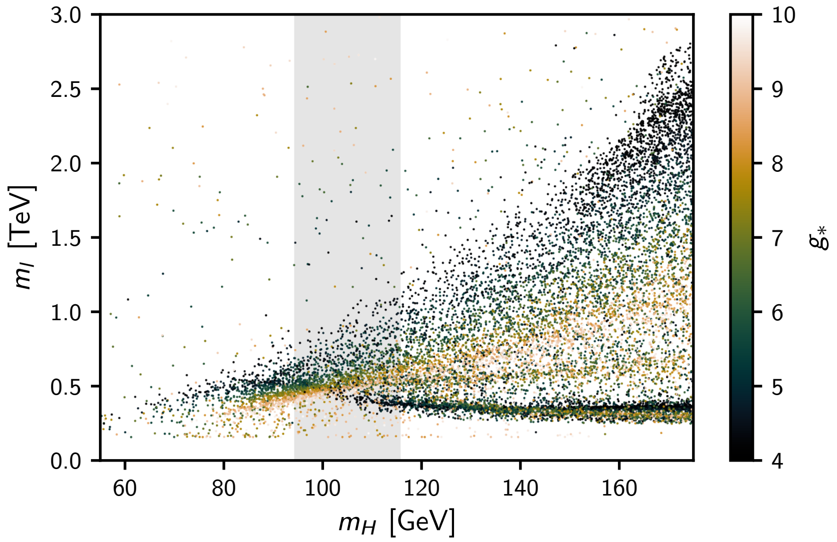

(b) Scatter plot for $\kappa, \kappa' \in [0, 5.25]$ corresponding to $g_* \in [4, 10]$, which is color-coded for each valid point.

Figure 3.8: The lightest top partner state in dependence of the Higgs mass for $c_\psi, c_\chi \in [-0.5, 0.5]$, $c_1, c_2 \in [-1.4, 1.4]$ and $c_s, c_v, c_w \in [10^{-10}, 1]$ in the full sMCHM_5. The grey band denotes a variation of $\pm 10\,\%$ around a Higgs mass of $m_H(f) = 105\,\mathrm{GeV}$.

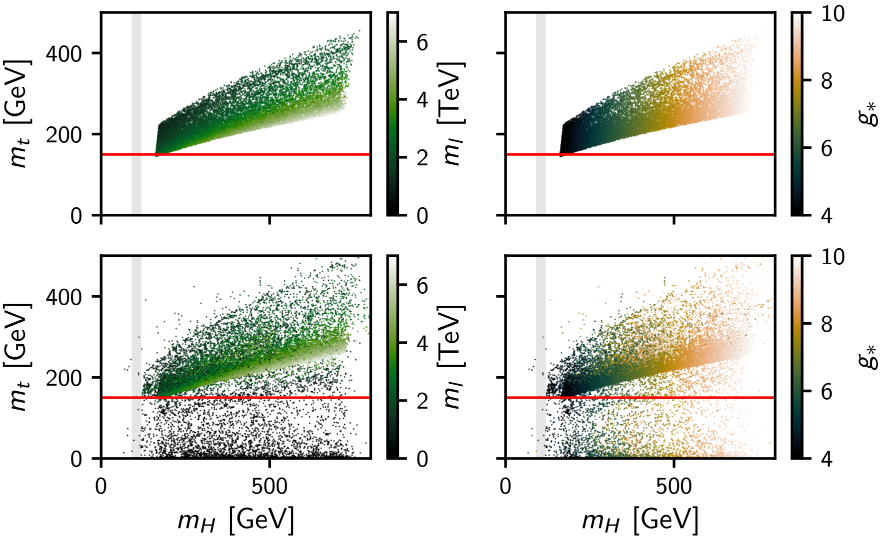

Figure 3.9: In all plots the top mass m_t is plotted against the Higgs mass m_H in the maximally symmetric sMCHM$_5$. For the upper two plots, the new vector like fermions have been decoupled and besides $\kappa, \kappa' \in [0, 5.25]$ only the bulk fermion masses $c_\psi, c_\chi \in [-0.5, 0.5]$ are varied. In the lower two plots, also $c_s, c_v, c_{w_R}, c_{w_L} \in [10^{-10}, 1]$ have been varied. In both scenarios, the lightest top partner masses m_l (left) as well as the 5D coupling strength g_* (right) have been color-coded. The grey band in all plots denotes a variation of $\pm 10\,\%$ around a Higgs mass of $m_H(f) = 105\,\text{GeV}$, whereas the red line refers to a fixed top mass at $m_t = 150\,\text{GeV}$.

in order to achieve a 5D coupling strength g_* between 4 and 10. It can be seen here that the region within the grey band can be populated easily up to top partner masses of $\lesssim 3\,\text{TeV}$ and has points up to $\lesssim 2\,\text{TeV}$, which (as has been checked) do not suffer from a significantly enhanced fine-tuning compared to points of lower top partner mass. However, all points above $2\,\text{TeV}$ in this region are strongly tuned which is reasonable because they have a high 5D coupling strength of $g_* \gtrsim 7$ which corresponds to critical values of $N_{\text{CFT}} \lesssim 3$.[40] The latter is problematic with regard to the validity of the theory.

3.4 A new symmetry - The maximally symmetric sMCHM$_5$

It has been discussed in Section 2.5 and shown in Section 3.3 that the sMCHM$_5$ does not solve the double-tuning issue of the MCHM$_5$. Therefore, a combination of this theory with the concept of maximal symmetry has been suggested and theoretically derived in Section 2.5.2. The quantitative results of a 5D implementation will be discussed in the following.

[40] Critical in the sense, that for low N_{CFT} the theory becomes non-perturbative and AdS/CFT duality is lost.

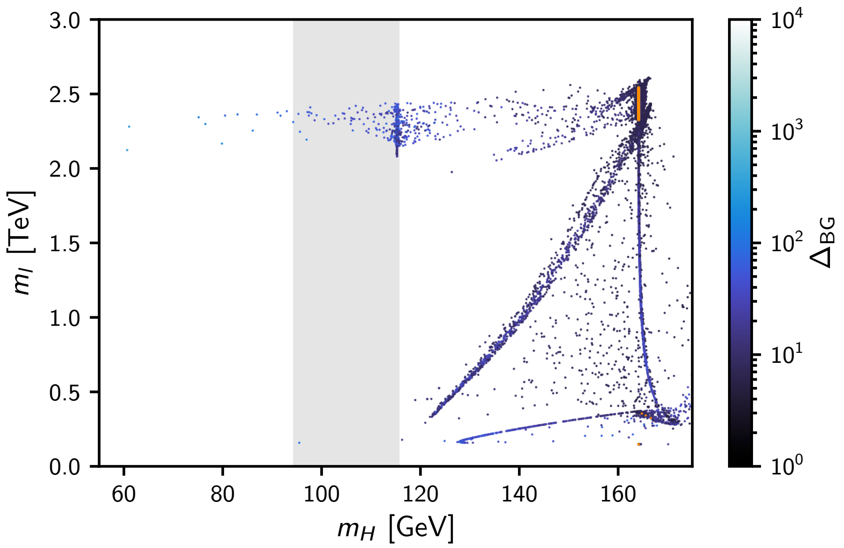

Figure 3.10: Displayed is the lightest top partner state in dependence of the Higgs mass for $c_\psi \in [-0.5, 0.5]$, $c_s, c_v, c_{w_R}, c_{w_L} \in [10^{-10}, 1]$ and $\kappa = \kappa' = 0$ in the maximally symmetric sMCHM$_5$. The grey band denotes a variation of $\pm 10\,\%$ around a Higgs mass of $m_H(f) = 105\,\text{GeV}$. The fine-tuning Δ_{BG} for each valid point is color-coded. Points with $c_s, c_v, c_{w_R}, c_{w_L} > 0.1$ are indicated in orange referring to the situation in the maximally symmetric MCHM$_5$. The tuning of all orange points is (as expected) of $\mathcal{O}(10)$.

To get an idea of the theoretical power of this approach, it is useful to look at the accessible regime of the top quark within the model. This is on the one hand important, because a fixed top quark mass restricts the degrees of freedom for the other free parameters. On the other hand, it serves as a consistency check for the approach. In Figure 3.9 two possibilities are displayed. The lower plots refers to the maximally symmetric model with soft breaking, where the parameters c_s, c_v, c_{w_R} and c_{w_L} are freely varied. In the upper plots, these parameters were taken to infinity, effectively decoupling the new vector-like fermions from the theory. These plots show the MCHM$_5$ where $c_1 = -c_2$ has been assumed.[41]

In the upper two plots one can see that for fixed g_* and m_H, according to Eq. 2.5.11 the top mass m_t is antiproportional to its partner mass m_l. The range of the bulk mass parameters c_ψ and c_χ (which correspond to the top-top partner mixings $\sin\theta_{t_{L,R}}$ in the 4D) then determines the range for the m_t and m_l. Higher g_* in general correspond to a higher scale for all masses. The Higgs mass range for a fixed top mass at $m_t = 150\,\text{GeV}$ is resembled by the overlap of the valid points with the red line. Performing a parameter scan one would expect in this case only a vertical line of valid points around $m_H \simeq 165\,\text{TeV}$ in the m_H-m_l plot. In order to broaden the parameter space towards the grey band of valid Higgs masses in the maximally symmetric MCHM$_5$ one would need to raise

[41] Again, as expected, the MCHM$_5$ with this constraint serves as a special case of the theory.

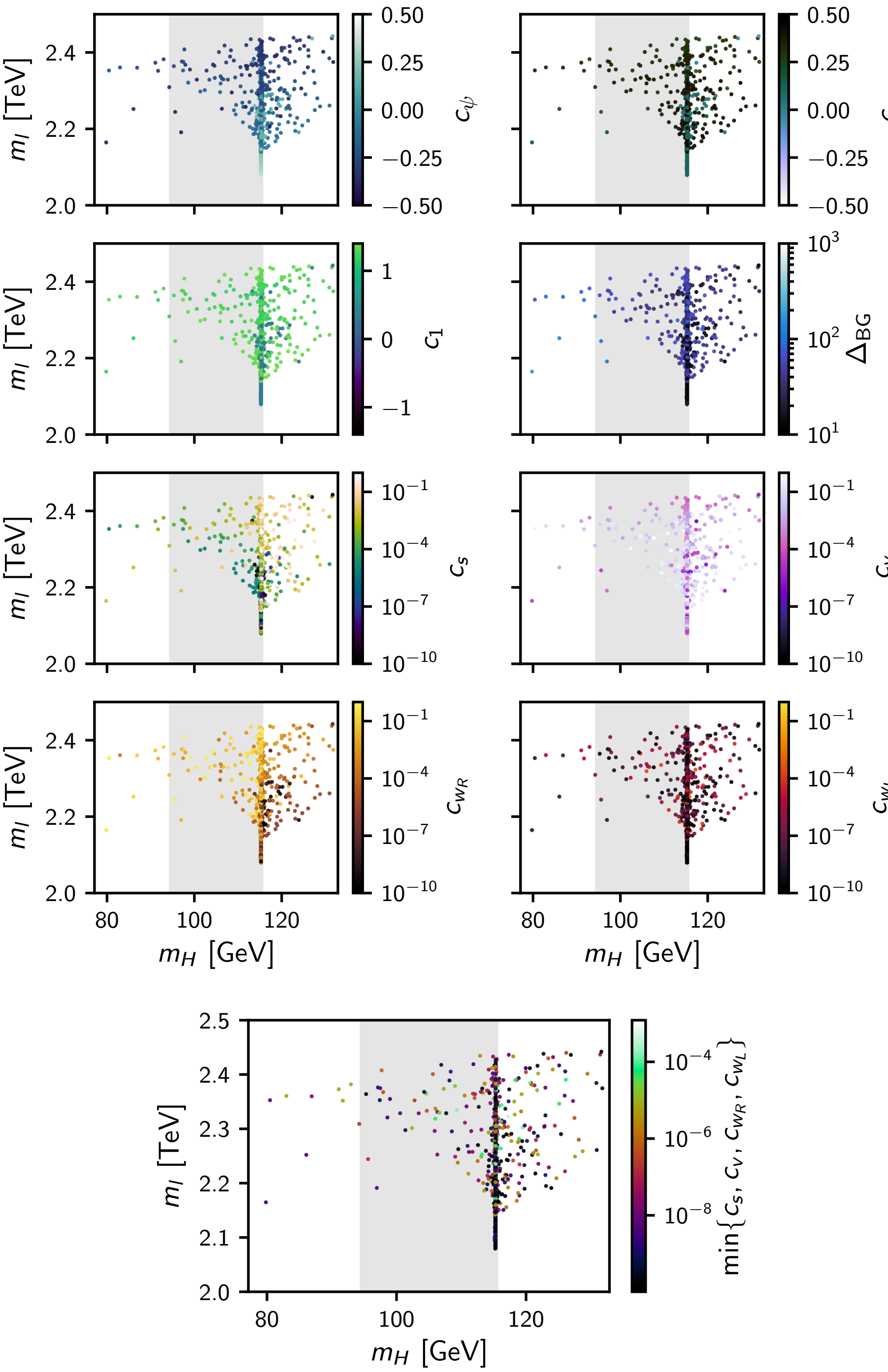

Figure 3.11: A picture detail of Figure 3.10 is displayed, color-coding each of the 7 input parameters of the model as well as the fine-tuning Δ_{BG}. c_χ and c_1 are fixed by the observational constraints of Eq. 2.4.63. The last plot displays the minimum of the new mass parameters for each point, where it should be noted, that the range for the $\min\{c_s, c_v, c_{w_R}, c_{w_L}\}$ within this sector has not been fixed externally.

f which will also raise the tuning.

Another possibility to obtain valid Higgs masses which is explored in the lower two plots of Figure 3.9 is to consider a maximally symmetric sMCHM_5. Here one can see that the previous constraints are significantly weakened and the regime of valid Higgs masses can be populated without the need of raising the breaking scale. It can also be observed that the grey band of the Higgs mass region for a fixed top mass is accessible for $g_* \sim 4$, which means that one might be able to get sufficient results without introducing gauge kinetic terms.

The result of these considerations can be seen in Figure 3.10. Here, apart from the new fermionic mass parameters, only the left-handed bulk mass parameter c_ψ has been varied, which significantly lowers the phase space of the valid points. However, one can clearly see a branch of points emerging at $2\,\mathrm{TeV} \lesssim m_l \lesssim 2.5\,\mathrm{TeV}$ proving the existence of heavy top partner states for a light Higgs mass within the model. In principle, the height of this branch can be varied by introducing brane kinetic gauge terms or by adjusting f. Also indicated in orange are points of $c_s, c_v, c_{w_R}, c_{w_L} > 0.1$ so high, that the initial maximally symmetric MCHM_5 is restored. As can be easily seen, all points match the expectations discussed above which means that the results on m_H from the maximally MCHM_5 alone are in great tension with the current bounds on the Higgs mass from the LHC. Adjusting f or g_* as can be seen in Figure 3.4 for the "normal" MCHM_5 does not cure this issue.

The characteristics of points within the important region around the physical Higgs mass with regard to their input parameters as well as their tuning have been exploited in Figure 3.11. Here, a few aspects should be mentioned. Firstly, both bulk mass parameters c_ψ and c_χ are not as IR-localized as one would have assumed in the regular case. This is achieved due to softened breaking and has already been discussed in Section 3.2. The brane mass terms c_1 and $c_2 = -c_1$ are of $\mathcal{O}(1)$ which is favored by naturalness arguments. In contrast to the conventional sMCHM_5, points can be found, where all new fermionic mass parameters c_s, c_v, c_{w_R} and c_{w_L} are above 10^{-4}. Nevertheless, one can also see that it is essential for a light Higgs that none of the new fermions decouples completely from the theory (i.e. $c_s, c_v, c_{w_R}, c_{w_L} < 1$). Scaled with R these numbers correspond to dimensionful masses of orders between the Planck scale $M_{\mathrm{Pl}} \sim 10^{19}\,\mathrm{GeV}$ and the scale of a *Grand Unified Theory* (GUT) around $M_{\mathrm{GUT}} \sim 10^{15}\,\mathrm{GeV}$ at the UV-brane, which are both desirable energies for a UV-cutoff as explained in Section 1. The tuning Δ_{BG} of these points at $\mathcal{O}(10)$ is consistent with the estimation in Eq. 2.5.22 and thus significantly lower than in the sMCHM_5.

4 Conclusion and Outlook

In this thesis, the question has been raised, if it is possible to obtain top partner masses for the experimentally observed Higgs mass around $m_h = 125\,\mathrm{GeV}$ above the current exclusion limits of $1.37\,\mathrm{TeV}$ in CHMs without raising the breaking scale f. The latter requirement has been linked to the request of finding a solution featuring a minimal amount of fine-tuning.

For this purpose it has been exclusively focussed on the quark content of the MCHM_5. Other possible implementations, like changing the representation of the quark multiplets to a sizable **14** [99], including a realistic lepton sector [45] or moving to a non-minimal coset [66] have been discussed elsewhere. Within this framework, two explicit models have been considered. The first model, called sMCHM_5 [46], introduces new vector-like fermions which break the global symmetry in a "softer" way. The second combines this idea with a maximally symmetric approach [51]. In order to quantitatively study these theories, 5D holographic implementations have been derived for both in Section 2.

In Section 3 parameter studies of these models have been performed. First, in Section 3.1 the results of the already studied MCHM_5 model [45] have been reproduced and shown to be consistent with prior analyses. In a second step in Section 3.2, a toy model containing only one of the three vector-like fermions has been analyzed. Here, it has been shown that the mass for the top partners can already increase moderately while keeping the Higgs light. Considering the full model in Section 3.3, it has been possible to raise the top partner masses to almost $2\,\mathrm{TeV}$ without gauge kinetic terms, including such terms (making the 5D model more flexible such as to reproduce a more general Composite Higgs setup) allows for masses above $2.5\,\mathrm{TeV}$ at the price of an enhanced tuning.

Studying a maximally symmetric version of the sMCHM_5 has been shown to solve these issue. It has been possible in this setup to obtain top partner masses above $2\,\mathrm{TeV}$ around the observed Higgs mass, which have a fine-tuning of $\mathcal{O}(10)$ and fundamental (5D) vector-like fermion masses in a natural spectrum around the GUT-scale. Therefore, it has been proven that especially the maximally symmetric sMCHM_5 can provide a natural environment to produce heavy top partner masses in a regime, which is just about to be tested by the *High Luminosity LHC* (HL-LHC) [104] or the *Future Circular Collider* (FCC) [105].

Certainly, this is not the end of the line and more analyses could be performed to further scrutinize the scenario. Especially estimates for EWPOs as well as constraints from hadronic and leptonic decay channels and FCNCs are left for future work. Moreover, it would be interesting to see, if it is possible to distinguish this model from others in an experiment. Studies on changes in the cross-section for Higgs+jet as well as double Higgs production [106–109] are currently ongoing. Perspectively, it might be even possible to include this approach into CHMs with higher symmetries to be able to study other yet unsolved problems like the origin of dark matter or neutrino masses.

Acknowledgements

I owe my gratitude to my supervisor Dr. Florian Goertz and Dr. Simone Blasi, who did an excellent job in supporting me and helping me out in any situation while guiding my way throughout the last year. Special thanks also goes to the theory devision of my second referee Prof. Dr. Manfred Lindner, who made it possible for me to write my thesis at the MPIK. In particular I would like to thank Thomas Rink, Thomas Hugle and Valentin Tenorth, who helped me with any IT-related problem at any time, as well as my office neighbors Jonas Rezacek and Deniz Gündüz for fruitful discussions and a comfortable work environment. Moreover, I am obliged to Thomas Pfeil, Karsten Roth and Oliver Scholer, who made the effort to proofread this thesis. Finally, I deeply thank my friends and my family who supported me unconditionally along the way.

Appendix

A Calculations in 4D

A.1 Integrating out Q^T and $\tilde{T}^t$

Starting with the sMCHM$_5$ mass Lagrangian

$$\mathcal{L}_{\text{Mass}}^{\text{MCHM}_5} = - \sum_{r,r'=T,t} \Big(m_{rr'} \bar{Q}_L^r Q_R^{r'} + \tilde{m}_{rr'} \bar{\tilde{T}}_L^r \tilde{T}_R^{r'} \Big) - \lambda_{t_L} f (\bar{q}_L \Delta_L)_I \Big(U_{Ii} Q_R^{T\,i} + U_{I5} \tilde{T}_R^T \Big) - \lambda_{t_R} f (\bar{t}_R \Delta_R)_I \Big(U_{Ii} Q_L^{t\,i} + U_{I5} \tilde{T}_L^t \Big) + h.c., \tag{A.1.1}$$

where $I = 1, ..., 5$, $i = 1, ..., 4$, the Q^T and $\tilde{T}^t$ are integrated out at zero momentum. This can be done as follows: First one takes the derivative of the action with respect to $\bar{Q}_L^T$ and Q_R^T where the kinetic can be ignored contributions. This gives the relations to the $Q_{L,R}^t$ fields

$$Q_R^T = -\frac{m_{Tt}}{m_{TT}} Q_R^t, \quad \bar{Q}_L^T = -\frac{m_{tT}}{m_{TT}} \bar{Q}_L^t - \frac{\lambda_{t_L} f}{m_{TT}} (\bar{q}_L \Delta_L)_I U_{Ii} \tag{A.1.2}$$

which can be inserted back into the Lagrangian. This yields

$$\mathcal{L}_{\text{Mass}}^{\text{MCHM}_5} \supset -\Big(m_{tt} - \frac{m_{tT} m_{Tt}}{m_{TT}} \Big) \bar{Q}_L^t Q_R^t - \lambda_{t_L} f (\bar{q}_L \Delta_L)_I U_{Ii} \Big(-\frac{m_{Tt}}{m_{TT}} Q_R^{t\,i} \Big), \tag{A.1.3}$$

where the $m_{Tt} m_{tT}/m_{TT}$ term can be neglected because it is assumed that the non-diagonal masses are subleading. The procedure for $\tilde{T}^t$ is equivalent, yielding

$$\mathcal{L}_{\text{Mass}}^{\text{MCHM}_5} \supset -\Big(\tilde{m}_{TT} - \frac{\tilde{m}_{tT}^* \tilde{m}_{Tt}^*}{\tilde{m}_{tt}^*} \Big) \bar{\tilde{T}}_L^T \tilde{T}_R^T - \lambda_{t_R} f (\bar{t}_R \Delta_R)_I U_{I5} \Big(-\frac{\tilde{m}_{Tt}^*}{\tilde{m}_{tt}^*} \tilde{T}_L^T \Big). \tag{A.1.4}$$

Neglecting again the subleading term and redefining $\lambda_{t_L} = b_L y_{t_L}$ ($\lambda_{t_R} = a_R y_{t_R}$) one arrives at

$$\mathcal{L}_{\text{Mass}}^{\text{MCHM}_5} = - m_Q^t \bar{Q}_L Q_R^t - \tilde{m}_T \bar{\tilde{T}}_L^T \tilde{T}_R^T - y_{t_L} f (\bar{q}_L \Delta_L)_I \big(a_L U_{Ii} Q_R^{t\,i} + b_L U_{I5} \tilde{T}_R^T \big) - y_{t_R} f (\bar{t}_R \Delta_R)_I \big(a_R U_{Ii} Q_L^{t\,i} + b_R U_{I5} \tilde{T}_L^T \big) + h.c. \;, \tag{A.1.5}$$

with $a_L = -m_{Tt}/m_{TT} b_L$ ($b_R = -\tilde{m}_{Tt}^*/\tilde{m}_{tt}^* a_R$).

B Calculations in 5D

B.1 Mapping between an exponentially suppressed and a conformally flat 5D metric

The exponentially suppressed metric is given by

$$\mathrm{d}s^2 = e^{-2ky} \eta_{\mu\nu} \mathrm{d}x^\mu \mathrm{d}x^\nu - \mathrm{d}y^2, \tag{B.1.1}$$

with L the length of the interval, $k > 0$ the warping factor and $y \in [0, L]$. The square root of the metric determinant equals $\sqrt{G_{\text{exp}}} = \exp(-4ky)$. Setting

$$z \equiv \frac{e^{ky}}{k}, \quad R \equiv \frac{1}{k}, \tag{B.1.2}$$

one can rewrite Eq. B.1.1 using $\mathrm{d}y = \frac{R}{z}\mathrm{d}z$ into its conformally flat form

$$\mathrm{d}s^2 = \left(\frac{R}{z}\right)^2 (\eta_{\mu\nu}\mathrm{d}x^\mu \mathrm{d}x^\nu - \mathrm{d}z^2), \tag{B.1.3}$$

with a metric determinant square root of $\sqrt{G_{\text{conf}}} = (R/z)^5$. Looking at the integration boundaries

$$\int_0^L \mathrm{d}y \sqrt{G_{\text{exp}}} = \int_0^L \mathrm{d}y e^{-4ky} \stackrel{!}{=} \int_R^{R'} \mathrm{d}z \left(\frac{R}{z}\right)^5 = \int_R^{R'} \mathrm{d}z \sqrt{G_{\text{conf}}} \tag{B.1.4}$$

one can further identify

$$L \equiv R \ln \frac{R'}{R}, \tag{B.1.5}$$

which can be used to relate the 4D and 5D couplings. See [110] for a more detailed discussion.

B.2 Dirac matrices in 5D and supersymmetric notation

The 5D gamma matrices on an AdS_5 with signature $(+, -, -, -, -)$ are given by

$$\Gamma^M = \{\gamma^\mu, i\gamma^5\} \tag{B.2.1}$$

$\mu = 0, 1, 2, 3$, with γ^μ, γ^5 being the 4D gamma matrices in reverse Weyl representation

$$\gamma^\mu = \begin{pmatrix} 0 & \sigma^\mu \\ \bar{\sigma}^\mu & 0 \end{pmatrix}, \quad \gamma^5 = \begin{pmatrix} \mathbb{1}_2 & 0 \\ 0 & -\mathbb{1}_2 \end{pmatrix}, \tag{B.2.2}$$

where $\bar{\sigma}^\mu = \eta^{\mu\nu}\sigma_\nu$. The σ^μ are the Pauli matrices

$$\sigma^0 = -\mathbb{1}_2, \quad \sigma^1 = \begin{pmatrix} 0 & 1 \\ 1 & 0 \end{pmatrix}, \quad \sigma^2 = \begin{pmatrix} 0 & -i \\ i & 0 \end{pmatrix}, \quad \sigma^3 = \begin{pmatrix} 1 & 0 \\ 0 & -1 \end{pmatrix}. \tag{B.2.3}$$

In this basis a 5D Dirac spinor can be written as

$$\Psi = \begin{pmatrix} \Psi_L \\ \Psi_R \end{pmatrix} = \begin{pmatrix} \chi_\alpha \\ \psi^{\dot{\alpha}} \end{pmatrix}, \tag{B.2.4}$$

with $\Psi_{L,R} = \frac{1}{2}(\mathbb{1}_4 \pm \gamma^5)\Psi$. The α and $\dot{\alpha}$ denote supersymmetric indices which obey the following relations

$$\chi_\alpha = i\sigma^2_{\alpha\beta}\chi^\beta, \quad \bar{\psi}^{\dot{\alpha}} = \left(-i\sigma^2\right)^{\dot{\alpha}\dot{\beta}} \bar{\psi}_{\dot{\beta}}, \quad \left(\chi^\dagger\right)_\alpha = \bar{\chi}_{\dot{\alpha}}, \quad \left(\bar{\psi}^\dagger\right)^{\dot{\alpha}} = \psi^\alpha. \tag{B.2.5}$$

Therefore, the Dirac adjoint in terms of these spinors yields

$$\bar{\Psi} = \left(\Psi_L^\dagger, \Psi_R^\dagger\right)\gamma^0 = -\left(\left(\bar{\psi}^\dagger\right)^{\dot{\alpha}}, \left(\chi^\dagger\right)_\alpha\right) = -\left(\psi^\alpha, \bar{\chi}_{\dot{\alpha}}\right). \tag{B.2.6}$$

The symmetric Lorentz invariants from this notation are

$$\chi\psi = \chi^\alpha\psi_\alpha = \psi^\alpha\chi_\alpha = \psi\chi \tag{B.2.7}$$

$$\bar{\chi}\bar{\psi} = \bar{\chi}_{\dot{\alpha}}\bar{\psi}^{\dot{\alpha}} = \bar{\psi}_{\dot{\alpha}}\bar{\chi}^{\dot{\alpha}} = \bar{\psi}\bar{\chi}. \tag{B.2.8}$$

B.3 Decoupling of mixed equations

In the flat case the two mixed equations can simply be decoupled

$$s_n' + m_\psi s_n - m_n f_n = 0 \tag{B.3.1}$$

$$f_n' - m_\psi f_n + m_n s_n = 0 \tag{B.3.2}$$

by taking the derivative of one equation and inserting the equations into each other multiple times. One arrives at

$$\begin{aligned}
(\text{B.3.1})' &= s_n'' + m_\psi s_n' - m_n f_n' \\
&= s_n'' + m_\psi s_n' - m_n(m_\psi f_n - m_n s_n) \\
&= s_n'' + m_\psi s_n' - m_n\left(\frac{m_\psi}{m_n}(s_n' + m_\psi s_n) - m_n s_n\right) \\
&= s_n'' + (m_n^2 - m_\psi^2)s_n^2 = 0
\end{aligned} \tag{B.3.3}$$

and similar for f_n. The warped case is methodically equivalent with the addition, that one also has to consider other z-dependent quantities in the equations

$$s_n' + \frac{c_\psi - 2}{z}s_n - m_n f_n = 0 \tag{B.3.4}$$

$$f_n' - \frac{c_\psi + 2}{z}f_n + m_n s_n = 0. \tag{B.3.5}$$

For s_n this means

$$\begin{aligned}
(\text{B.3.4})' &= s_n'' + \frac{c_\psi - 2}{z}\left(s_n' - \frac{1}{z}s_n\right) - m_n f_n' \\
&= s_n'' + \frac{c_\psi - 2}{z}\left(s_n' - \frac{1}{z}s_n\right) - m_n\left(\frac{c_\psi + 2}{z}f_n - m_n s_n\right) \\
&= s_n'' + \frac{c_\psi - 2}{z}\left(s_n' - \frac{1}{z}s_n\right) - m_n\left(\frac{c_\psi + 2}{m_n z}\left(s_n' + \frac{c_\psi - 2}{z}s_n\right) - m_n s_n\right) \\
&= s_n'' - \frac{4}{z}s_n' + \left(m_n^2 - \frac{c_\psi^2 + c_\psi - 6}{z^2}\right)s_n = 0.
\end{aligned} \tag{B.3.6}$$

The result for f_n is given in Eq. 2.3.75. The solution is equivalent for the t_n and f_n.

B.4 Bessel equations and warped trigonometric functions

Starting with

$$s_n'' - \frac{4}{z}s_n' + \left(m_n^2 - \frac{c_\psi^2 + c_\psi - 6}{z^2}\right)s_n = 0, \tag{B.4.1}$$

it is useful to first redefine $s_n \equiv z^{5/2}\tilde{s}_n$. Plugging this into equation B.4.1 and deviding by $z^{1/2}$

$$z^2\tilde{s}_n'' + z\tilde{s}_n' + \left(m_n^2 z^2 - \left(c_\psi + \frac{1}{2}\right)^2\right)\tilde{s}_n = 0 \tag{B.4.2}$$

is obtained which corresponds to the Bessel equation

$$x^2\frac{\mathrm{d}^2 y}{\mathrm{d}x^2} + x\frac{\mathrm{d}y}{\mathrm{d}x} + (x^2 - \nu^2)y = 0, \tag{B.4.3}$$

with $y \equiv \tilde{s}_n$, $x \equiv m_n z$ and $\nu = c_\psi + 1/2$. For $\tilde{f}_n$ the same differential equation with $\nu = 1/2 - c_\psi$ are derived. Solutions to this differential equation will therefore be a combination of Bessel functions of the first and second kind

$$y = AJ_\nu(x) + BY_\nu(x), \tag{B.4.4}$$

with definitions

$$J_\nu(x) = \sum_{k=0}^{\infty}\frac{(-1)^k\left(\frac{x}{2}\right)^{\nu+2k}}{k!\Gamma(\nu+k+1)} \quad \text{and} \quad Y_\nu(x) = \frac{J_\nu(x)\cos(\nu\pi) - J_{-\nu}(x)}{\sin(\nu\pi)}. \tag{B.4.5}$$

For this case, this means that the solutions of s_n and f_n can be written as

$$s_n(z) = z^{\frac{5}{2}}\left(\tilde{A}_n J_{c_\psi+\frac{1}{2}}(m_n z) + \tilde{B}_n Y_{c_\psi+\frac{1}{2}}(m_n z)\right) \tag{B.4.6}$$

$$f_n(z) = z^{\frac{5}{2}}\left(\tilde{C}_n J_{\frac{1}{2}-c_\psi}(m_n z) + \tilde{D}_n Y_{\frac{1}{2}-c_\psi}(m_n z)\right). \tag{B.4.7}$$

Since it is easier in the calculations to deal with functions which behave like sine and cosine functions, the mode basis will be redefined into

$$s_n(z) = \left(\frac{R}{z}\right)^{c_\psi-2}\left(A_n C_{c_\psi}(z) + B_n S_{c_\psi}(z)\right) \tag{B.4.8}$$

$$f_n(z) = \left(\frac{R}{z}\right)^{-c_\psi-2}\left(C_n C_{-c_\psi}(z) + D_n S_{-c_\psi}(z)\right), \tag{B.4.9}$$

with

$$C_c(z) \equiv \frac{\pi}{2}m_n R\left(\frac{z}{R}\right)^{c+\frac{1}{2}}\left(Y_{c-\frac{1}{2}}(m_n R)J_{c+\frac{1}{2}}(m_n z) - J_{c-\frac{1}{2}}(m_n R)Y_{c+\frac{1}{2}}(m_n z)\right) \tag{B.4.10}$$

$$S_c(z) \equiv \frac{\pi}{2}m_n R\left(\frac{z}{R}\right)^{c+\frac{1}{2}}\left(J_{c+\frac{1}{2}}(m_n R)Y_{c+\frac{1}{2}}(m_n z) - Y_{c+\frac{1}{2}}(m_n R)J_{c+\frac{1}{2}}(m_n z)\right) \tag{B.4.11}$$

and the relations

$$\tilde{A}_n = m_n R^{-\frac{3}{2}} \frac{\pi}{2} \Big(A_n Y_{c-\frac{1}{2}}(m_n R) - B_n Y_{c+\frac{1}{2}}(m_n R) \Big) \tag{B.4.12}$$

$$\tilde{B}_n = m_n R^{-\frac{3}{2}} \frac{\pi}{2} \Big(B_n J_{c+\frac{1}{2}}(m_n R) - A_n J_{c-\frac{1}{2}}(m_n R) \Big) \tag{B.4.13}$$

$$\tilde{C}_n = m_n R^{-\frac{3}{2}} \frac{\pi}{2} \Big(C_n Y_{-c-\frac{1}{2}}(m_n R) - D_n Y_{-c+\frac{1}{2}}(m_n R) \Big) \tag{B.4.14}$$

$$\tilde{D}_n = m_n R^{-\frac{3}{2}} \frac{\pi}{2} \Big(D_n J_{-c+\frac{1}{2}}(m_n R) - C_n J_{-c-\frac{1}{2}}(m_n R) \Big). \tag{B.4.15}$$

Using $J'_\nu(x) = J_{\nu-1}(x) - \nu/x J_\nu(x)$ and $Y'_\nu(x) = Y_{\nu-1}(x) - \nu/x Y_\nu(x)$ their derivative

$$C'_c(z) = \frac{\pi}{2} m_n^2 R \Big(\frac{z}{R}\Big)^{c+\frac{1}{2}} \Big(Y_{c-\frac{1}{2}}(m_n R) J_{c-\frac{1}{2}}(m_n z) - J_{c-\frac{1}{2}}(m_n R) Y_{c-\frac{1}{2}}(m_n z) \Big) \tag{B.4.16}$$

$$S'_c(z) = \frac{\pi}{2} m_n^2 R \Big(\frac{z}{R}\Big)^{c+\frac{1}{2}} \Big(J_{c+\frac{1}{2}}(m_n R) Y_{c-\frac{1}{2}}(m_n z) - Y_{c+\frac{1}{2}}(m_n R) J_{c-\frac{1}{2}}(m_n z) \Big) \tag{B.4.17}$$

can also be obtained quite easily. They are also called warped sine and cosine functions because they show a similar behavior to the normal ones in the UV, i.e. $S_c(R) = 0$, $C_c(R) = 1$, $S'_c(R) = m_n$ and $C'_c(R) = 0$.

Since it is more useful for calculations of the Higgs potential to work with the momentum instead of the mass, the formulas for these functions can be rewritten using $m_n = ip$. Doing this, one needs to make use of the modified Bessel functions which translate to the normal ones as

$$I_\nu(x) = i^\nu J_\nu(ix) \quad \text{and} \quad K_\nu(x) = \frac{\pi}{2} \frac{I_{-\nu}(x) - I_\nu(x)}{\sin(\nu\pi)} \tag{B.4.18}$$

with similar derivation rules $I'_\nu(x) = I_{\nu-1}(x) - \nu/x I_\nu(x)$ and $K'_\nu(x) = -K_{\nu-1}(x) - \nu/x K_\nu(x)$. The warped trigonometric functions and their derivatives in terms of the momentum read

$$C_c(z) = pR \Big(\frac{z}{R}\Big)^{c+\frac{1}{2}} \Big(K_{c-\frac{1}{2}}(pR) I_{c+\frac{1}{2}}(pz) + I_{c-\frac{1}{2}}(pR) K_{c+\frac{1}{2}}(pz) \Big) \tag{B.4.19}$$

$$S_c(z) = ipR \Big(\frac{z}{R}\Big)^{c+\frac{1}{2}} \Big(K_{c+\frac{1}{2}}(pR) I_{c+\frac{1}{2}}(pz) - I_{c+\frac{1}{2}}(pR) K_{c+\frac{1}{2}}(pz) \Big) \tag{B.4.20}$$

$$C'_c(z) = p^2 R \Big(\frac{z}{R}\Big)^{c+\frac{1}{2}} \Big(K_{c-\frac{1}{2}}(pR) I_{c-\frac{1}{2}}(pz) - I_{c-\frac{1}{2}}(pR) K_{c-\frac{1}{2}}(pz) \Big) \tag{B.4.21}$$

$$S'_c(z) = ip^2 R \Big(\frac{z}{R}\Big)^{c+\frac{1}{2}} \Big(K_{c+\frac{1}{2}}(pR) I_{c-\frac{1}{2}}(pz) + I_{c+\frac{1}{2}}(pR) K_{c-\frac{1}{2}}(pz) \Big). \tag{B.4.22}$$

For $m_n R \ll 1$ and $m_n z \ll 1$ small, the trigonometric functions can be approximated up to linear oder in m_n

$$C_c(z) = 1 + \mathcal{O}\big(m_n^2\big) \qquad S_c(z) = m_n R \frac{\big(\frac{z}{R}\big)^{2c+1} - 1}{2c+1} + \mathcal{O}\big(m_n^3\big). \tag{B.4.23}$$

B.5 The warped equations of motion for gauge fields

Deriving the solutions for the ζ_n is very similar to the procedure in Section B.4. Starting with

$$\zeta_n'' - \frac{1}{z}\zeta_n' + m_n^2 \zeta_n = 0 \tag{B.5.1}$$

one can again redefine $\zeta_n = z\tilde{\zeta}_n$ and multiply with z yielding

$$z^2 \zeta_n'' + z\zeta_n' + (m_n^2 - 1)\zeta_n = 0. \tag{B.5.2}$$

This again is the Bessel equations with $\nu = 1$ which has solutions expressed in terms of the warped trigonometric functions defined in Eq. 2.3.77 and 2.3.76

$$\zeta_n(z) = A_n C(z) + B_n S(z) \tag{B.5.3}$$

with

$$C(z) \equiv C_{\frac{1}{2}}(z) = \frac{\pi}{2} m_n z \Big(Y_0(m_n R) J_1(m_n z) - J_0(m_n R) Y_1(m_n z) \Big) \tag{B.5.4}$$

$$S(z) \equiv S_{\frac{1}{2}}(z) = \frac{\pi}{2} m_n z \Big(J_1(m_n R) Y_1(m_n z) - Y_1(m_n R) J_1(m_n z) \Big). \tag{B.5.5}$$

The functions ϑ_n can be defined accordingly

$$\vartheta_n(z) = \frac{1}{m_n} (A_n C'(z) + B_n S'(z)) \tag{B.5.6}$$

with

$$C'(z) \equiv C'_{\frac{1}{2}}(z) = \frac{\pi}{2} m_n^2 z \Big(Y_0(m_n R) J_0(m_n z) - J_0(m_n R) Y_0(m_n z) \Big) \tag{B.5.7}$$

$$S'(z) \equiv S'_{\frac{1}{2}}(z) = \frac{\pi}{2} m_n^2 z \Big(J_1(m_n R) Y_0(m_n z) - Y_1(m_n R) J_0(m_n z) \Big). \tag{B.5.8}$$

B.6 Spectral functions of the gauge towers

In order to derive the spectral functions for the gauge towers one can proceed in a similar way as for the fermion towers in Section 2.4.2. Starting from a KK-decomposition of the gauge fields given in general by Eq. 2.4.10

$$L_\mu^a(x,z) = \sum_n l_n^a(z,h) A_\mu^{(n)}(x) \qquad R_\mu^b(x,z) = \sum_n r_n^b(z,h) A_\mu^{(n)}(x)$$

$$B_\mu(x,z) = \sum_n b_n(z,h) A_\mu^{(n)}(x) \qquad Z'_\mu(x,z) = \sum_n z'_n(z,h) A_\mu^{(n)}(x) \tag{B.6.1}$$

$$C_\mu^{\hat{a}}(x,z) = \sum_n c_n^{\hat{a}}(z,h) A_\mu^{(n)}(x), \tag{B.6.2}$$

it is first noticed that if one wants to solve the bulk equations of motion, the ζ_n^A (which are labelled according to the 5D fields) will usually dependent on the VEV $h \equiv \langle h^{\hat{a}} \rangle$

of the Higgs. This additional feature has been dropped in the previous discussion for a reason which will become clear in a moment. Rewriting Eq. 2.4.16

$$S_A = \sum_n \int \mathrm{d}^4x \Big(-\frac{1}{4} F^{(n)}_{\mu\nu} F^{(n)\mu\nu} + \frac{1}{2}\Big(\partial_\mu A_5^{(n)} - m_n A_\mu^{(n)}\Big)^2 \Big), \tag{B.6.3}$$

one can see, that the $A_5^{(n)}$ which belong to the Higgs cannot be gauged away leaving it present in the bulk. This will make it in general very complicated to solve for the equations of motion since h mixes Dirichlet and Neumann modes. Fortunately, it is possible, as in the fermionic case, to get rid of h in the entire bulk via the Wilson line transformation $\Omega(x,z)$ of 2.4.40 which makes all $A_5^{(n)}(x)$ vanish for $z \neq R'$. This reduces the 4D KK-action to

$$S_A = \sum_n \int \mathrm{d}^4x \Big(-\frac{1}{4} F^{(n)}_{\mu\nu} F^{(n)\mu\nu} + \frac{1}{2} m_n^2 A_\mu^{(n)} A^{(n)\mu} \Big) \tag{B.6.4}$$

which results in the usual Proca equation of motions

$$\partial_\mu F^{(n)\mu\nu} + m_n^2 A^{(n)\nu} = 0 \tag{B.6.5}$$

for massive 4D gauge fields. This in hindsight justifies the requirement in Eq. 2.4.18 making it now the actual equation of motion for the ζ_n^A in absence of the h. Therefore, one can derive from Eq. B.5.3

$$\zeta_n^A(z,0) = F_n^A C(z) + G_n^A S(z) \tag{B.6.6}$$

the full equations of motions for the base functions via

$$\zeta_n^A(z,h) T^A = \Omega^\dagger(x,z) \zeta_n^B(z,0) T^B \Omega(x,z). \tag{B.6.7}$$

where it will be summed over A and B. Since the T^A together with $\mathbb{1}_5$ are a basis for the mass eigenstates for the gauge fields of $SO(5) \times U(1)_X$ they can be used to identify the $\zeta_n^A(z,h)$ within this equation.[42] For this purpose it is also beneficial to rewrite the b_n and z'_n in terms of the unmixed base functions

$$r_n^3(z,h) = s_\phi b_n(z,h) + c_\phi z'_n(z,h) \tag{B.6.8}$$

$$x_n(z,h) = c_\phi b_n(z,h) - s_\phi z'_n(z,h) \tag{B.6.9}$$

of R_μ^3 and X_μ with generators T_R^3 and $\mathbb{1}_5$.

One can translate the imposed BCs for the fields

$$L_\mu^a(+,+) \quad R_\mu^b(-,+) \quad B_\mu(+,+) \quad Z'_\mu(-,+) \quad C_\mu^{\hat{a}}(-,-) \tag{B.6.10}$$

into BCs for the z-dependent KK-functions yielding

$$\begin{aligned} \partial_5 l_n^a(z,h)_{|R} = \partial_5 b_n(z,h)_{|R} = r_n^b(z,h)_{|R} = z'_n(z,h)_{|R} = c_n^{\hat{a}}(z,h)_{|R} = 0 \\ \partial_5 l_n^a(z,h)_{|R'} = \partial_5 b_n(z,h)_{|R'} = \partial_5 r_n^b(z,h)_{|R'} = \partial_5 z'_n(z,h)_{|R'} = c_n^{\hat{a}}(z,h)_{|R'} = 0. \end{aligned} \tag{B.6.11}$$

[42] Actually, the basis of the mass eigenstates consists of $\mathbb{1}_5$, $\hat{T}^{\hat{a}}$ and $T_L^a \pm T_R^a$.

Because of $\Omega(x,R)=1$ one obtaines $\zeta_n^A(R,h)=\zeta_n^A(R,0)$ leaving the boundary condition unchanged by the Wilson line transformation on the UV-brane. Using B.6.6 the relations $G_n^{l,a}=F_n^{r,b}=G_n^b=F_n^{z'}=F^{c,\hat{a}}=0$ are obtained as the first 11 constraints. Introducing brane kinetic terms for the SM gauge fields on the UV

$$S_A^{\mathrm{UV}}=\int \mathrm{d}^4x\left[-\frac{1}{4}\kappa^2R\ln\frac{R'}{R}L_{\mu\nu}^aL^{a\mu\nu}-\frac{1}{4}\kappa'^2R\ln\frac{R'}{R}B_{\mu\nu}B^{\mu\nu}\right] \tag{B.6.12}$$

alters some of the conditions. This can again be done by pushing the brane kinetic term ε away from the UV-brane. Requiring the $A_\mu^{(n)}$ still to fulfill the Proca equations of motion, one has to alter the free equations of motion for the KK-functions l_n^a and b_n in order to cancel the extra contribution. This can be achieved by

$$-\partial_5\partial^5l_n^a+\frac{1}{z}\partial_5l_n^a=\left(1+\kappa^2R\ln\frac{R'}{R}\,\delta(z-R+\varepsilon)\right)m_n^2l_n^a \tag{B.6.13}$$

and equivalent for the b_n with κ'. Assuming l_n^a to be smooth, one can, by integrating from 0 to ε and taking $\varepsilon\to0^+$

$$\partial_5l^a_{n|_{R^+}}=-\kappa^2m_n^2R\ln\frac{R'}{R}l^a_{n|_{R^+}} \tag{B.6.14}$$

derive the mass dependent BCs in the gauge sector. Therefore, the BC for l_n^a at $z=R$ is changed to the one in Eq. B.6.14 proceeding in the same way for b_n. This changes the relations of the corresponding parameters to $G_n^{l,a}=-\kappa^2m_nR\ln(R'/R)F_n^{l,a}$ and $G_n^b=-\kappa'^2m_nR\ln(R'/R)F_n^b$, respectively. The corresponding free base functions now yield

$$\begin{aligned}
l_n^a(z,0)&=F_n^{l,a}\left(C(z)-\kappa^2m_nR\ln\frac{R'}{R}S(z)\right) &\qquad r_n^b(z,0)&=G_n^{r,a}S(z)\\
b_n(z,0)&=F_n^b\left(C(z)-\kappa'^2m_nR\ln\frac{R'}{R}S(z)\right) &\qquad z_n'(z,0)&=G_n^{z'}S(z)\\
&\qquad c_n^{\hat{a}}(z,0)=F^{c,\hat{a}}S(z).
\end{aligned} \tag{B.6.15}$$

Inserting these functions into Eq. B.6.7 the $\zeta_n^A(z,h)$ are obtained. An evaluation at $z=R'$ with respect to their BCs yields a system of linear differential equations which can be solved for the remaining 11 parameters $F^{l,a}$, $G^{r,a}$, F^b, $G^{z'}$ and $F^{c,\hat{a}}$. Using the corresponding parameter matrix M_g one can determine the spectral functions of $\rho(m_n^2(h))$ by looking at

$$\begin{aligned}
\det M_g=&\left(m_n\frac{R'}{R}s_h^2\Big(K'(R')+s_\phi^2K(R')\Big)+2K(R')K'(R')\right)\\
&\cdot\left(m_n\frac{R'}{R}s_h^2+2K(R')\right)^2S'(R')^3\stackrel{!}{=}0,
\end{aligned} \tag{B.6.16}$$

with the definition

$$K^{(\prime)}(R')\equiv S(R')\left(C'(R')-m_nR\frac{R'}{R}\kappa^{(\prime)2}S'(R')\right), \tag{B.6.17}$$

where the Wronskian relation

$$S'(z)C(z) - C'(z)S(z) = m_n \frac{z}{R} \tag{B.6.18}$$

has been used to simplify the expression. The first root term can be identified with the spectral function for the Z and the second with the function for the $W^{\pm}$

$$\rho_{W,Z}(m_n^2) = 1 + f_{W,Z}(m_n^2) s_h^2, \tag{B.6.19}$$

with form factors

$$f_W(-p^2) = \frac{m_n}{2} \frac{R'}{R} \frac{1}{S(R')(C'(R') - m_n R \ln(R'/R)\kappa^2 S'(R'))} \tag{B.6.20}$$

$$\begin{aligned} f_Z(-p^2) =& \frac{m_n}{2} \frac{R'}{R} \left[\frac{1}{S(R')(C'(R') - m_n \ln(R'/R)\kappa^2 S'(R'))} \right. \\ &+ \left. \frac{s_\phi^2}{S(R')(C'(R') - m_n R \ln(R'/R)\kappa'^2 S'(R'))} \right]. \end{aligned} \tag{B.6.21}$$

B.7 Numerical Calculation of the Higgs potential

Due to the quite lengthy expression of the spectral function for fermionic KK-towers (here for the top quark), it is beneficial for computational implementation to work in terms of the 10×10 matrix M_t. For an easier calculation the derivations will be performed in terms of $s_h^2 \equiv \sin^2((\tilde{v} + h)/f)$ with $s_0^2 = \xi = v^2/f^2$. The potential and its derivative therefore look like

$$V_t(0) = -\frac{3}{4\pi^2} \int_0^\infty \mathrm{d}p\, p^3 \log\left(\frac{\det M(\xi)}{\det M(0)}\right) \tag{B.7.1}$$

$$\begin{aligned} \left.\frac{\partial V_t(h)}{\partial h}\right|_{h=0} &= \left.\frac{\partial s_h^2}{\partial h}\right|_{h=0} \left.\frac{\partial V_t(s_h^2)}{\partial s_h^2}\right|_{s_h^2=\xi} \\ &= -\frac{3\sqrt{\xi - \xi^2}}{2\pi^2 f} \int_0^\infty \mathrm{d}p\, p^3 \,\mathrm{tr}\left(M^{-1}(\xi) \left.\frac{\partial M(s_h^2)}{\partial s_h^2}\right|_{s_h^2=\xi} \right) \end{aligned} \tag{B.7.2}$$

$$\begin{aligned} \left.\frac{\partial^2 V_t(h)}{\partial h^2}\right|_{h=0} &= \left.\frac{\partial^2 s_h^2}{\partial h^2}\right|_{h=0} \left.\frac{\partial V_t(s_h^2)}{\partial s_h^2}\right|_{s_h^2=\xi} + \left.\left(\frac{\partial s_h^2}{\partial h}\right)^2\right|_{h=0} \left.\frac{\partial^2 V_t(s_h^2)}{(\partial s_h^2)^2}\right|_{s_h^2=\xi} \\ &= -\frac{3(1-2\xi)}{2\pi^2 f^2} \int_0^\infty \mathrm{d}p\, p^3 \,\mathrm{tr}\left(M^{-1}(\xi) \left.\frac{\partial M(s_h^2)}{\partial s_h^2}\right|_{s_h^2=\xi} \right) \\ &\quad - \frac{3\xi(1-\xi)}{\pi^2 f^2} \int_0^\infty \mathrm{d}p\, p^3 \,\mathrm{tr}\left(M^{-1}(\xi) \left.\frac{\partial^2 M(s_h^2)}{(\partial s_h^2)^2}\right|_{s_h^2=\xi} \right. \\ &\qquad \left. - \left[M^{-1}(\xi) \left.\frac{\partial M(s_h^2)}{\partial s_h^2}\right|_{s_h^2=\xi} \right]^2 \right). \end{aligned} \tag{B.7.3}$$

References

[1] Y. Fukuda et al. "Evidence for Oscillation of Atmospheric Neutrinos". In: *Physical Review Letters* 81.8 (1998), pp. 1562–1567. arXiv: hep-ex/9807003.

[2] P. Minkowski. "$\mu \to e\gamma$ at a rate of one out of 109 muon decays?" In: *Physics Letters B* 67.4 (1977), pp. 421–428.

[3] W. Konetschny and W. Kummer. "Nonconservation of total lepton number with scalar bosons". In: *Physics Letters B* 70.4 (1977), pp. 433–435.

[4] R. Foot, H. Lew, X. G. He, and G. C. Joshi. "See-saw neutrino masses induced by a triplet of leptons". In: *Zeitschrift für Physik C: Particles and Fields* 44.3 (1989), pp. 441–444.

[5] E. Ma. "Verifiable radiative seesaw mechanism of neutrino mass and dark matter". In: *Physical Review D* 73.7, 077301 (2006). arXiv: hep-ph/0601225.

[6] F. Zwicky. "Die Rotverschiebung von extragalaktischen Nebeln". In: *Helvetica Physica Acta* 6 (1933), pp. 110–127.

[7] K. G. Begeman, A. H. Broeils, and R. H. Sanders. "Extended rotation curves of spiral galaxies: dark haloes and modified dynamics". In: *Monthly Notices of the Royal Astronomical Society* 249.3 (1991), pp. 523–537.

[8] E. Corbelli and P. Salucci. "The extended rotation curve and the dark matter halo of M33". In: *Monthly Notices of the Royal Astronomical Society* 311.2 (2000), pp. 441–447. eprint: astro-ph/9909252.

[9] D. Clowe et al. "A Direct Empirical Proof of the Existence of Dark Matter". In: *The Astrophysical Journal* 648.2 (2006), pp. L109–L113. eprint: astro-ph/0608407.

[10] G. Bertone, D. Hooper, and J. Silk. "Particle dark matter: evidence, candidates and constraints". In: *Physics Reports* 405.5-6 (2005), pp. 279–390. arXiv: hep-ph/0404175.

[11] Planck Collaboration. "Planck 2013 results. I. Overview of products and scientific results". In: *Astronomy & Astrophysics* 571.A1 (2014). arXiv: 1303.5062 [astro-ph].

[12] A. Friedman. "Über die Krümmung des Raumes". In: *Zeitschrift für Physik* 10.1 (1922), pp. 377–386.

[13] G. Lemaître. "Un Univers homogène de masse constante et de rayon croissant rendant compte de la vitesse radiale des nébuleuses extra-galactiques". In: *Annales de la Société Scientifique de Bruxelles* 47 (1927), pp. 49–59.

[14] B. P. Abbott et al. "A gravitational-wave standard siren measurement of the Hubble constant". In: *Nature* 551.7678 (2017), pp. 85–88. arXiv: 1710.05835 [astro-ph].

[15] A. G. Riess. "The expansion of the Universe is faster than expected". In: *Nature Reviews Physics* 2.1 (2020), pp. 10–12. arXiv: 2001.03624 [astro-ph].

[16] S. Carlip. "Quantum gravity: a progress report". In: *Reports on Progress in Physics* 64.8 (2001), pp. 885–942. arXiv: gr-qc/0108040v1.

[17] R. Penrose. *The road to reality: A complete guide to the laws of the universe*. Random house, 2006.

[18] D. Oriti. *Approaches to quantum gravity: Toward a new understanding of space, time and matter*. Cambridge University Press, Mar. 2009.

[19] G. 't Hooft. "Naturalness, chiral symmetry, and spontaneous chiral symmetry breaking". In: *NATO Science Series B* 59 (1980). Ed. by G. 't Hooft et al., pp. 135–157.

[20] P. Nelson. "Naturalness in Theoretical Physics". In: *American Scientist* 73.1 (1985), pp. 60–67.

[21] G. F. Giudice. "Naturally Speaking: The Naturalness Criterion and Physics at the LHC". In: *Perspectives on LHC Physics* (2008), pp. 155–178. arXiv: 0801.2562 [hep-ph].

[22] A. Hook. "TASI Lectures on the Strong CP Problem and Axions". In: *Proceeding of Science* TASI2018 (2019). arXiv: 1812.02669 [hep-ph].

[23] F. Feruglio. "Pieces of the flavour puzzle". In: *The European Physical Journal C* 75.8 (2015), p. 373. arXiv: 1503.04071 [hep-ph].

[24] K. G. Wilson. "Renormalization Group and Strong Interactions". In: *Physical Review D* 3.8 (1971), pp. 1818–1846.

[25] E. Gildener and S. Weinberg. "Symmetry breaking and scalar bosons". In: *Physical Review D* 13.12 (1976), pp. 3333–3341.

[26] E. Gildener. "Gauge-symmetry hierarchies revisited". In: *Physics Letters B* 92.1-2 (1980), pp. 111–114.

[27] G. Altarelli. "The Higgs: so simple yet so unnatural". In: *Physica Scripta* T158. 014011 (2013). arXiv: 1308.0545 [hep-ph].

[28] A. de Gouvea, D. Hernandez, and T. M. P. Tait. "Criteria for Natural Hierarchies". In: *Physical Review D - Particles, Fields, Gravitation and Cosmology* 89.11 (2014), pp. 1–8. arXiv: 1402.2658 [hep-ph].

[29] D. Kazakov. "Beyond the Standard Model' 17". In: *CERN Yellow Reports: School Proceedings* 3.0 (2018). arXiv: 1807.00148 [hep-ph].

[30] L. Susskind. "Dynamics of spontaneous symmetry breaking in the Weinberg-Salam theory". In: *Physical Review D* 20.10 (1979), pp. 2619–2625.

[31] S. Weinberg. "Implications of dynamical symmetry breaking". In: *Physical Review D* 13.4 (1976), pp. 974–996.

[32] S. Weinberg. "Implications of dynamical symmetry breaking: An addendum". In: *Physical Review D* 19.4 (1979), pp. 1277–1280.

[33] C. T. Hill and E. H. Simmons. “Strong dynamics and electroweak symmetry breaking”. In: *Physics Reports* 381.4-6 (2003), pp. 235–402. arXiv: hep-ph/0203079.

[34] Y. A. Golfand and E. P. Likhtman. “Extension of the Algebra of Poincare Group Generators and Violation of P Invariance”. In: *JETP Letters* 13 (1971), pp. 323–326.

[35] J. Wess and B. Zumino. “Supergauge transformations in four dimensions”. In: *Nuclear Physics B* 70.1 (1974), pp. 39–50.

[36] S. P. Martin. “A Supersymmetry primer”. In: *Perspectives on supersymmetry. Vol.2*. Ed. by G. L. Kane. Vol. 21. 2010, pp. 1–153. arXiv: hep-ph/9709356.

[37] J. D. Lykken. “Introduction to supersymmetry”. In: *Theoretical Advanced Study Institute in Elementary Particle Physics (TASI 96): Fields, Strings, and Duality*. June 1996, pp. 85–153. arXiv: hep-th/9612114.

[38] ATLAS Collaboration. “Combination of the searches for pair-produced vector-like partners of the third-generation quarks at $\sqrt{s} = 13$ TeV with the ATLAS detector”. In: *Physical Review Letters* 121.21, 211801 (2018). arXiv: 1808.02343 [hep-ex].

[39] P. W. Higgs. “Broken Symmetries and the Masses of Gauge Bosons”. In: *Physical Review Letters* 13.16 (1964), pp. 508–509.

[40] F. Englert and R. Brout. “Broken Symmetry and the Mass of Gauge Vector Mesons”. In: *Physical Review Letters* 13.9 (1964), pp. 321–323.

[41] G. S. Guralnik, C. R. Hagen, and T. W. B. Kibble. “Global Conservation Laws and Massless Particles”. In: *Physical Review Letters* 13.20 (1964), pp. 585–587.

[42] ATLAS Collaboration. “Observation of a new particle in the search for the Standard Model Higgs boson with the ATLAS detector at the LHC”. In: *Physics Letters B* 716.1 (2012), pp. 1–29. arXiv: 1207.7214 [hep-ex].

[43] L. Serkin. “Top quarks and exotics at ATLAS and CMS”. In: *11th International Workshop on Top Quark Physics*. Jan. 2019. arXiv: 1901.01765 [hep-ex].

[44] O. Matsedonskyi, G. Panico, and A. Wulzer. “Light top partners for a light composite Higgs”. In: *Journal of High Energy Physics* 2013.1 (2013). arXiv: 1204.6333 [hep-th].

[45] A. Carmona and F. Goertz. “A naturally light Higgs without light Top Partners”. In: *Journal of High Energy Physics* 2015.5 (2014). arXiv: 1410.8555 [hep-ph].

[46] S. Blasi and F. Goertz. “Softened Goldstone-Symmetry Breaking”. In: *Physical Review Letters* 123.22, 221801 (2019). arXiv: 1903.06146 [hep-ph].

[47] G. Panico and A. Wulzer. *The Composite Nambu-Goldstone Higgs*. Vol. 913. Springer, 2016. arXiv: 1506.01961 [hep-ph].

[48] R. Contino. “The Higgs as a Composite Nambu-Goldstone Boson”. In: *Theoretical Advanced Study Institute in Elementary Particle Physics: Physics of the Large and the Small*. 2011, pp. 235–306. arXiv: 1005.4269 [hep-ph].

[49] G. Panico, M. Serone, and A. Wulzer. “Electroweak symmetry breaking and precision tests with a fifth dimension”. In: *Nuclear Physics B* 762.1-2 (2007), pp. 189–211. arXiv: 0605292 [hep-ph].

[50] C. Csáki, T. Ma, and J. Shu. “Maximally Symmetric Composite Higgs Models”. In: *Physical Review Letters* 119.13, 131803 (2017). arXiv: 1702.00405 [hep-ph].

[51] S. Blasi, C. Csaki, and F. Goertz. *A Natural Composite Higgs via Universal Boundary Conditions [Preprint]*. Apr. 2020. arXiv: 2004.06120 [hep-ph].

[52] S. Dimopoulos and J. Preskill. “Massless composites with massive constituents”. In: *Nuclear Physics B* 199.2 (1982), pp. 206–222.

[53] D. B. Kaplan, H. Georgi, and S. Dimopoulos. “Composite Higgs scalars”. In: *Physics Letters B* 136.3 (1984), pp. 187–190.

[54] D. B. Kaplan and H. Georgi. “SU(2)×U(1) breaking by vacuum misalignment”. In: *Physics Letters B* 136.3 (1984), pp. 183–186.

[55] H. Georgi and D. B. Kaplan. “Composite Higgs and custodial SU(2)”. In: *Physics Letters B* 145.3-4 (1984), pp. 216–220.

[56] H. Georgi, D. B. Kaplan, and P. Galison. “Calculation of the composite Higgs mass”. In: *Physics Letters B* 143.1-3 (1984), pp. 152–154.

[57] M. J. Dugan, H. Georgi, and D. B. Kaplan. “Anatomy of a composite Higgs model”. In: *Nuclear Physics B* 254 (1985), pp. 299–326.

[58] T. Banks. “Constraints on SU(2)×U(1) breaking by vacuum misalignment”. In: *Nuclear Physics B* 243.1 (1984), pp. 125–130.

[59] J. A. Evans, J. Galloway, M. A. Luty, and R. A. Tacchi. “Minimal conformal technicolor and precision electroweak tests”. In: *Journal of High Energy Physics* 2010.10 (2010). arXiv: 1001.1361 [hep-ph].

[60] N. Arkani-Hamed, A. G. Cohen, and H. Georgi. “Electroweak symmetry breaking from dimensional deconstruction”. In: *Physics Letters B* 513.1-2 (2001), pp. 232–240. arXiv: hep-ph/0105239.

[61] N. Arkani-Hamed et al. “The Minimal Moose for a Little Higgs”. In: *Journal of High Energy Physics* 2002.08 (2002). arXiv: hep-ph/0206020.

[62] R. Contino, Y. Nomura, and A. Pomarol. “Higgs as a holographic pseudo-Goldstone boson”. In: *Nuclear Physics B* 671 (2003), pp. 148–174. arXiv: hep-ph/0306259.

[63] Z. Chacko, H.-S. Goh, and R. Harnik. “Natural Electroweak Breaking from a Mirror Symmetry”. In: *Physical Review Letters* 96.23, 231802 (2006). arXiv: hep-ph/0506256.

[64] W. D. Goldberger, B. Grinstein, and W. Skiba. “Light scalar at LHC: the Higgs or the dilaton?” In: *Physical Review Letters* 100.11, 111802 (2007). arXiv: 0708.1463 [hep-ph].

[65] G. Panico and A. Wulzer. “The Discrete Composite Higgs Model”. In: *Journal of High Energy Physics* 2011.09 (2011). arXiv: 1106.2719 [hep-ph].

[66] B. Bellazzini, C. Csáki, and J. Serra. "Composite Higgses". In: *The European Physical Journal C* 74.5 (2014). arXiv: 1401.2457 [hep-th].

[67] S. Dimopoulos and L. Susskind. "Mass without scalars". In: *Nuclear Physics B* 155.1 (1979), pp. 237–252.

[68] C. Grojean, O. Matsedonskyi, and G. Panico. "Light top partners and precision physics". In: *Journal of High Energy Physics* 2013.10 (2013). arXiv: 1306.4655 [hep-ph].

[69] N. Arkani-Hamed, A. G. Cohen, E. Katz, and A. E. Nelson. "The Littlest Higgs". In: *Journal of High Energy Physics* 2002.07 (2002). arXiv: hep-ph/0206021.

[70] I. Low, W. Skiba, and D. Smith. "Little Higgs bosons from an antisymmetric condensate". In: *Physical Review D* 66.7, 072001 (2002). arXiv: hep-ph/0207243.

[71] S. Chang. "A "littlest Higgs" model with custodial SU(2) symmetry". In: *Journal of High Energy Physics* 2003.12 (2003). arXiv: hep-ph/0306034.

[72] M. Schmaltz, D. Stolarski, and J. Thaler. "The bestest little Higgs". In: *Journal of High Energy Physics* 2010.9 (2010). arXiv: 1006.1356 [hep-ph].

[73] E. Bertuzzo, T. S. Ray, H. de Sandes, and C. A. Savoy. "On composite two Higgs doublet models". In: *Journal of High Energy Physics* 2013.5 (2013). arXiv: 1206.2623 [hep-ph].

[74] K. Agashe, R. Contino, and A. Pomarol. "The Minimal Composite Higgs Model". In: *Nuclear Physics B* 719.1-2 (2004), pp. 165–187. arXiv: hep-ph/0412089.

[75] G. F. Giudice, C. Grojean, A. Pomarol, and R. Rattazzi. "The strongly-interacting light Higgs". In: *Journal of High Energy Physics* 2007.06 (2007). arXiv: hep-ph/0703164.

[76] S. Coleman, J. Wess, and B. Zumino. "Structure of Phenomenological Lagrangians. I". In: *Physical Review* 177.5 (1969), pp. 2239–2247.

[77] C. G. Callan, S. Coleman, J. Wess, and B. Zumino. "Structure of Phenomenological Lagrangians. II". In: *Physical Review* 177.5 (1969), pp. 2247–2250.

[78] P. Sikivie, L. Susskind, M. Voloshin, and V. Zakharov. "Isospin breaking in technicolor models". In: *Nuclear Physics B* 173.2 (1980), pp. 189–207.

[79] D. B. Kaplan. "Flavor at SSC energies: A new mechanism for dynamically generated fermion masses". In: *Nuclear Physics B* 365.2 (1991), pp. 259–278.

[80] R. Contino, L. Da Rold, and A. Pomarol. "Light custodians in natural composite Higgs models". In: *Physical Review D* 75.5, 055014 (2007). arXiv: hep-ph/0612048.

[81] C. Csáki, A. Falkowski, and A. Weiler. "The flavor of the composite pseudo-goldstone Higgs". In: *Journal of High Energy Physics* 2008.09 (2008). arXiv: 0804.1954 [hep-ph].

[82] A. Pomarol and F. Riva. "The composite Higgs and light resonance connection". In: *Journal of High Energy Physics* 2012.8 (2012). arXiv: 1205.6434 [hep-ph].

[83] S. De Curtis, M. Redi, and A. Tesi. "The 4D composite Higgs". In: *Journal of High Energy Physics* 2012.4 (2012). arXiv: 1110.1613 [hep-ph].

[84] J. M. Maldacena. "The Large N Limit of Superconformal Field Theories and Supergravity". In: *International Journal of Theoretical Physics* 38.4 (1997). arXiv: hep-th/9711200.

[85] T. Kaluza. "Zum Unitätsproblem der Physik". In: *Sitzungsberichte der Preussischen Akademie der Wissenschaften zu Berlin (Mathematik Physik)* (1921).

[86] O. Klein. "Quantentheorie und fünfdimensionale Relativitätstheorie". In: *Zeitschrift für Physik* 37.12 (1926), pp. 895–906.

[87] R. Rattazzi and A. Zaffaroni. "Comments on the Holographic Picture of the Randall-Sundrum Model". In: *Journal of High Energy Physics* 2001.04 (2001). arXiv: hep-th/0012248.

[88] L. Randall and R. Sundrum. "Large Mass Hierarchy from a Small Extra Dimension". In: *Physical Review Letters* 83.17 (1999), pp. 3370–3373. arXiv: hep-ph/9905221.

[89] C. Csaki, J. Hubisz, and P. Meade. "TASI lectures on electroweak symmetry breaking from extra dimensions". In: *Theoretical Advanced Study Institute in Elementary Particle Physics: Physics in $D \geqq 4$*. Oct. 2005, pp. 703–776. arXiv: hep-ph/0510275.

[90] C. Csáki, C. Grojean, J. Hubisz, Y. Shirman, and J. Terning. "Fermions on an interval: Quark and lepton masses without a Higgs". In: *Physical Review D* 70.1, 015012 (2004). arXiv: hep-ph/0310355v1.

[91] A. Falkowski. "Holographic pseudo-Goldstone boson". In: *Physical Review D* 75.2, 025017 (2007). arXiv: hep-ph/0610336.

[92] H. Davoudiasl, J. L. Hewett, and T. G. Rizzo. "Brane-localized kinetic terms in the Randall-Sundrum model". In: *Physical Review D* 68.4, 045002 (2003). arXiv: hep-ph/0212279.

[93] S. Coleman and E. Weinberg. "Radiative Corrections as the Origin of Spontaneous Symmetry Breaking". In: *Physical Review D* 7.6 (1973), pp. 1888–1910.

[94] K. Oda and A. Weiler. "Wilson lines in warped space: dynamical symmetry breaking and restoration". In: *Physics Letters B* 606.3-4 (2005), pp. 408–416. arXiv: hep-ph/0410061.

[95] R. Sundrum. "Tasi 2004 lectures: To the fifth dimension and back". In: *Theoretical Advanced Study Institute in Elementary Particle Physics: Physics in $D \geqq 4$*. Aug. 2005, pp. 585–630. arXiv: hep-th/0508134.

[96] A. D. Medina, N. R. Shah, and C. E. M. Wagner. "Gauge-Higgs unification and radiative electroweak symmetry breaking in warped extra dimensions". In: *Physical Review D* 76.9, 095010 (2007). arXiv: 0706.1281 [hep-ph].

[97] A. Falkowski, S. Pokorski, and J. Roberts. "Modelling strong interactions and longitudinally polarized vector boson scattering". In: *Journal of High Energy Physics* 2007 (2007).

[98] G. Panico, E. Pontón, J. Santiago, and M. Serone. "Dark matter and electroweak symmetry breaking in models with warped extra dimensions". In: *Physical Review D* 77.11, 115012 (2008). arXiv: 0801.1645 [hep-ph].

[99] G. Panico, M. Redi, A. Tesi, and A. Wulzer. "On the tuning and the mass of the composite Higgs". In: *Journal of High Energy Physics* 2013.3 (2013). arXiv: 1210.7114 [hep-ph].

[100] M. Baak et al. "The electroweak fit of the standard model after the discovery of a new boson at the LHC". In: *The European Physical Journal C* 72.11 (2012). arXiv: 1209.2716 [hep-ph].

[101] R. Barbieri and G. Giudice. "Upper bounds on supersymmetric particle masses". In: *Nuclear Physics B* 306.1 (1988), pp. 63–76.

[102] C. Csáki, T. Ma, J. Shu, and J.-H. Yu. *Emergence of Maximal Symmetry [Preprint]*. 2018. arXiv: 1810.07704 [hep-ph].

[103] D. B. N. Eite Tiesinga Peter J. Mohr and B. N. Taylor. *The 2018 CODATA Recommended Values of the Fundamental Physical Constants (Web Version 8.1)*. Database developed by J. Baker, M. Douma, and S. Kotochigova. Available at http://physics.nist.gov/constants, National Institute of Standards and Technology, Gaithersburg, MD 20899. 2020.

[104] I. Bejar et al. *High-Luminosity Large Hadron Collider (HL-LHC) Technical Design Report V. 0.1*. Sept. 2017.

[105] F. Collaboration. "FCC-hh: The Hadron Collider". In: *The European Physical Journal Special Topics* 228.4 (2019), pp. 755–1107.

[106] A. Banfi, A. Martin, and V. Sanz. "Probing top-partners in Higgs + jets". In: *Journal of High Energy Physics* 2014.8 (2014). arXiv: 1308.4771 [hep-ph].

[107] S. Dawson, A. Ismail, and I. Low. "What's in the loop? the anatomy of double Higgs production". In: *Physical Review D - Particles, Fields, Gravitation and Cosmology* 91.11 (2015), pp. 1–31. arXiv: 1504.05596 [hep-ph].

[108] A. Azatov, C. Grojean, A. Paul, and E. Salvioni. "Resolving gluon fusion loops at current and future hadron colliders". In: *Journal of High Energy Physics* 2016.9 (2016). arXiv: 1608.00977 [hep-ph].

[109] A. Banfi, B. M. Dillon, W. Ketaiam, and S. Kvedaraitė. "Composite Higgs at high transverse momentum". In: *Journal of High Energy Physics* 2020.1 (2020). arXiv: 1905.12747 [hep-ph].

[110] S. Casagrande, F. Goertz, U. Haisch, M. Neubert, and T. Pfoh. "Flavor physics in the Randall-Sundrum model I. Theoretical setup and electroweak precision tests". In: *Journal of High Energy Physics* 2008.10 (2008). arXiv: 0807.4937 [hep-ph].

Declaration of authorship:

I, Julian Bollig, declare that this thesis and the work presented in it is entirely my own. Where I have consulted the work of others, it is always clearly stated.

Heidelberg, July 31, 2020